# DESIGN OF TWO WHEELED TWIN ROTORED HYBRID ROBOTIC PLATFORM

A MASTER'S THESIS

in

Mechatronics Engineering

Atilim University

by

DOĞANÇ KÜÇÜK

JULY 2010

# DESIGN OF TWO WHEELED TWIN ROTORED HYBRID ROBOTIC PLATFORM

A THESIS SUBMITTED TO

THE GRADUATE SCHOOL OF NATURAL AND APPLIED SCIENCES

OF

ATILIM UNIVERSITY

BY

DOĞANÇ KÜÇÜK

IN PARTIAL FULFILLMENT OF THE REQUIREMENTS

FOR

THE DEGREE OF MASTER OF SCIENCE

IN

MECHATRONICS ENGINEERING

JULY 2010

Approval of the Graduate School of Natural and Applied Sciences, Atılım University.

_____

Prof. Dr. İbrahim Akman

Director

I certify that this thesis satisfies all the requirements as a thesis for the degree of Master of Science.

_____

Prof. Dr. Abdulkadir Erden

Head of Department

This is to certify that we have read the thesis "Design of Two Wheeled Twin Rotored Hybrid Robotic Platform" submitted by "Doğanç Küçük" and that in our opinion it is fully adequate, in scope and quality, as a thesis for the degree of Master of Science.

| | |
|---|---|
| _____ | _____ |
| Asst. Prof. Dr. Bülent İrfanoğlu | Asst. Prof. Dr. Kutluk Bilge Arıkan |
| Co-Supervisor | Supervisor |

Examining Committee Members

| | | |
|---|---|---|
| Prof. Dr. Bülent Emre Platin | (METU, M.E. Dept.) | _____ |
| Prof. Dr. Kemal Leblebicioğlu | (METU, E.E.E. Dept.) | _____ |
| Assoc. Prof. Dr. Veysel Gazi | (TOBB E.E.E. Dept.) | _____ |
| Asst. Prof. Dr. Bülent İrfanoğlu | (AT.U. M.E. Dept.) | _____ |
| Asst. Prof. Dr. Kutluk Bilge Arıkan | (AT.U. M.E. Dept.) | _____ |

Date: 23.07.2010

I declare and guarantee that all data, knowledge and information in this document has been obtained, processed and presented in accordance with academic rules and ethical conduct. Based on these rules and conduct, I have fully cited and referenced all material and results that are not original to this work.

Name, Last Name: Doğanç KÜÇÜK

Signature:

# ABSTRACT

## DESIGN OF TWO WHEELED TWIN ROTORED HYBRID ROBOTIC PLATFORM

Küçük, Doğanç

M.S., Mechatronics Engineering Department

Supervisor: Asst.Prof.Dr. Kutluk Bilge Arıkan

Co-Supervisor: Asst.Prof.Dr. Bülent İrfanoğlu

July 2010, 113 pages

The design of the two wheeled twin rotored hybrid robot (TWTR) structure is explained in the thesis. This study is the initial phase of the project to reach a hybrid platform that can navigate on ground and hover and navigate in air whenever necessary. This initial phase includes the design of the initial version of the physical system and design of basic controllers depending on the mathematical models and simulations. The system is designed and physically constructed based on the mechatronics design principles. Selection of actuators, sensor set, and the control hardware and the physical structure design are all considered simultaneously with the mathematical model and controller design phases. Nonlinear equations of motion of the physical system are derived and linearized in state space form for both ground and flying modes of motion. Linear Quadratic Regulator (LQR) and Error Space Approach type of controllers are designed employing the mathematical model and simulations. For ground motion, LQR and Error Space Approach controllers are designed and implemented on the real system; whereas PID and LQR type control systems are designed and implemented for the flying motion of the real robotic

platform. Stabilization of the attitude dynamics is considered for the flying motion in this study. Designed control systems are implemented on the physical system and the control parameters are tuned experimentally. The control system is developed in Matlab/Simulink and real time implementation is achieved by using Simulink Real Time Windows Target utility. Embedded controllers are not utilized in this first stage. Control systems are designed for the stabilization of the system and error space approach is applied for tracking a reference for the motion of the robot on ground. LQR's are designed to stabilize the attitude dynamics of the robot for flying motion. Switching between the control systems on ground and in air modes are achieved using a proximity sensor that can sense the distance of the platform body to the ground. Experiments show that system can be stabilized on ground and the attitude dynamics can be stabilized in air. The system will be developed to fully guide on ground and in air.

**Keywords:** Hybrid Robot, Self-balancing Pendulum Robot, Twin Rotor, Flying Robot, Attitude Stabilization, Linear Quadratic Regulator, Error Space Approach, Real Time Windows Target.

# ÖZ

## İKİ TEKERLEKLİ İKİ DÖNERKANAT SİSTEMİNE SAHİP MELEZ ROBOTİK SİSTEM TASARIMI

Küçük, Doğanç

Yüksek Lisans, Mekatronik Mühendisliği Bölümü

Tez Yöneticisi: Yrd. Doç. Dr. Kutluk Bilge Arıkan

Ortak Tez Yöneticisi: Yrd. Doç. Dr. Bülent İrfanoğlu

Temmuz 2010, 113 sayfa

Tez kapsamında iki tekerlekli iki dönerkanat sistemine sahip melez robotik sistem yapısı ayrıntılarıyla açıklanmıştır. Bu çalışma, yerde seyredebilen, gerektiğinde dikey kalkış gerçekleştirip havada seyredebilen melez sistem projesinin ilk aşamasıdır. Fiziksel sistemin ilk tasarımını, matematiksel modele göre tasarlanmış çeşitli kontrol sistemlerini ve bu kontrol sistemlerinin benzetimlerini içermektedir. Sistem mekatronik tasarım prensiplerine göre tasarlanmış ve fiziksel olarak inşa edilmiştir. Eyleyiciler, algılayıcı sistemi, kontrol donanımı ve fiziksel yapı tasarımı konuları, matematiksel model ve kontrol sistem tasarımı süreçleri ile eş zamanlı olarak düşünülmüştür. Kara ve hava hareketleri için, doğrusal olmayan hareket denklemleri türetilmiştir ve bu denklemler durum uzayı biçiminde doğrusallaştırılmıştır. LQR ve hata uzayı yaklaşımı türünde kontrol sistemleri matematiksel model ve benzetimler kullanılarak tasarlanmıştır. Kara hareketi için LQR ve hata uzayı yaklaşımı türünde kontrol sistemleri tasarlanıp gerçek sistem üzerinde uygulanmıştır. Hava hareketi içinse PID ve LQR tipi kontrol sistemleri

gerçek sistem üzerinde uygulanmıştır. Bu çalışmada, hava hareketi kısmında sistemin yönelim dinamiklerinin dengelenmesi düşünülmüştür. Tasarlanan kontrol sistemleri fiziksel sistem üzerinde uygulanmış ve deneysel olarak ayarlanmıştır. Kontrol sistemleri, Matlab ortamında geliştirilmiş ve gerçek zamanlı uygulaması Simulink arayüzü ile gerçekleştirilmiştir. Gömülü kontrolcü tasarımı ve uygulanması bu aşamada çalışmaya dahil edilmemiştir. Kara hareketinde, LQR ve PID tipi kontrol sistemleri sistemin davranışının kararlı hale getirilmesi için, hata uzay yaklaşımı ise referans takip kontrolü için kullanılmıştır. Hava hareketinde ise sistemin davranışının kararlı hale getirilmesi için LQR tipi kontrolcü kullanılmıştır. Hava ve Kara hareketleri kontrol sistemleri arasındaki geçiş, sistemin yer ile arasında olan mesafeyi ölçen bir mesafe ölçüm algılayıcısı ile sağlanması öngörülmüştür. Gerçekleştirilen deneyler, sistemin kara ve hava hareketlerinde davranışının dengelenebildiğini göstermektedir. Sistem kara ve hava hareketlerinde seyir kontrolünün gerçekleştirilmesine açıktır.

**Anahtar Kelimeler:** Melez Robot, Kendini Dengeleyen Sarkaç Robot, İkiz Dönerkanat Sistemi, Uçan Robot, Yönelim Denetimi, Doğrusal Kuadratik Regülator, Hata Uzayı Yaklaşımı, Real Time Windows Target.

To My Father, Mother and Brother;

# ACKNOWLEDGEMENTS

I express sincere appreciation to my supervisor Asst. Prof. Dr. Kutluk Bilge Arıkan for his guidance and insight throughout the research. Thanks also go to my co-supervisor Asst. Prof. Dr. Bülent İrfanoğlu. The technical and mental assistance of Ayça Göçmen, Cahit Gürel, Meral Aday, Handan Kara, Selçuk Kahraman, Sefa Boyacıoğlu and Aybike Çetin are gratefully acknowledged.

# TABLE OF CONTENTS

# LIST OF TABLES

# LIST OF FIGURES

# LIST OF ABBREVIATIONS

| | | |
|---|---|---|
| A/D | - | Analog/Digital |
| AHRS | - | Attitude and Heading Reference System |
| D/A | - | Digital/Analog |
| DAQ | - | Data Acquisition |
| DC | - | Direct Current |
| DSP | - | Digital Signal Processing |
| ESC | - | Electronic Speed Controller |
| FBD | - | Free Body Diagram |
| FPGA | - | Field Programmable Gate Arrays |
| I/O | - | Input / Output |
| IEEE | - | The Institute of Electrical and Electronics Engineers |
| IMU | - | Inertial Measurement Unit |
| LQR | - | Linear Quadratic Regulator |
| MEMS | - | Micro Electro Mechanical Systems |
| PC | - | Personal Computer |
| PIC | - | Programmable Interface Controller |
| PID | - | Proportional Integral Derivative |
| PT | - | Personal Transporter |
| PWM | - | Pulse Width Modulation |
| RTWT | - | Real Time Windows Target |

| | | |
|---|---|---|
| TWTR | - | Two Wheeled Twin Rotor Hybrid Robotic Platform |
| UAV | - | Unmanned Aerial/Air Vehicle |
| UGV | - | Unmanned Ground Vehicle |
| USB | - | Universal Serial Bus |
| VTOL | - | Vertical Take-off and Landing |

# NOMENCLATURE

The following are the list of variables used in this thesis:

$\phi$ -Angular position of body (radian)

$\dot{\phi}$ -Angular velocity of body (radian/s)

$\ddot{\phi}$ -Angular acceleration of body (radian/$s^2$)

x -Linear displacement of body in x direction (m)

$\dot{x}$ –Linear velocity of body in x direction (m/s)

$\ddot{x}$ -Linear acceleration of body in x direction ($m/s^2$)

$\theta_w$ -Angular position of wheel (radian)

$\dot{\theta}_w$-Angular velocity of wheel (radian/s)

$\ddot{\theta}_w$-Angular acceleration of wheel (radian/$s^2$)

$\theta_m$ -Angular position of motor shaft (radian)

$\dot{\theta}_m$ -Angular velocity of motor shaft (radian/s)

$\ddot{\theta}_m$ -Angular acceleration of motor shaft (radian/$s^2$)

y -Linear displacement of body in y direction (m)

$\dot{y}$ -Linear velocity of body in y direction (m/s)

$\ddot{y}$ -Linear acceleration of body in y direction ($m/s^2$)

$\alpha$ -Angular acceleration (radian/$s^2$)

$I_w$ -Mass moment of inertia of wheel ($kgm^2$)

$I_b$ -Mass moment of inertia of body ($kgm^2$)

T -Torque applied by wheels (Nm)

$b_f$ -Friction coefficient

a –Acceleration ($m/s^2$)

m –Mass (kg)

$M_w$ -Mass of wheel (kg)

$M_b$ -Mass of body (kg)

$F_x$ -Force in x direction (N)

$F_y$ -Force in y direction (N)

g –Gravitational acceleration (m /$s^2$)

N -Normal Force (N)

M –Moment (Nm)

L -Length of body to the center of mass (m)

R -Terminal resistance of DC motor (Ohm)

l -Inductance of DC motor (Henry)

V -Voltage applied (Volt)

$V_e$ -Terminal Voltage (Volt)

$T_m$ -Torque produced by DC Motor (Nm)

i -Current passing terminal of DC motor (Amper)

$K_t$ -Torque Constant

$K_e$ -Back EMF constant

n -Gear Ratio

$C_g$ -Center of gravity (m)

$I_{cm}$ -Mass moment of inertia around center of mass (kg$m^2$)

$I$ - Inertia Matrix

$I_{xx,xy,xz,zx,zy,zz,yx,yy,yz}$ - Inertia Matrix Elemelements (kg$m^2$)

d – Drag factor

b – Thrust factor

R – Rotation Matrix

p , q, r – Angular velocity components expressed in body reference frame (rad/s)

$\dot{p}, \dot{q}, \dot{r}$ - Angular acceleration components expressed in body reference frame (rad/$s^2$)

$\theta$, $\phi$, $\psi$ – Euler anglers (rad)

$\dot{\theta}, \dot{\phi}, \dot{\psi}$ – Euler angular rates (rad/s)

$\omega$ – Angular velocity matrix

$\omega_{x,y,z}$ - Angular velocity matrix components (rad/s)

Ω - Angular velocity of propellers (rad/s)

$\tau_f$ - Frictional torque (Nm)

$F_t$ - Frictional force (N)

$V_{app}$ - Applied voltage (V)

A, B, C, D – State space representation matrices

$x_{1,2,3,4,5\ldots}$ - States

$F_{z,1,2}$ - Thrust force (N)

$M_{1,2}$ - Drag force (N)

$T_g$ - Torque generated by the flywheel (Nm)

$M_p$ – Total mass (kg)

$\beta$ - Pendulum angle (rad)

$V_{1,2}$ – Applied voltage to brushless motors (V)

# CHAPTER 1

# INTRODUCTION

In recent years, there are increasing amount of investigations on two wheeled balance robots. The system has inherently unstable dynamics and several types of controllers can be applied on the platform. The system has many advantages for usage in various applications. Similar systems are used as personal transportation vehicles and improved wheeled chairs. In the same way, flying systems are one of the important fields in academic and military type of researches. The topic has also an importance for civil applications. Stabilization of the flying robots is the first task of a development of an Unmanned Aerial Vehicle (UAV) or a flying robot. UAV's are mainly used for military applications, search and rescue operations, hobbies, forecasting and broadcasting operations.

Another important research topic that gained importance in recent years is hybrid systems. Especially in robotics combining different systems with different locomotion systems may reveal an optimal solution for certain types of applications. Wheeled and legged mechanisms are the most researched and implemented locomotion systems for hybrid robots, but some other hybrid systems are also investigated and implemented. For example, flying and wheeled hybrid systems gained importance especially in military applications. The idea of combining the motion capabilities of two wheeled balance system and twin robot flying system is the starting point of this study and the hybrid robot concept covered in this study combines a twin rotor flying system and two wheeled self-balancing pendulum robot. The overall hybrid system is a unique system and the illustration of the system is shown in the Figure 1. The TWTR (Two Wheeled Twin Rotor Hybrid Robotic

Platform) system is capable of moving on the ground and flying in the air. The system is a Vertical Take-off and Landing (VTOL) platform, inherently unstable for both modes of motion. This requires to design stabilizing control systems at first. The schematic representation of the designed system is given in Figure 1.

In order to stabilize the system and track a reference position on ground, optimal control solutions are utilized basically. The Linear Quadratic Regulator (LQR) is a well-known design technique that provides practical feedback gains. As it is named, LQR is a regulatory controller which forces the states of the system to the zero position. In addition to the regulation, tracking a reference position is expected on ground motion. Error space approach is a LQR based controller, the main difference of error space approach is adding extra states to the system; these extra states are the difference between reference and output. When the regulatory control system leads the states to zero, output of the systems becomes equal with the reference; this means the system tracks reference with a regulatory controller. These types of controllers are used in this study in addition to the PID (Proportional Integral Derivative) controllers.

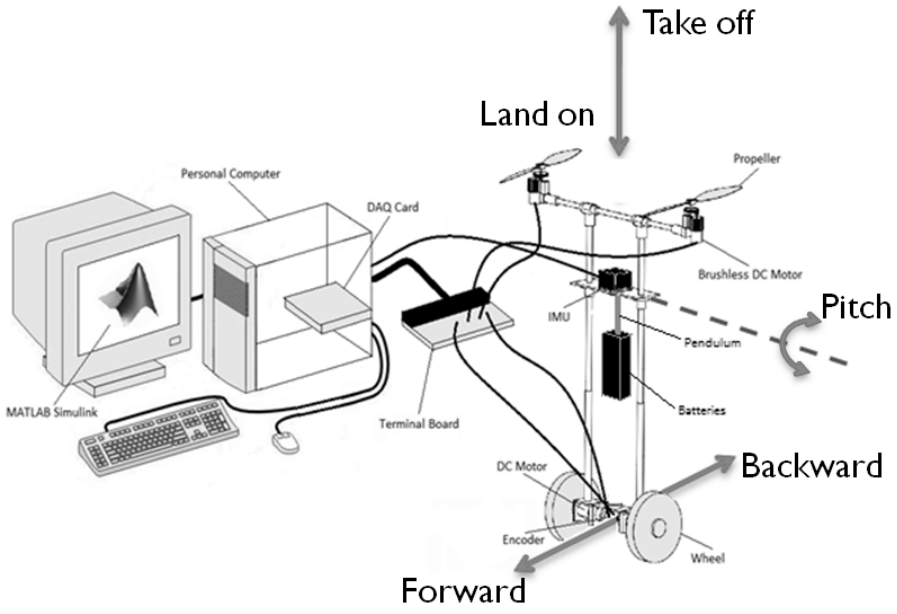


*Figure 1 Twin Rotor Two Wheeled Hybrid System*

Considering the physical system, it is easy to see the need to use a sensor set to sense the quantities that describe the dynamics of the system. Basic element in this set is the inertial measurement unit (IMU). An IMU detects motion using a combination of accelerometers and gyroscopes. An accelerometer gives a noisy output when it is used to determine the tilt angle and the orientation from the integral of a gyroscope measurement has a drift. This drift may be due to the operating temperature or inherent characteristics of the gyroscope itself. To overcome these problems, a signal-level sensor fusion technique using estimators such as Kalman filter or complementary filter which thrusts the measurements of accelerometer in low frequencies and measurements of gyroscopes in high frequencies. With the aid of the filters, the gyroscope drift and accelerometer noise is eliminated. In flying and balancing robotics operations these types IMU's should be used, but the heading angle of these systems needs magnetometer to be measured, the magnetometer implemented systems are named as Attitude and Heading Reference System (AHRS).

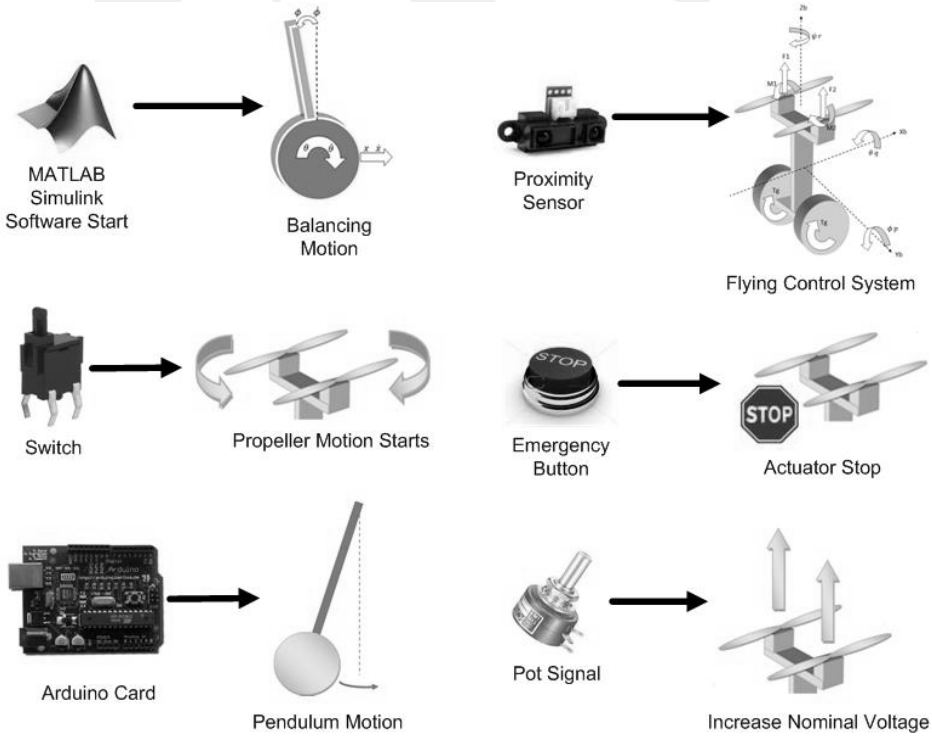


*Figure 2 Theory of Operation*

In the TWTR system, it is desired to have a moving robot which has the switching conditions that are shown in Figure 2, that can avoid obstacles by flying, or that can use its flying ability to record visual data from environment, but the frame of this work is mainly to stabilize the TWTR system on ground and to stabilize the attitude dynamics in flying mode. The system is designed and physically constructed based on the mechatronics design principles. Selection of actuators, sensor set, and the control hardware and the physical structure design are all considered simultaneously with the mathematical model and controller design phases. Based on the design procedure, an IMU, an encoder to detect the translational position and velocity of the hybrid system on ground and a proximity sensor to detect the distance of the platform to the ground build the required sensor set. Sensorial data are processed within LQR, PID, error space approach type control systems. Different control systems are required for each mode of motion. Switching between these control systems are achieved depending on the information coming from the proximity sensor.

### 1.1. Aim and Scope

Aims of this thesis are stated below. Prior to list them, it is important to express the ultimate aim of the project of which the thesis is the initial part. The major aim is to design and produce a hybrid robotic system that can navigate on ground and hover whenever necessary. After hovering, the system will navigate in air. Additional sensors will be placed on the system for further navigation purposes and defined tasks. Aims and scope of this thesis are stated as below.

- *Designing and producing the hybrid robotic platform that can move on ground with two wheels and that can hover vertically with two propellers:* The system is designed based on the mechatronic design principles. Mechanical structure, sensor set, actuators, electronic components, control hardware and control algorithm are all designed and selected simultaneously with the mathematical models and simulations. The system should be able to stabilize itself on ground by using the dc motors coupled to wheels. In addition, the attitude of the platform should be stabilized by using the propellers and wheels with dc motors. Propellers give the ability to achieve

hovering, control roll and yaw dynamics. Whereas wheels with DC motors are utilized to actuate the pitch dynamics in the air. The control system is implemented via a desktop PC. Embedded control is not required in this thesis. Designed control systems are implemented in such a rapid prototyping based system architecture. In the further parts of the study, embedded control is compulsory.

- *Constructing the mathematical models of the hybrid system and designing basic control systems:* Nonlinear and linear mathematical models are required for both of the motion modes. Translational and pitch dynamics of the robot on ground are required to be modeled in the scope of the thesis. Roll, pitch and yaw dynamics are required to be modeled for the motion in the air. State-space models are constructed. Controller designs are performed employing the linearized mathematical models. Designed controllers for the ground motion are aimed to stabilize the hybrid system on two wheels and track a reference translational position. Designed controllers for the motion in the air include regulation of the attitude dynamics together with heading. Simple altitude control is also implemented to track a reference altitude by using the information from the proximity sensor. PID, LQR and error space type basic control structures are designed and implemented. Real-time implementations are performed by a desktop PC, data acquisition board, MatLab Simulink, and the Real-time Windows Target blockset. More complex control algorithms will be employed in the further stages and aims of the study.

# CHAPTER 2

# LITERATURE SURVEY

Hybrid robotic movement strategies have been recently used in robotic design and applications. Hybrid robot concept provides the systems the flexibility of different movement capabilities, which makes the system more suitable for different purposes in robotics applications. The most investigated hybrid movement strategy is to combine wheeled and legged motions on a hybrid design [1], [2], [3]. Paw and Hylos can be stated as examples of hybrid legged and wheeled robots which are shown in Figure 3 below;

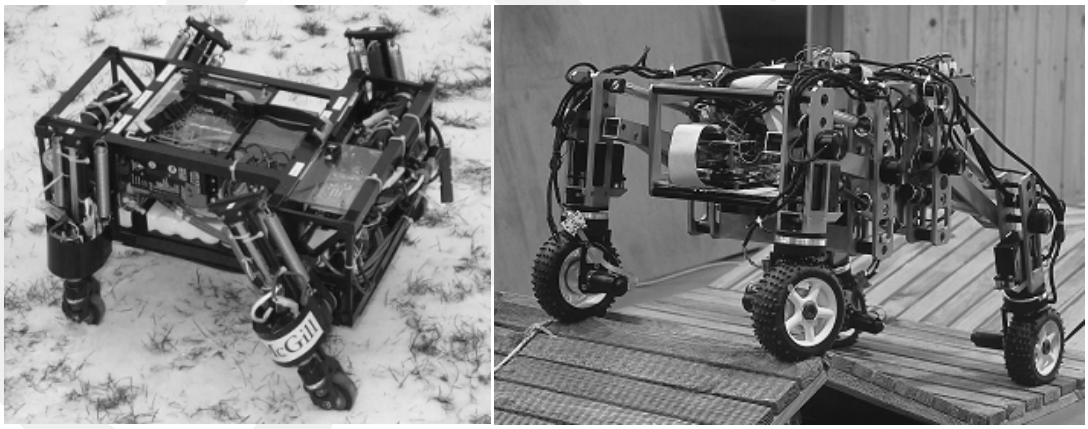

*Figure 3 Wheeled Legged Hybrid Robots Paw and Hylos [1], [2]*

During the increasing amount of hybrid movement systems in robotics applications, the hybrid air-land vechiles topic is also gained importance. Some of these hybrid air-land vechiles are designed for military reasons and some of them are for civil

applitaions line research and rescue operations. Griffon which is stated as a hybrid Unmanned Ground Vechile (UGV) / Unmanned Air Vechile (UAV). The system combines an iRobot Packbot structure and a steerable parafoil structure [4]. There are also flying and crawling hybrid systems on the literature [5]. These hybrid air-land vehicles are shown in Figure 4;

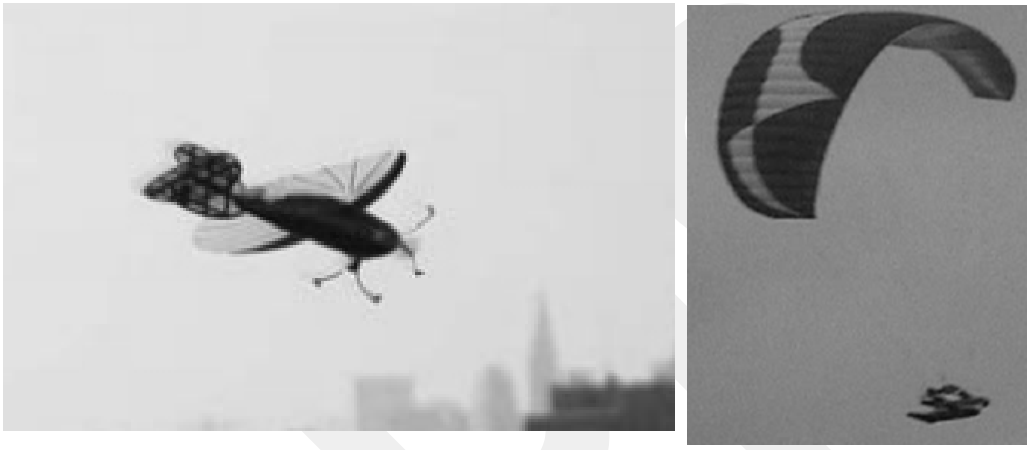

*Figure 4 Air-Land Hybrid Vehicles [5][4]*

Two wheeled balance robot system became a popular research system in recent years. The system is an inherently unstable system and easy to implement several types of controllers on it. That's why there are large amount of literature mentions two wheeled balance robot systems.

There was some research before, but two wheeled balance robot concept is started with the announcement of the arrival of the first self balancing, zero emissions personal transportation vehicle; The Segway Personal Transporter (Segway PT) by Dean Kamen. This was a commercial product. The 'SEGWAY PT' which can be seen in Figure 5 is able to balance a human standing on its platform while the user traverses the terrain with it. This innovation uses five gyroscopes and a collection of other tilt sensors to keep itself upright. Only three gyroscopes are needed for the whole system, the additional sensors are included as a safety precaution.

*Figure 5 Segway PT*

The two wheeled balance system is used for several applications in literature. Manipulator design for two wheeled balance system in order to carry or hold objects in robotics applications is one of the research areas [6]. The two wheeled balance system is also used in wheelchair systems for some applications [7]. The system has several usage areas up to take role as a moving platform for a music reading and singing robot [8]. This music reading and singing two wheeled balance robot is shown in Figure 6.

In order to use the two wheeled balance system as a robot or transporter, the system should be stabilized because the system is inherently unstable. In order to design this controller, the mathematical model of the structure should be derived. The derived equations of motions are nonlinear, so these equations should be linearised in order to implement linear control systems. In some researches nonlinear mathematical model is used in the controller design [9], [10]. In some researches, feedback linearization is applied to the system [11]. The states of the linear form of mathematical model are generally pendulum angular position, pendulum angular velocity, robots linear position and robots linear velocity [12], [13], [14]. But in some researches the robots turning angular position and robots turning angular velocity are stated as states in mathematical model [15], [16]. In addition, there are researches

which use four states in stabilization of the platform and use other two states for navigation of the system with decoupling control structures [17], [18].

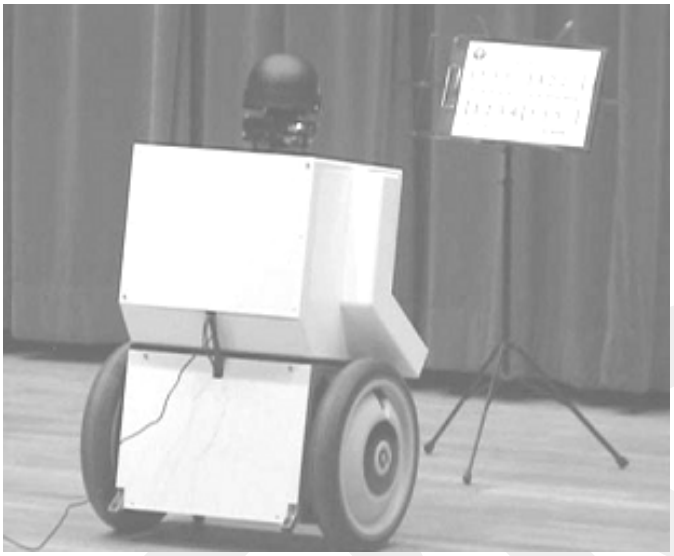

*Figure 6 Music Reading and Singing Two Wheeled Balance Robot on Stage* [8]

As the designed and implemented controller, most of the researches use LQ or LQR for the stabilization of the two wheeled balance robot system [13], [15], [16], [19]. As the optimal controller, instead of LQR type of controllers, pole placement technique is another popular control system for the stabilization of the system [17], [18]. PID control technique is designed and implemented in some researches also [14]. After the stabilization of the two wheeled balance robot system, the trajectory control is applied with a PID controller in general but some other control systems are designed and implemented for the trajectory control [17], [18], [19]. However, trajectory control of the two wheeled balancing system is not applied in some works. As robust controller, sliding mode based techniques are used to design the robust controllers on two wheeled balancing systems [16]. Fuzzy Logic Controllers are also implemented on the system also [10].

In some works, two wheeled balancing system is designed as a transportation vehicle [14], [20]. The system is controlled by the torque disturbance of the driver [14]. Segway PT can be stated as one of the examples for this type of systems, but in some

works; the trajectory is fully controlled by a steering computer. The motion of the passenger is a disturbance that should be rejected in these types of systems [20]. B2 PT which is shown in Figure 7, can be stated as an example of these types of designs.

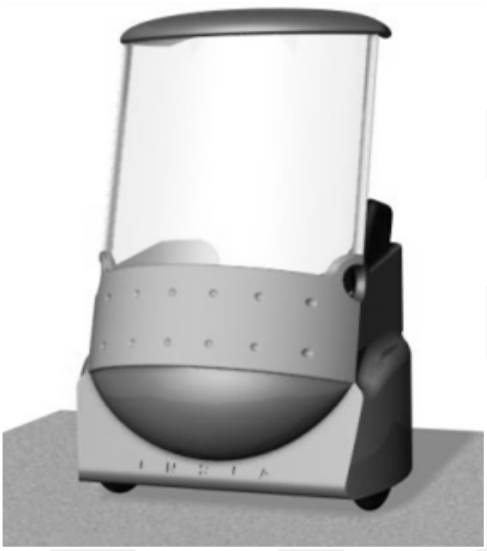

*Figure 7 B2 Two Wheeled Balancing Vehicle [20]*

As the sensor system, in nearly all of the works, encoders are used to measure the linear displacement of the two wheeled balance system; numerical integration of the linear displacement is used in order to measure the linear velocity of the system [13], [15], [17], [18], [19], [21]. Encoders are also used in order to measure the two wheeled systems turning angular position and turning angular velocity, these measurements are used when applying turning angular position and turning angular velocity as the states of the mathematical model [15], [17], [18].

The critical point in two wheeled balance systems sensor unit is measuring the tilt angular position and tilt angular velocity. For measuring the tilt angle, 2 axis accelerometers are used in order to sense the gravitational acceleration and a trigonometric function of these 2 axis measurement gives the tilt angular position, the tilt angular velocity is measured by the derivative of the angular position [18]. Another approach is using a gyroscope sensor in order to measure the tilt angular

velocity and the tilt angular position is measured by the numerical integration of the tilt angular velocity [7], [15], [18], [21]. Tilt angular position is also measured by mounting two proximity sensors on the front and back parts of the body; the angular position is calculated from the subtraction of distances of the front part and back parts of the body [12].

The angular position and angular velocity on tilt axis are measured separately also, this means angular position is measured by an accelerometer, inclinometer or proximity sensor and angular velocity is measured by a gyroscope [12], [19]. Numerical integration of gyroscope has a bias because of the change in the temperature of the sensor, calibration problems and the measurement of the accelerometer for tilt angular position is too noisy. In some works, the change in the temperature of the gyroscope is measured in order to dismiss this bias [10]. Because of these reasons sensor fusion techniques are used in some works [10], [13]. This sensor fusion technique combines the measurement of two sensors and gives a better angle output. As it is mentioned before, the integration of gyroscope output has a bias, and the angle output of accelerometer is noisy, a complementary filter combines these two sensor output. Filter rely the integration of gyroscope output in high frequencies and angle output of accelerometer in low frequencies [10]. Kalman filter and Extended Kalman filter are other used sensor fusion methods in two wheeled balancing action [13].

In sensing system, as accelerometers, analog devices accelerometers ADXL 330 and ADXL 202 are used generally [13], [14]. Instead of using accelerometers, SEIKA N3 digital inclinometer is used in the literature [13]. Another sensor used instead of accelerometers is Sharp GP2D120 proximity sensor [12]. As gyroscopes, piezzo electronics gyros are used generally [18], [21]. Micro-electromechanical technology gyroscopes are also used in works, Analog devices ADX300EB and ADXRS150 gyroscopes are generally used [10], [12]. HITEC GY-130 digital rate gyroscope is stated as another gyroscope used in literature [13]. Inertial measurement units combining some accelerometers and gyroscopes are also used in the literature [10], [17]. As Inertial measurement unit Microstrain FAS-G IMU is generally used [17].

In order to design the control system, nearly all of the literature used Matlab Simulink software [13], [17], [18], [19]. In implementing the designed control systems, two ways are followed in the literature. Implementing designed controllers using embedded controller systems is one of these ways [10], [13], [14], [17], [18], [19]. The second way is implementing control systems with using PC and data acquisition card [7], [12], [15].

As embedded control systems, PC 104 based computer Athena with Matlab software and xPC Target Tool of Matlab software are used [19]. The implementation of Athena PC 104 on two wheeled balance system is shown in Figure 8. Digital Signal Processing (DSP) boards are used in implementing embedded control systems also [17], [18]. Field Programmable Gate Arrays (FPGA) are another type of control unit which are used in order to implement the designed controller system in some researches [10] Microchip PIC series microcontrollers and other controllers used in basic robotic actions like Mark 4 Eyebot controller are used in balancing system also [13], [14]. In implementing the control systems with using PC and data acquisition card, Matlab with Real time windows target and C++ Programs are generally used [7], [12], [15].

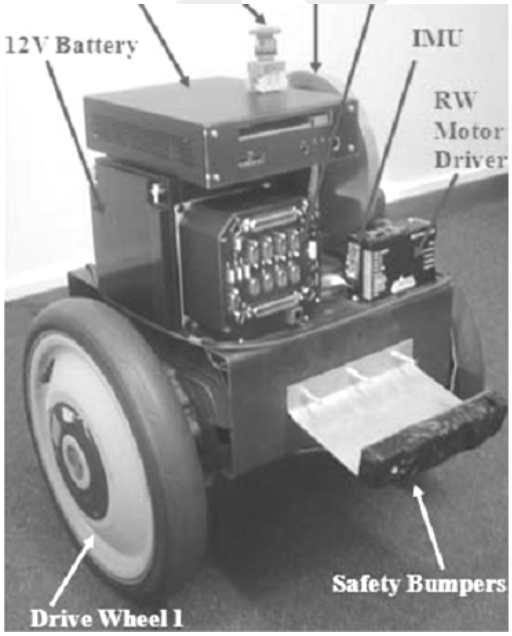


*Figure 8 Athena PC 104 System Placed on Two Wheeled Balance System [19]*

With the increasing interest on Unmanned Air Vechiles (UAV), Vertical Take-off and Landing (VTOL) flying systems are the most popular flying robotic topic in recent years. Because VTOL systems are highly maneuverable and extremely stable and these types of the systems are more suitable for robotic applications because the system can hover on a desired point in the air.

VTOL property is gained by the motor and the propeller pair added to the system. In the litetature most studied VTOL UAV structure is the quadrotor structure which has four motor propeller pair mounted vertically. Some of the quadrotor structures used in experimental works in the literature are shown in Figure 9 [22], [23], [24], [25], [26], [27], [28], [29], [30].

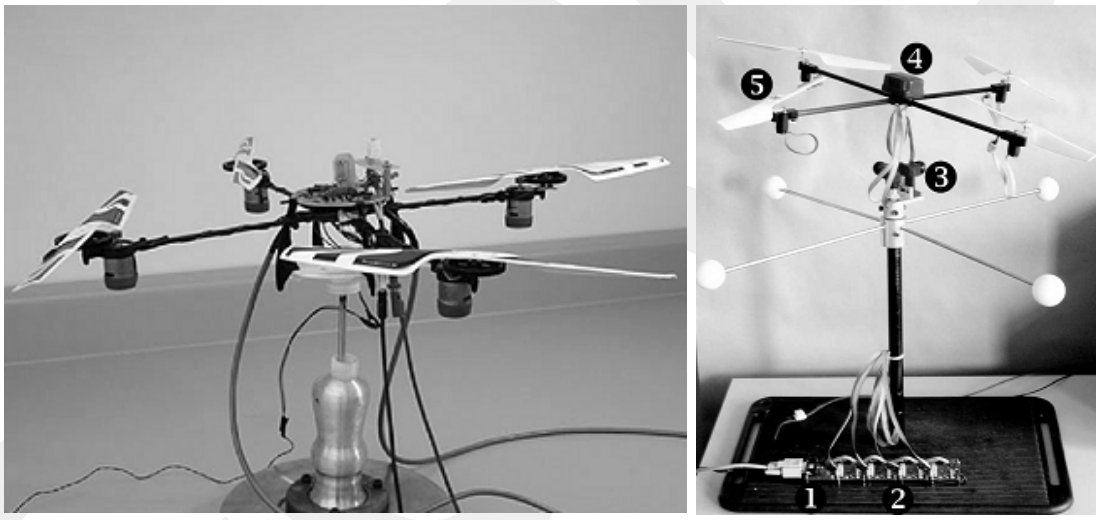


*Figure 9 Some Quadrotor Structures [22], [25]*

Except for quadrotor flying robots, trirotor flying robots are also studied in the literature. The reduction in the number of rotors from four to three allows to obtain more compact vehicles for rapid deployment, as well as longer flight autonomy. Reducing the amount of the rotors also has a gaining on energy consumption topic. These trirotor structures are shown in Figure 10 [31], [32], [33].

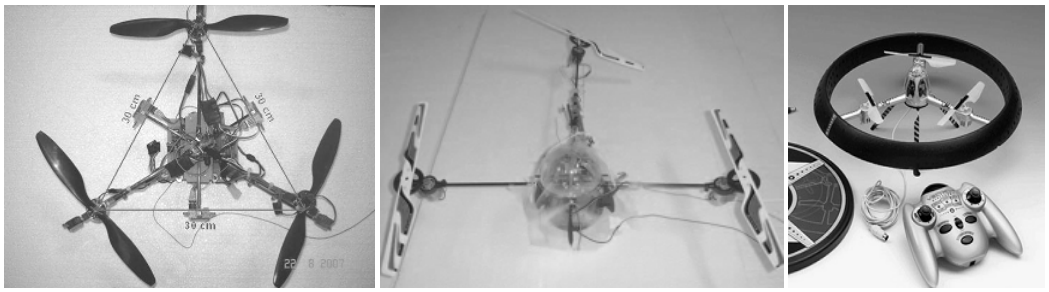

*Figure* 10 *Trirotor Structures [31], [32],[33]*

Twinrotor structures can be stated as another topic studied in the literature. These twin rotor systems have generally two rotors like the the classical helicopter [34], [35], [36]. In addition, there are twinrotor structures which has two rotors placed laterally and the direction of the thrust can be redirected by tilting the propellers laterally and longitudinally [37]. Twinrotor structures used in some experimental works in the literature are shown in Figure 11.

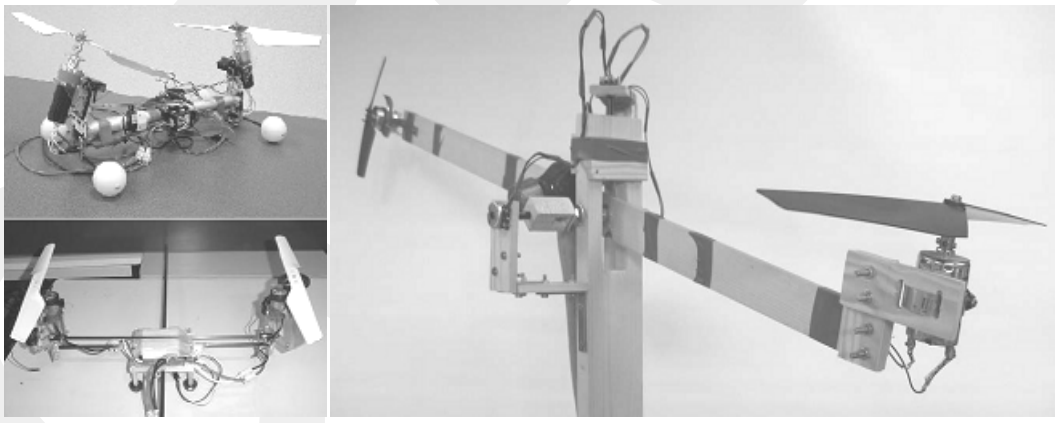

*Figure 11 Twinrotor Structures [36],[37]*

In the flying robotics researches, there are several approaches on modelling the flying system mathematically. In generally, yaw, pitch and roll dynamics and the actuator equations of the flying system are included in the mathematical model [22], [24], [26], [31]. In some works, only yaw and pitch dynamics and actuator equations are included in the mathematical model [36]. Another approach is to add altitude

dynamics to the yaw, pitch and roll dynamics and the actuator equations [23], [29], [32]. More complex models are created by including x, y and z position dynamics to the yaw, pitch and roll dynamics and the actuator equations [25], [30].

The derived mathematical models are linearised in order to implement linear control systems [22], [24], [26], [28], [34], [36]. But in some of the works nonlinear control systems are applied to the flying systems, these type of systems does not require the linearization of the mathematical model [25], [30]. The nonlinear control systems which are mostly designed and applied to the flying system can be stated as backstepping techniques [25], [25] , sliding mode techniques [25] and Hinfinity controllers [30].

There are several ways to implement control systems to the linear systems. The basic way can be stated as implementing PID, PI or PD type controllers on each axis [24], [28], [29], [36]. $PD^2$ feedback structure is also applied to the systems in order to stabilization control of each axis [38].

In the stabilization of the flying robots, optimal controllers like LQ, LQR and Pole Placement Controllers are implemented on the systems also[24], [26], [34] In some systems, LQR based regulatory controllers are used in path tracking applications. To use the LQR design for path tracking control, the regulator problem must be recast as a tracking problem. In a tracking problem, the output y is compared to a reference signal r. The goal is to drive the error between the reference and the output to zero [34]. Error space approach based control systems which have a difference of having integral of the error term as a state is applied on several systems in path tracking systems. Other control systems are used in the path tracking also. Backstepping type controllers are the most preferred controllers in path tracking applications in the literature [25], [30], [37]. PI and PID type control systems are also used in the altitude control of flying systems [29].

In the sensing system of the flying structures, the critical point is to measure the pitch, roll and yaw angles and angular rates, in the test setups which have connections to the ground or fixed parts potentiometers are used to measure angles for the stabilization control of the flying robots. [28], [36]. But, these type of systems

cannot be used in flying applications because there are no fixed frame in the air. The most preferred way is to use gyroscopes and accelerometer in order to measure pitch, roll and yaw angle and angular velocities, magnetometers and inclonometers are also used in these measurement systems [22], [26], [27], [28], [39]. In some works in the literature, accelerometers or inclonometers are used to measure the angles and gyroscopes are used in order to angular velocities [26], [27], [28]. Although the average value of the sensor readings, especially the angle measurement should not be accurate. Because of this reason sensor fusion techniques like complementary filters and kalman filters combining the accelerometer reading and gyroscope reading are used in order to measure accurate angle and angular rate measurement [38, 39]. Inertial Measurement Units (IMU) which operates sensor fusion techniques inside, are used in the flying robotics applications also [23], [24], [25]. As the accelerometer, Analog Devices accelerometer ADXL203, ADXL202 and ADXL210 are the most preffered sensor in the litelature, again Analog Devices gyroscope ADXRS150 is used as gyroscope sensor [26], [27], [28]. The Xsens MT9-B Inertial Measurement Unit is used as the IMU sensor in the literature also [23], [24], [25]. Magnetic sensors, encoders and hall effect sensors are used to measure the rotational velocity of the propellers also [22].

In implementing the designed control systems on the real system, personnel computers and PC104 type computers equipped with data acquisiton systems or RS 232 type serial communication ports are used as the control hardware frequently in the literature [23], [24], [25], [26], [32], [36]. Dspace controller boards, Microchip PIC controller boards and Gumstix boards are also used as the controller hardware in flying robotics applications [22], [28], [29]. As the control software, Matlab and Real Time Windows Target are the most preferred platform to implement the designed control systems on the real platforms [22], [26]. Matlab and XPC Target are a preferred platform in embedded applications [32]. Labwiev software is preffered instead of Matlab software in some of the literature [36]. Coding with C Language is another method, this method can be used in PC based systems and embedded systems also [24], [28].

# CHAPTER 3

# MATHEMATICAL MODELLING

The mathematical model of TWTR system is derived for two different motion modes, namely on ground and in the air modes. In mathematical model for ground mode, translational and pitch dynamics are modeled. This is due to the fact that forward, backward, and the tilt motions of the robot are examined in this study. In the flying mode, yaw, roll, and the pitch dynamics are modeled, i.e. attitude and heading dynamics are modeled.

## 3.1. Mathematical Model for Ground Movement

The dynamics of the system is described by a mathematical model in order to develop an efficient control system to stabilize the dynamics. Positive directions of linear and rotational motions of the platform and wheels are shown in Figure 12. Following assumptions are made in deriving the mathematical model of the ground motion.

- System has a rigid structure.

- No slip occurs between ground and wheels.

- Two DC motor have identical characteristics and gives the same output for the same input.

- The inductance of DC motors is assumed as zero.

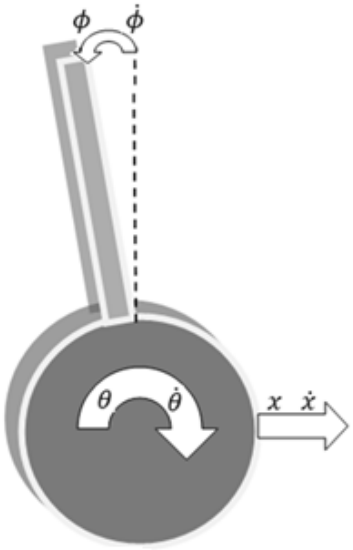


*Figure 12 Positive Directions of Motion Variables for Ground Motion*

Wheel dynamics is modeled to couple the translational dynamics of the hybrid robot in x direction and applied torque by dc motors. The freebody diagram of a wheel is shown in Figure 13.

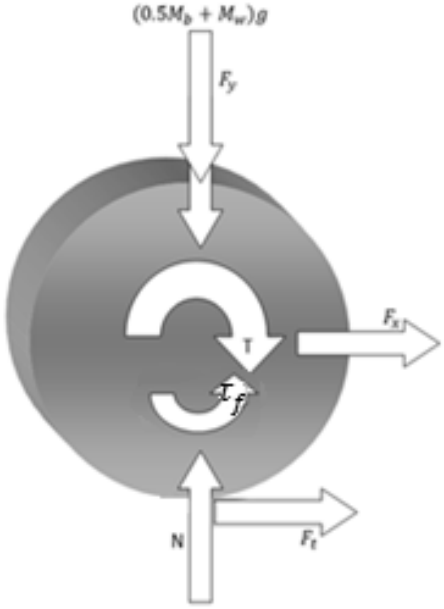


*Figure 13 FBD of Wheel*

Using the Newton's Laws, equations of motion can be derived for the wheel dynamics.

$$\sum M = I\alpha \tag{3.1}$$

$$I_w \ddot{\theta}_w = T - rF_t - \tau_f \tag{3.2}$$

The frictional torque is defined as;

$$\tau_f = b(\dot{\theta}_w - \dot{\phi}) \tag{3.3}$$

If equation 3.3 is writen in equation 3.2;

$$I_w \ddot{\theta}_w = T - rF_t - b(\dot{\theta}_w - \dot{\phi}) \tag{3.4}$$

Equation of motion in x direction can be derived as below.

$$\sum F_x = ma \tag{3.5}$$

$$M_w \ddot{x} = F_x - F_t \tag{3.6}$$

Sum of the forces in vertical (y) direction gives;

$$\sum F_y = ma \tag{3.7}$$

$$N = (0.5M_b + M_w)g + F_y \tag{3.8}$$

Freebody diagram of the robot body is shown in Figure 14. Dynamic equations of the robot body are derived using the following equations considering the resultant moment about the center of gravity and resultant forces in x and y directions.

$$\sum M = I\alpha \tag{3.9}$$

$$I_b \ddot{\phi} = T - rF_t L\cos\phi + 2F_y L\sin\phi + 2b(\dot{\theta}_w - \dot{\phi}) \tag{3.10}$$

$$\sum F_x = ma \tag{3.11}$$

$$M_b \ddot{x}_b = 2F_x \tag{3.12}$$

$$\sum F_y = ma \tag{3.13}$$

$$M_b \ddot{y}_b = 2F_y - M_b g \tag{3.14}$$

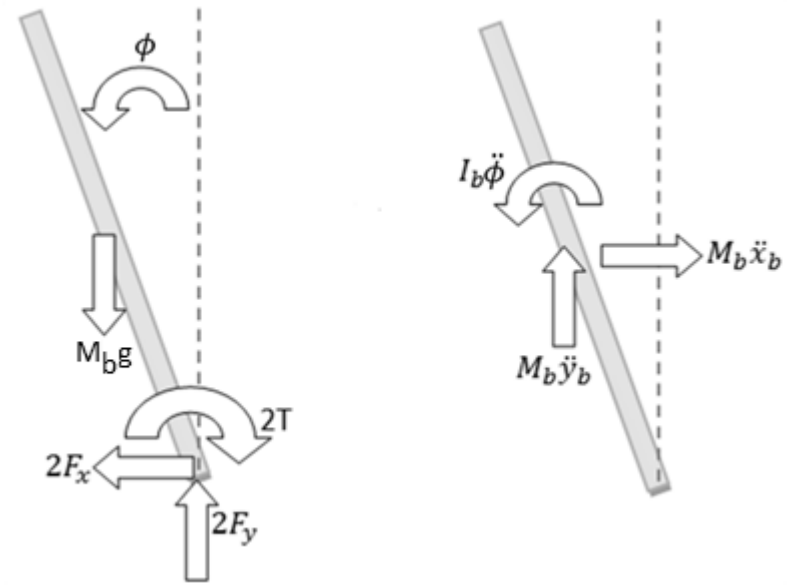


*Figure 14 Free Body Diagram (FBD) of the Robot Body*

In order to relate the wheel dynamics and body dynamics following kinematic equations are employed.

$$x_b = x - L\sin\phi \tag{3.15}$$

$$\dot{x}_b = \dot{x} - \dot{\phi}L\cos\phi \tag{3.16}$$

$$\ddot{x}_b = \ddot{x} - \ddot{\phi}L\cos\phi + \dot{\phi}^2 L\sin\phi \tag{3.17}$$

$$y_b = L\cos\phi \tag{3.18}$$

$$\dot{y}_b = -\dot{\phi} L \sin\phi \tag{3.19}$$

$$\ddot{y}_b = -\ddot{\phi} L \sin\phi - \dot{\phi}^2 L \cos\phi \tag{3.20}$$

Assuming no slip in the wheel-ground contact, following equations can be utilized to relate the translational motion with the rotational dynamics of the wheels.

$$x = r\theta_w \tag{3.21}$$

$$\dot{x} = r\dot{\theta}_w \tag{3.22}$$

$$\ddot{x} = r\ddot{\theta}_w \tag{3.23}$$

Using the above equations dynamic equations in x and pitch directions are obtained as follows.

$$I_w \ddot{\theta}_w + r[(-0.5M_b(\ddot{x} - \ddot{\phi} L \cos\phi + \dot{\phi}^2 L \sin\phi) - M_w \ddot{x})] + b\left(\dot{\theta}_w - \dot{\phi}\right) = T \tag{3.24}$$

$$\begin{aligned} &I_b \ddot{\phi} + r[(-0.5M_b(\ddot{x} - \ddot{\phi} L \cos\phi + \dot{\phi}^2 L \sin\phi) - M_w \ddot{x})] L \cos\phi - \\ &M_b(-\ddot{\phi} L \sin\phi - \dot{\phi}^2 L \cos\phi + g) L \sin\phi - 2b\left(\dot{\theta}_w - \dot{\phi}\right) = -2T \end{aligned} \tag{3.25}$$

In Equations 3.24 and 3.25, T is the torque input provided by the DC motors to the wheels. Torque input can be stated using the DC motor model with gearbox. Figure 15 shows the assumed DC motor model in detail.

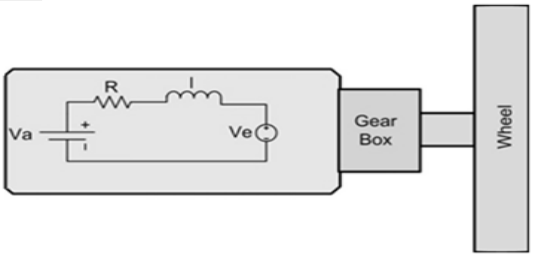


*Figure 15 DC Motor Model*

The torque which is produced by motor is related with the current produced by the motor armature. This relation is;

$$T_m = K_t i \tag{3.26}$$

The electrical circuit is modeled as a resistor and inductor circuit. The produced voltage by the coils of motor is related with the shaft velocity and this relation is;

$$V_e = K_e \dot{\theta}_m \tag{3.27}$$

According to the Kirchoff's Voltage Law, The electrical circuit is stated as;

$$V - Ri - l\frac{di}{dt} - Ve = 0 \tag{3.28}$$

Inductance of the motor is assumed zero. Therefore Equation 3.28 can be used to express the current in terms of an algebraic equation, Equation. 3.29.

$$i = \frac{V}{R} - \frac{K_e}{R}\dot{\theta}_m \tag{3.29}$$

Rotation of the motor shaft can be related to the rotation of the wheel considering the gearbox reduction ratio, n, and body tilt, ϕ.

$$\theta_m = n\theta_w - \phi \tag{3.30}$$

$$\dot{\theta}_m = n\dot{\theta}_w - \dot{\phi} \tag{3.31}$$

Put equation 3.31 into equation 3.29 in order to get the current produced by the motor armature;

$$i = \frac{V}{R} - \frac{K_e}{R}(n\dot{\theta}_w - \dot{\phi}) \tag{3.32}$$

Torque produced by the motor, T, and torque applied to the wheel, $T_m$, are expressed as below.

$$T_m = \frac{K_t V}{R} - \frac{K_t K_e}{R}(n\dot{\theta}_w - \dot{\phi}) \tag{3.33}$$

$$T = nT_m \tag{3.34}$$

$$T = \frac{nK_t V}{R} - \frac{nK_t K_e}{R}(n\dot{\theta}_w - \dot{\phi}) \tag{3.35}$$

Considering the equations of motions together with the torque equations, following equations are reached as equations that define the dynamics of hybrid robot on ground.

$$\ddot{\phi} = \dot{\phi}\left(\frac{-2(K_t K_e + bR)}{\alpha R}\right) + \ddot{x}\left(\frac{2M_b L\cos\phi}{\alpha}\right) + \dot{x}\left(\frac{2(n^2 K_t K_e + bR)}{\alpha R r}\right) - V\left(\frac{2nK_t}{\alpha R}\right) - \beta\sin\phi \tag{3.36}$$

$$\alpha = I_b + 2M_b L^2$$
$$\beta = 2M_b g L \tag{3.37}$$

$$\ddot{x} = \ddot{\phi}\left(\frac{-0.5M_b r^2 L\cos\phi}{\gamma}\right) + \dot{\phi}^2\left(\frac{0.5M_b r^2 L\sin\phi}{\gamma}\right) + \dot{\phi}\left(\frac{nK_t K_e r + bRr}{\gamma R}\right) + \dot{x}\left(\frac{-n^2 K_t K_e r - bRr}{\gamma R r}\right) + V\left(\frac{nK_t r}{\gamma}\right) \tag{3.38}$$

$$\gamma = (-0.5M_b - M_w)r - I_w \tag{3.39}$$

### 3.1.1. Linearisation of Nonlinear State Equations for Ground Movement

Equations of motion derived above are used to derive the nonlinear state equations as the mathematical model of the system on ground mode. Followings are the state variables that define the dynamics of the system.

$$
\begin{aligned}
x_1 &= \dot{x} \\
x_2 &= \ddot{x} \\
x_3 &= \dot{\phi} \\
x_4 &= \ddot{\phi}
\end{aligned}
\tag{3.40}
$$

Voltage input to the DC motors is the only input to the system on ground mode. Since the yaw control on ground is not concerned, same voltage input is applied to both of the motors. The linearized form of nonlinear state equations is given as below.

$$
\begin{aligned}
\dot{x} &= Ax + Bu \\
y &= Cx + Du
\end{aligned}
\tag{3.41}
$$

A, B, C, and the D matrices are found by using the Jacobian of the nonlinear state equations with respect to the states and the input term. The system is linearized around the origin of the state vector that is where the hybrid robot stands with zero pitch angle and velocity at the origin of the x axis with zero translational velocity. These linearisation operations are carried out in Matlab and the related m-file is given in Appendix A. The linearized model becomes;

$$
\begin{bmatrix} \dot{x} \\ \ddot{x} \\ \dot{\phi} \\ \ddot{\phi} \end{bmatrix} = \begin{bmatrix} 0 & 1 & 0 & 0 \\ 0 & A2{,}2 & A2{,}3 & A2{,}4 \\ 0 & 0 & 0 & 1 \\ 0 & A4{,}2 & A4{,}3 & A4{,}4 \end{bmatrix} \begin{bmatrix} x \\ \dot{x} \\ \phi \\ \dot{\phi} \end{bmatrix} + \begin{bmatrix} 0 \\ B2{,}1 \\ 0 \\ B4{,}1 \end{bmatrix} V \tag{3.42}
$$

where;

$$
A2{,}2 = \frac{2\begin{pmatrix} M_b L^2 R n^2 K_t K_e + I_w R I_b + I_b R^2 b + 2M_b L^2 R^2 b \\ + I_b R n^2 K_t K_e + 2M_b L^2 R I_w - M_b L r n^2 K_t K_e + M_b L r^2 n \end{pmatrix}}{\left((M_b I_b + 2M_b I_b + 4M_w M_b L^2) R r^2\right)}
$$

$$
A2{,}3 = 2\frac{{M_b}^2 L^2 g R}{M_b I_b + 2M_w I_b + 4M_w M_b L^2}
$$

$$
A2{,}4 = \frac{-2(M_b L^2 K_t K_e + 2M_b L^2 b R + I_b b R + I_b n K_t K_e + M_b L R n K_t K_e - M_b L r b R)}{\left(r R (M_b I_b + 2M_w I_b + 4M_w M_b L^2)\right)}
$$

$$A4,2 = \frac{2\begin{pmatrix} M_b r^2 n - 2M_w r n^2 K_t K_e + 2M_w r^2 n + 2M_b LRI_w \\ +2M_b LRn^2 K_t K_e + 2M_b LR^2 b - M_b r n^2 K_t K_e \end{pmatrix}}{\left(Rr^2(M_b I_b + 2M_w I_b + 4M_w M_b L^2)\right)}$$

$$A4,3 = 2\frac{M_b gLR(M_b + 2M_w)}{M_b I_b + 2M_b I_b + 4M_w M_b L^2} \tag{3.43}$$

$$A4,4 = \frac{-2(2M_b LnK_t K_e + 2M_b LbR + M_b RnK_t K_e - M_b rbR - 2M_w rbR + 2M_w RnK_t K_e)}{\left(rR(M_b I_b + 2M_w I_b + 4M_w M_b L^2)\right)}$$

and;

$$B2,1 = -2\frac{nK_t(M_b Lr + I_b + 2M_b L^2)}{\left(rR(M_b I_b + 2M_w I_b + 4M_w M_b L^2)\right)}$$

$$B4,1 = -2\frac{nK_t(2LM_b + M_b r + 2rM_w)}{\left(rR(M_b I_b + 2M_w I_b + 4M_w M_b L^2)\right)} \tag{3.44}$$

All states are measured by using the sensor set, namely the inertial measurement unit and the encoder. Therefore C matrix is a 4x4 identity matrix and D matrix is a 4x1 zero vector. Details of the employed sensor set and hardware are given in the following chapter.

### 3.2. Mathematical Modeling for Flying Motion

In order to derive the mathematical model of TWTR system in flying mode, following assumptions are made.

- System structure is supposed to be rigid.

- The inductance of DC motor is assumed to be too small and can be neglected.

- The two DC motors are assumed to have identical characteristics (DC motors attached to the wheels).

- The two DC motors are assumed to have same voltage input (DC motors attached to the wheels).

Attitude and heading dynamics are considered in this thesis. It is desired to stabilize the robot in the hovering condition in flying mode. Therefore, related dynamics are modeled in this part. Euler Angles are employed to model the orientation of the platform. Figure 16 shows the body and inertial reference frames and the directions of related quantities of the flying dynamics.

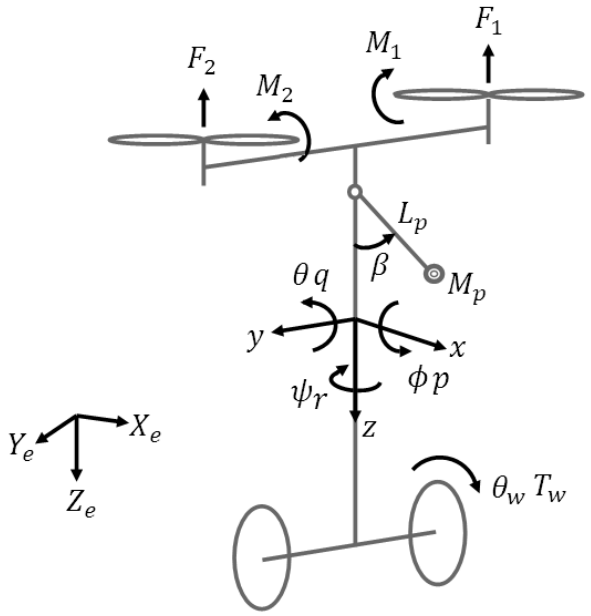


*Figure 16 FBD and States of the System*

The Euler's angles for TWTR system are defined in terms of (ψ, θ, ϕ), namely yaw, pitch, and the roll angles. At each rotation, following rotation matrices are employed.

$$\psi\ Rotation \qquad \begin{bmatrix} x_1 \\ y_1 \\ z_1 \end{bmatrix} = \begin{bmatrix} 1 & 0 & 0 \\ 0 & \cos\phi & -\sin\phi \\ 0 & \sin\phi & \cos\phi \end{bmatrix} \begin{bmatrix} x_b \\ y_b \\ z_b \end{bmatrix} \tag{3.45}$$

$$\theta\ Rotation \qquad \begin{bmatrix} x_2 \\ y_2 \\ z_2 \end{bmatrix} = \begin{bmatrix} \cos\theta & 0 & \sin\theta \\ 0 & 1 & 0 \\ -\sin\theta & 0 & \cos\theta \end{bmatrix} \begin{bmatrix} x_1 \\ y_1 \\ z_1 \end{bmatrix} \tag{3.46}$$

$$\phi\ Rotation \qquad \begin{bmatrix} x_E \\ y_E \\ z_E \end{bmatrix} = \begin{bmatrix} \cos\psi & -\sin\psi & 0 \\ \sin\psi & \cos\psi & 0 \\ 0 & 0 & 1 \end{bmatrix} \begin{bmatrix} x_2 \\ y_2 \\ z_2 \end{bmatrix} \tag{3.47}$$

$$R_1 = \begin{bmatrix} 1 & 0 & 0 \\ 0 & \cos\phi & -\sin\phi \\ 0 & \sin\phi & \cos\phi \end{bmatrix},\ R_2 = \begin{bmatrix} \cos\theta & 0 & \sin\theta \\ 0 & 1 & 0 \\ -\sin\theta & 0 & \cos\theta \end{bmatrix},$$
$$R_3 = \begin{bmatrix} \cos\psi & -\sin\psi & 0 \\ \sin\psi & \cos\psi & 0 \\ 0 & 0 & 1 \end{bmatrix} \tag{3.48}$$

The resultant transformation matrix from body reference frame to the Earth (inertial) reference frame is given below.

$$R = R_1 R_2 R_3 \tag{3.49}$$

$$\begin{bmatrix} \cos\psi\cos\theta & \cos\psi\sin\theta\sin\phi - \cos\phi\sin\psi & \cos\psi\sin\theta\cos\phi + \sin\psi\sin\phi \\ \sin\psi\cos\theta & \sin\psi\sin\theta\sin\phi + \cos\psi\cos\phi & \sin\psi\sin\theta\cos\phi - \sin\phi\cos\psi \\ -\sin\theta & \sin\phi\cos\theta & \cos\theta\cos\phi \end{bmatrix} \tag{3.50}$$

Components of the angular velocity of the platform expressed in the body reference frame are given as below.

$$\omega = \begin{bmatrix} \omega_x \\ \omega_y \\ \omega_z \end{bmatrix} = \begin{bmatrix} p \\ q \\ r \end{bmatrix} \tag{3.51}$$

By using the rotation matrices, time derivatives of the Euler angles can be expressed in terms of angular velocity components, p, q, and the r.

$$\dot{\phi} = p + q\tan\theta\sin\phi + r\tan\theta\cos\phi \tag{3.52}$$

$$\dot{\theta} = q\cos\phi - r\sin\phi \tag{3.53}$$

$$\dot{\psi} = q\sec\theta\sin\phi + r\sec\theta\cos\phi \tag{3.54}$$

Angular momentum equation given below is used to find the time derivatives of the angular velocity terms.

$$H_c = I\omega \tag{3.55}$$

Inertia matrix, I, can be expressed as below.

$$I = \begin{bmatrix} I_{xx} & -I_{xy} & -I_{xz} \\ -I_{yx} & I_{yy} & -I_{yz} \\ -I_{zx} & -I_{zy} & I_{zz} \end{bmatrix} \tag{3.56}$$

It is assumed to be a diagonal matrix where the mass products of inertia terms are assumed to be zero. Dynamic equations regarding the angular velocities are derived using the Newton's Law.

$$\left(\frac{dH_c}{dt}\right)\Big|_{OX_EY_EZ_E} = \left(\frac{dH_c}{dt}\right)\Big|_{Ox_by_bz_b} + \omega\, x\, H_C = M \tag{3.57}$$

$$I\dot{\omega} + \omega\, x\, (I\omega) = M \tag{3.58}$$

$$\begin{bmatrix} \dot{p} \\ \dot{q} \\ \dot{r} \end{bmatrix} = I^{-1}.\begin{bmatrix} M_x \\ M_y \\ M_z \end{bmatrix} - I^{-1}.\begin{bmatrix} p \\ q \\ r \end{bmatrix} x\, I.\begin{bmatrix} p \\ q \\ r \end{bmatrix} \tag{3.59}$$

Resultant moments about roll, pitch, and the yaw axes are given below. Thrust forces generated by each motor-propeller pair is denoted by $F_1$ and $F_2$ below.

$$\sum M_x = (F_1 - F_2)\frac{L}{2} \tag{3.60}$$

$$\sum M_y = 2T_g + M_p g L_p cos\theta sin\beta \tag{3.61}$$

$$\sum M_z = M_1 - M_2 \tag{3.62}$$

Resultant moments about roll, pitch, and the yaw axes are given below.

$$\begin{bmatrix}\dot{p}\\ \dot{q}\\ \dot{r}\end{bmatrix}=\begin{bmatrix}\frac{qr}{I_x}(I_y-I_z)+\frac{L}{2I_x}(F_1-F_2)\\ \frac{pr}{I_y}(I_z-I_x)+\frac{2T_w}{I_y}+\frac{m_p g L_p cos\theta sin\beta}{I_y}\\ \frac{pq}{I_z}(I_x-I_y)+\frac{(F_1-F_2)d}{I_z b}\end{bmatrix} \tag{3.63}$$

State vector and state equations considering the yaw, roll, and the pitch dynamics of the platform are expressed below.

$$x=\begin{bmatrix}\phi\\ \theta\\ \psi\\ p\\ q\\ r\end{bmatrix} \tag{3.64}$$

$$\begin{bmatrix}\dot{\phi}\\ \dot{\theta}\\ \dot{\psi}\\ \dot{p}\\ \dot{q}\\ \dot{r}\end{bmatrix}=\begin{bmatrix}p+q\tan\theta\sin\phi+r\tan\theta\cos\phi\\ q\cos\phi-r\sin\phi\\ q\sec\theta\sin\phi+r\sec\theta\cos\phi\\ \frac{qr}{I_x}(I_y-I_z)+\frac{L}{2I_x}(F_1-F_2)\\ \frac{pr}{I_y}(I_z-I_x)+\frac{2T_w}{I_y}+\frac{m_p g L_p cos\theta sin\beta}{I_y}\\ \frac{pq}{I_z}(I_x-I_y)+\frac{(F_1-F_2)d}{I_z b}\end{bmatrix} \tag{3.65}$$

Brushless motors are used as the actuators of propellers of the hybrid robot. Therefore, force and moment terms in the previous equations should be expressed in terms of voltage input to the motors.

### 3.2.1. Motor and Propeller Model

Brushless motors in the system are driven by Electronic Speed Controllers (ESC) that makes the brushless motor behave like a continuous servo motor. Mathematical model of the motor-propeller unit is derived by experimental means. A test setup is

built up to measure the thrust of the system due to the applied voltage. In addition the angular velocity of the propeller is measured by a hand tachometer which is shown in Figure 17. Even, it is not so suitable to measure the transients in the velocity changes; use of this tachometer has provided information with certain accuracy.

*Figure 17 Ty1 Hand Type Tachometer*

Firstly, applied voltage to the motor-propeller unit is increased from 0 to 10 V. With 0.5 V increments, angular velocity of the propeller is measured by the hand tachometer. Variation of angular velocity with the applied voltage is given in Figure 18. A quadratic curve and a linear line are fitted to these measurements with using Matlab Curve Fitting tool. These results of fitted equations are also shown in Figure 18.

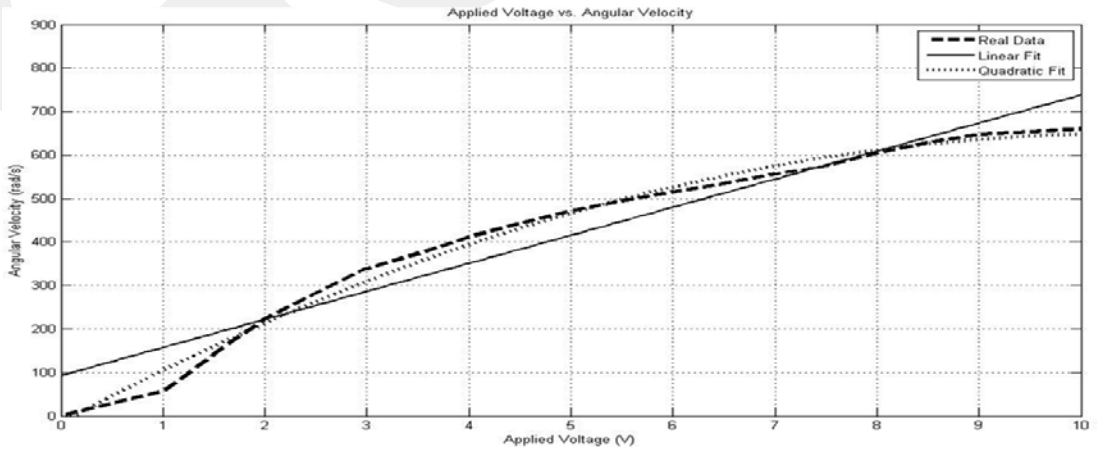


*Figure 18 Applied Voltage vs. Angular Velocity Curve and Fitted Equations*

The linear fit is given in below;

$$\Omega = 64.513V_{app} + 93.263 \text{ [rad/s]} \tag{3.66}$$

The quadratic fit is also given in below;

$$\Omega = -5.9877V^2 + 126.22V - 14.429 \text{ [rad/s]} \tag{3.67}$$

Due to the simplicity, linear fit is employed in the equations below. Consequently, thrust force generated due to the rotation of the propellers is generally expressed as below.

$$F_z = b\Omega^2 \tag{3.68}$$

Where b is the thrust factor. In order to find out this thrust factor, a test setup is employed in the Flying Robotics Laboratory of the Mechatronics Engineering Department at Atılım University. Figure 19 presents the details of the setup. There is a motor and a propeller in one side of the scale and a payload is assembled to the other side of the scale. A force sensor in placed under the payload in order to measure the thrust values depending on the applied motor voltage.

Voltage input to the motor-propeller pair is sent through a data acquisition system and the force sensor output is also measured and acquired by the same system. Various types of motor-propeller pairs are tested in addition to the pair used in the thesis. Chirp type voltage inputs are generally utilized.

Some detailed identification techniques are used to construct dynamic equations between the voltage input and thrust output of the pair. However, in this study a simplified relation is employed to simplify the model equations.

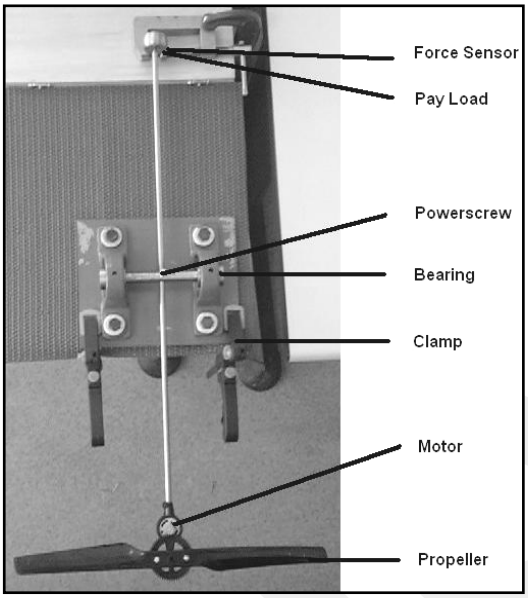


*Figure 19 Thrust Measurement Setup*

The force is the FS Series sensor of Honeywell. The payload should apply the force perpendicular to the sensor. Therefore the payload is designed to be spherical. This spherical shape will make the force applied perpendicular to the sensor. Output of the sensor is amplified by using Burr-Brown's INA2141 low power precision instrumentation amplifier to match the input range of the analog to digital converter of the data acquisition system. Humusoft MF 624 board is the data acquisition board of the system. Applied voltage input and the acquired thrust data are shown in Figure 20.

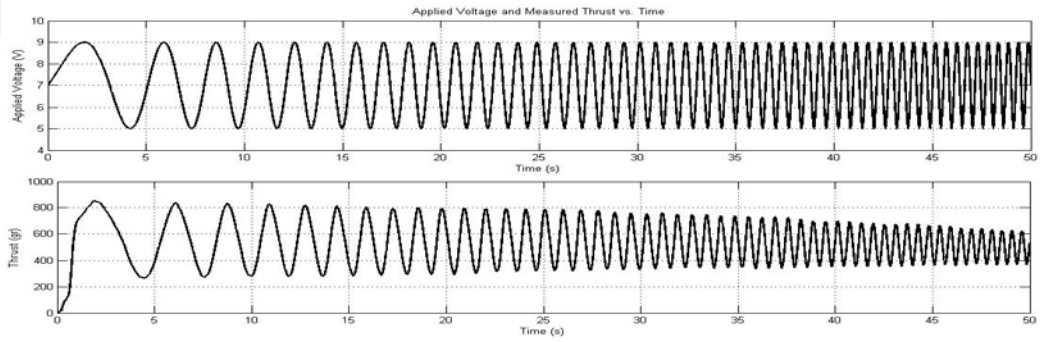


*Figure 20 Applied Voltage and Thrust versus Time Plot*

The thrust coefficient given in the Equation 3.68 is identified by using Simulink Parameter Estimation tool of Matlab. For the applied chirp signal as applied voltage, the thrust output of the real system and the identified model is shown in Figure 21. At low frequencies the proposed model has a better accuracy. Since it does not govern a dynamic equation the accuracy reduces at higher frequencies.

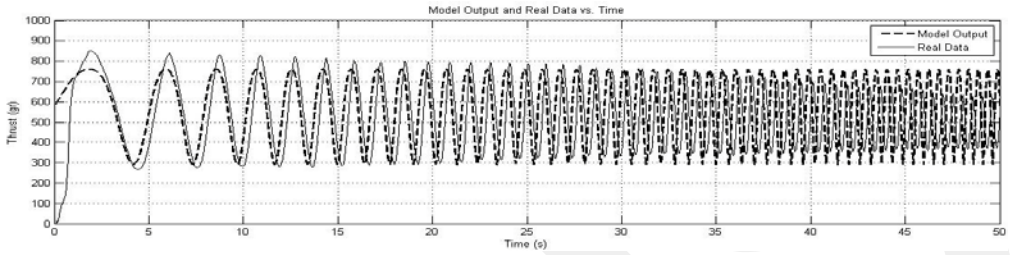


*Figure 21 Produced Thrust of Real System and Model for Chirp Input versus Time Plot*

As it can be seen in the figure 21, the identified model suits with the real data for low frequencies, but when the frequency is increased a difference between the model and real system occurs. The identification process of equation between applied voltage and angular velocity is carried out with a static measurement data, so it is expected to have some mismatches in dynamic systems. The identified model is validated on a 3 Hz sinusoidal type applied voltage signal. This validation data and the performance of the identified model is shown in Figure 22.

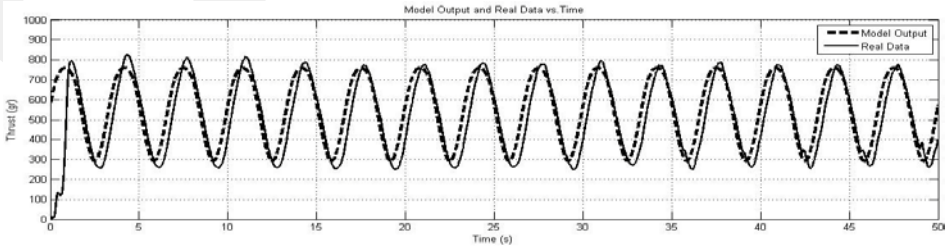


*Figure 22 Produced Thrust of Real System and Model for Sinusoidal Input versus Time Plot*

As it can be seen in the Figure 22, the identified model between the applied voltage and measured thrust suits the real data very well when sinusoidal type applied voltage is used. The identified thrust coefficient parameter is given in equation below;

$$b = 2x10^{-6} \left[\frac{N}{\left(\frac{rad}{s}\right)^2}\right] \tag{3.69}$$

If equation 3.66 is written in equation 3.68;

$$F_z = 23x10^{-6}(64.513V + 93.263)^2 \quad [N] \tag{3.70}$$

The generated drag moments by motor propeller pairs ($M_1, M_2$) are stated as;

$$M_{1,2} = d{\Omega_{1,2}}^2 \tag{3.71}$$

It is also possible to write the drag moments in terms of thrust forces as below.

$$M_{1,2} = \frac{d}{b} F_{1,2} \tag{3.72}$$

In literature it is seen that such a ratio is employed for thrust and drag coefficients;

$$\frac{b}{d} = \frac{1}{58} \tag{3.73}$$

The torque generated from DC motor is given in equation 3.35 as;

$$T_g = \frac{nK_tV}{R} - \frac{nK_tK_e}{R}(n\dot{\theta}_w - \dot{\phi}) \tag{3.74}$$

Torque applied to the ground wheels shall be manipulated to control the pitch dynamics. So as to achieve this, rotational velocities of the wheels should be added to the state vector of the flying dynamics. State equation for this term is given below.

$$\ddot{\theta}_w = \frac{nK_tV_3}{JR} - \frac{(nK_tK_e + Rb_w)\dot{\theta}_w}{JR} \tag{3.75}$$

When equation 3.75 is added, the attitude model becomes ready for linearisation;

$$\begin{bmatrix} \dot{\phi} \\ \dot{\theta} \\ \dot{\psi} \\ \dot{p} \\ \dot{q} \\ \dot{r} \\ \ddot{\theta}_w \end{bmatrix} = \begin{bmatrix} p + q\tan\theta\sin\phi + r\tan\theta\cos\phi \\ q\cos\phi - r\sin\phi \\ q\sec\theta\sin\phi + r\sec\theta\cos\phi \\ \frac{qr}{I_x}(I_y - I_z) + \frac{23x10^{-6}L}{2I_x}[(64.513V_1 + 93.263)^2 - (64.513V_2 + 93.263)^2] \\ \frac{pr}{I_y}(I_z - I_x) + \frac{2\left(\frac{nK_tV_3}{R} - \frac{nK_tK_e}{R}(n\dot{\theta}_w - \dot{\phi})\right)}{I_y} + \frac{m_pgL_pcos\theta sin\beta}{I_y} \\ \frac{pq}{I_z}(I_x - I_y) + \frac{(F_1 - F_2)d}{I_zb} \\ \frac{nK_tV_3}{JR} - \frac{(nK_tK_e + Rb_w)\dot{\theta}_w}{JR} \end{bmatrix} \tag{3.76}$$

Where $V_1$ and $V_2$ are the applied inputs to the propeller actuators, $V_3$ is the input voltage to the ground wheel actuators, and β is the angular position of the pendulum controlled by a digital servo motor. $V_{1,2,3}$ and β are the possible inputs to the system in flying mode. Instead of using all the inputs, either $V_3$ or β can be used. The inertia attached as wheels may not be enough to stabilize the pitch dynamics. Then, both can be used at the same time. Instead, only β can be used. It is seen in the controllability analysis that using one of them together with $V_{1,2}$ makes the system controllable. Tests on physical system show that using $V_3$ may not be enough.

### 3.2.2. Linearisation of Nonlinear State Equations for Flying Motion

Equation 3.76 is linearized around the hovering conditions where Euler angles and angular velocities are zero accept yaw angle. The state space representation is in the form of;

$$\dot{x} = Ax + Bu$$
$$y = Cx + Du \tag{3.77}$$

The state and input vector is constructed in the form of;

$$x = \begin{bmatrix} \phi \\ \theta \\ \psi \\ p \\ q \\ r \\ \dot{\theta}_w \end{bmatrix} \tag{3.78}$$

$$u = \begin{bmatrix} V_1 \\ V_2 \\ V_3 \\ \beta \end{bmatrix}$$

The linearized state-space equations are found;

$$A = jacobian\left(\begin{bmatrix} \dot{\phi} \\ \dot{\theta} \\ \dot{\psi} \\ \dot{p} \\ \dot{q} \\ \dot{r} \\ \ddot{\theta}_w \end{bmatrix}, \begin{bmatrix} \phi \\ \theta \\ \psi \\ p \\ q \\ r \\ \dot{\theta}_w \end{bmatrix}\right)$$
$$B = jacobian\left(\begin{bmatrix} \dot{\phi} \\ \dot{\theta} \\ \dot{\varphi} \\ \dot{p} \\ \dot{q} \\ \dot{r} \\ \ddot{\theta}_w \end{bmatrix}, \begin{bmatrix} V_1 \\ V_2 \\ V_3 \\ \beta \end{bmatrix}\right) \tag{3.79}$$

These operations are carried out in Matlab software and the m-file that utilized this linearization process is given in the Appendix A. The linearised state space

representation becomes in the form of Equation 3.77 and the state space matrices becomes;

$$\begin{bmatrix} \dot{\phi} \\ \dot{\theta} \\ \dot{\psi} \\ \dot{p} \\ \dot{q} \\ \dot{r} \end{bmatrix} = \begin{bmatrix} 0 & 0.01 & 0 & 1 & 0 & 0 \\ -0.01 & 0 & 0 & 0 & 1 & 0 \\ 0 & 0 & 0 & 0 & 0 & 1 \\ 0 & 0 & 0 & 0 & A_{45} & 0 \\ 0 & 0 & 0 & A_{54} & 0 & 0 \\ 0 & 0 & 0 & 0 & 0 & 0 \end{bmatrix} \begin{bmatrix} \phi \\ \theta \\ \psi \\ p \\ q \\ r \end{bmatrix} + \begin{bmatrix} 0 & 0 & 0 \\ 0 & 0 & 0 \\ 0 & 0 & 0 \\ B_{41} & B_{42} & 0 \\ 0 & 0 & B_{53} \\ B_{61} & B_{62} & 0 \end{bmatrix} \begin{bmatrix} V_1 \\ V_2 \\ \beta \end{bmatrix}$$

$$y = \begin{bmatrix} 1 & 0 & 0 & 0 & 0 & 0 & 0 \\ 0 & 1 & 0 & 0 & 0 & 0 & 0 \\ 0 & 0 & 1 & 0 & 0 & 0 & 0 \\ 0 & 0 & 0 & 1 & 0 & 0 & 0 \\ 0 & 0 & 0 & 0 & 1 & 0 & 0 \\ 0 & 0 & 0 & 0 & 0 & 1 & 0 \\ 0 & 0 & 0 & 0 & 0 & 0 & 1 \end{bmatrix} \begin{bmatrix} \phi \\ \theta \\ \psi \\ p \\ q \\ r \end{bmatrix} \tag{3.80}$$

Where;

$$A_{45} = \frac{\frac{I_y - I_z}{100}}{I_x}$$

$$A_{54} = -\frac{\frac{I_x - I_z}{100}}{I_y}$$

$$B_{41} = \frac{Lbk_1(k_2 + V_1 k_1)}{I_x}$$

$$B_{42} = -\frac{Lbk_1(k_2 + V_2 k_1)}{I_x} \tag{3.81}$$

$$B_{61} = \frac{L_p M_p g}{I_y}$$

$$B_{61} = \frac{2dk_1(k_2 + V_1 k_1)}{I_z}$$

$$B_{62} = -\frac{2dk_1(k_2 + V_2 k_1)}{I_z}$$

### 3.3. Basic Controllability and Observability Analysis

The state space representation of linear time invariant systems are given in equation 3.82, this form is the same for both flying and ground motions of the TWTR system.

$$\dot{x} = Ax + Bu$$
$$y = Cx + Du \tag{3.82}$$

Where;

*A* is the n x n "state matrix",
*B* is the n x r "input matrix",
*C* is the m x n "output matrix",
*D* is the m x r " feedforward matrix"

Controllability of the systems can be checked considering the rank of the following controllability matrix.

$$Co = [B \quad BA \quad BA^2 \quad \dots \quad BA^{n-1}] \tag{3.83}$$

The rank of the controllability matrix is calculated by using Matlab software for both flying and ground movements and the m-file calculates the rank of these controllability matrices is given in Appendix A. For ground movement of the TWTR system, the rank of the controllability matrix becomes;

$$Rank[B \quad BA \quad BA^2 \quad BA^3] = 4 \tag{3.84}$$

For flying movement of the TWTR system, the rank of the controllability matrix becomes;

$$Rank[B \quad BA \quad BA^2 \quad \dots \quad BA^6] = 7 \tag{3.85}$$

As it is seen from Equations 3.84 and 3.85, the system is controllable for both flying and ground modes. Since all states are measured for both of the modes, the system is observable in both types of motions.

# CHAPTER 4

# HYBRID ROBOT: PHYSICAL REALIZATION

This chapter describes the physical realization of the designed system as the Hybrid Robot. System components are classified and discussed. The robot platform consists of;

- Brushed DC motors attached to wheels
- Brushless dc motors attached to propellers
- Digital servo motor that handles the battery pack
- Motor drivers and electronic speed controllers,
- Inertial measurement unit that consists of accelerometers, gyros, magnetometers, and the complementary filter
- Encoder attached to the dc motor shaft
- Proximity sensor
- Real time control system with a desktop PC
- Data acquisition board
- Microcontroller unit to drive the servo motor
- Battery packs
- Desktop power supply.

The real-time controller software is generated in Matlab Simulink by using Realtime Windows Target Blockset. Controller hardware is not embedded onto the system. This is considered within the future work of thesis. The major aim is to design and develop a prototype system that is presented as a hybrid robot. Therefore, the physical implementation should be easy. Basic control algorithms are implemented on the system. Further developments and more complex control algorithms are

expected in the future steps of the study; they are not covered in the scope of the thesis. A simple schematic representation of the relation among the components is given in Figure 23. Sensor data is sent to the control PC via data acquisition board and serial port. This data is processed within the control algorithm and control inputs are sent to the actuators by the DAQ board and USB port. Brushless dc actuators are powered by the batteries attached on to the system. Digital servo and brushed dc ones are powered by desktop power supply modules. The main chasses that keeps all the onboard components is made from aluminum and plexiglas materials.

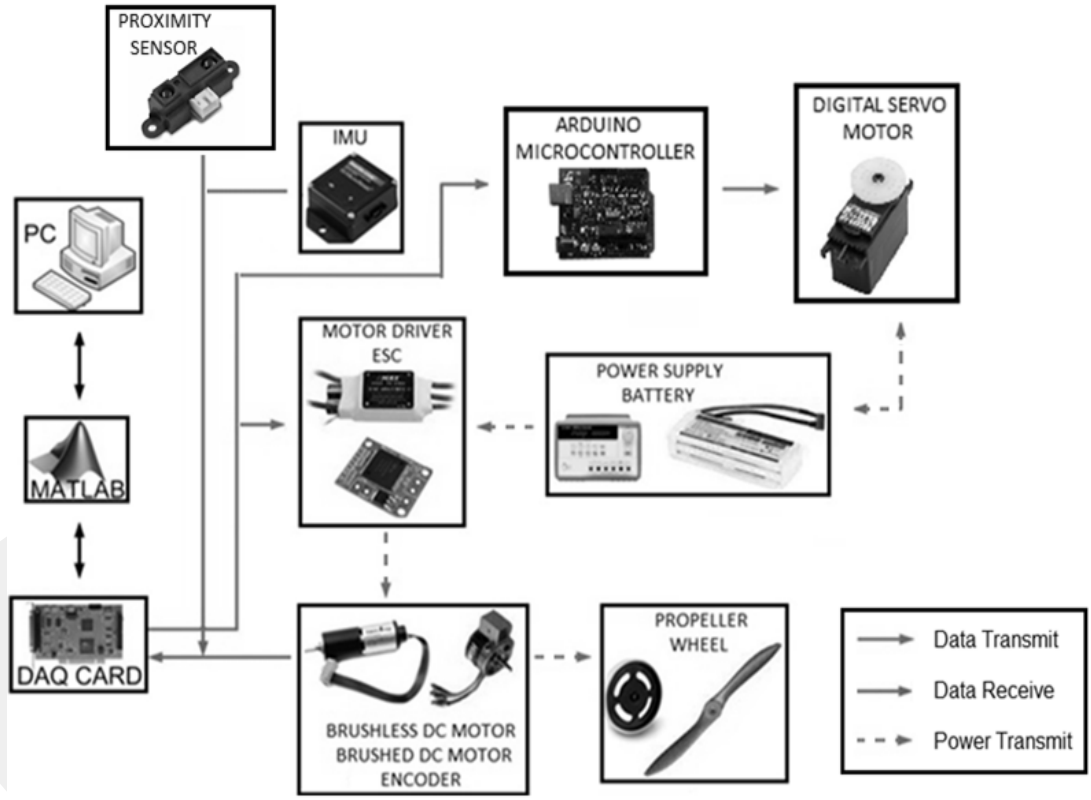


*Figure 23 Physical System*

A detailed information about the elements of the physical system is described in mechanical structure, sensor system, actuator system and controller system parts.

### 4.1. Mechanical Structure

In the design process of the mechanical structure, a prototype of the design is constructed. This constructed prototype is shown in Figure 24. The final design of the system is also shown in Figure 24. As it can be seen that the first prototype has a single rod on the body and has small wheels, because of some vibration problems the final design has two vertical rods on the body. In order to accomplish the pitch axis stabilization in flying movement, the inertia of the wheels are increased in the final design.

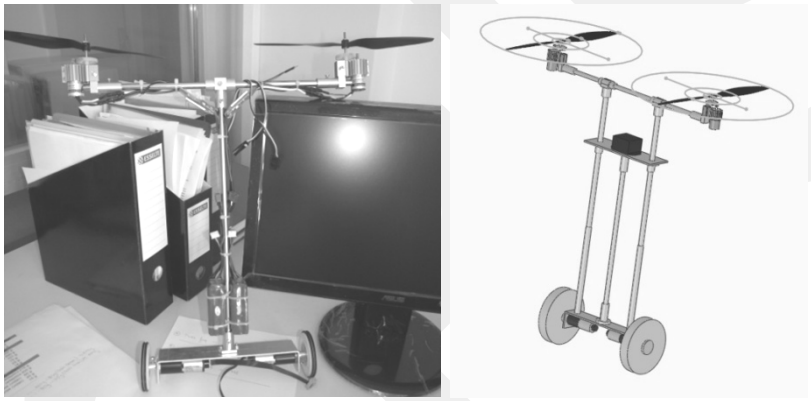

*Figure 24 First Prototype and Final Design of the System*

In the light of the experience gained from the first prototype, the design of the mechanical structure is improved. It is important to design a system with flexible parameters. This means the mass of the system, length of the system, center of mass of the system should be changed. A slider system is designed in order to slide between two vertical rods on the body which carries the sensor set and change the center of gravity of the robot. In order to change the length of the systems, these vertical rods can be elongated. For the vibration problem, the DC motors mounted to the wheels are beared in final desing. Finally a rod and connectors are designed for the system to mount with the test platform for flying movements. The illustration of the final design of the system is also shown in Figure 24 and the detailed mechanical

drawings of the TWTR system are given in Appendix B. In order to calculate the center of gravity of the system, the body is assumed as given in Figure 25.

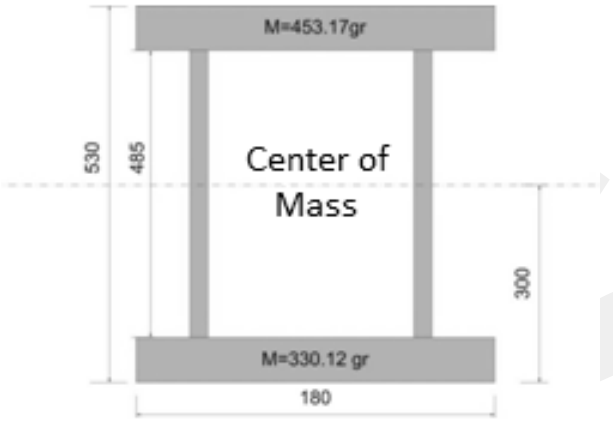


*Figure 25 Assumptions of the Body to Calculate the Center of Gravity*

From Figure 25 the center of mass of the body is calculated as;

$$C_g = \left(\frac{52}{453.17 + 330.12}\right) x453.17 = 30.01\ cm \tag{4.1}$$

As it is mentioned before, the inertia matrix of the system is in the form given in equation 4.2 and the total mass of the body is 1029.29 g.

$$I = \begin{bmatrix} I_{xx} & -I_{xy} & -I_{xz} \\ -I_{yx} & I_{yy} & -I_{yz} \\ -I_{zx} & -I_{zy} & I_{zz} \end{bmatrix} \tag{4.2}$$

The inertia matrix parameters, mass and center of mass of the system is given in Table 1;

*Table 1 Calculated Physical Parameters of the TWTR System*

| | |
|---|---|
| $I_{xx}$ | 0.0665 $kg.m^2$ |
| $I_{xy}$ | 7.904x$10^{-6} kg.m^2$ |
| $I_{xz}$ | -2.5396x$10^{-7}$ $kg.m^2$ |
| $I_{yx}$ | 7.904x$10^{-6}$ $kg.m^2$ |
| $I_{yy}$ | 0.0833 $kg.m^2$ |
| $I_{yz}$ | -4.7690x$10^{-5} kg.m^2$ |
| $I_{zx}$ | 7.904x$10^{-6}$ $kg.m^2$ |
| $I_{zy}$ | -4.7690x$10^{-5}$ $kg.m^2$ |
| $I_{zz}$ | 0.0177 $kg.m^2$ |
| Mass | 1.029 kg |
| $C_g$ | 30.08 cm |

As it can be seen in the Table 1, the non-diagonal elements of the inertia matrix are small enough compared to the diagonal elements of the inertia matrix to be assumed as zero.

### 4.2. Sensor System

In the hardware of the TWTR system, an IMU unit is used in order to measure the angular positions and angular velocities, shaft encoder mounted to the DC motors also used in order to measure the linear displacement and linear velocity of the system. The details about the sensor system are given in below.

#### 4.2.1. Encoder

Maxon 13mm Digital Magnetic 16 cpr quadrature Encoder is used to measure the displacement and the velocity of the TWTR system on ground movement. DC motor has a 19:1 planetary gear train, this means when encoder completes 19 rounds, the

wheel completes one round, so the one round of the wheel has 64x19 peaks. The displacement of the TWTR system on ground movement is calculated with the Equation 4.3.

$$Displacement_W = \frac{1216}{2\pi r_w} \tag{4.3}$$

As it can be seen from the Equation 4.3, the radius of the wheel is important for the TWTR system. Because of this reason several wheels has several radius values are used.

### 4.2.2 Inertial Measurement Unit

An IMU sensor is used in order to measure the angle and angular velocity. In order to measure these parameters Microstrain 3DM GX2 IMU which is shown in Figure 26, unit is used. 3DM-GX2 is a high-performance gyro enhanced orientation sensor which utilizes miniature MEMS sensor technology. It combines a triaxial accelerometer, triaxial gyro, triaxial magnetometer, temperature sensors, and an on-board processor running a sophisticated sensor fusion algorithm. It has a RS 232 connection with the computer.


*Figure 26 MicroStrain 3DM GX2 IMU*

The sampling rate of the IMU is set to 100 Hz, in this work it is desired to have a sampling rate of 200 Hz, so a sequence is sent to the IMU with Matlab software. In this work, Euler angles and angular rates data package is used, IMU sends a 31 bit package data which is shown in Table 2. The Matlab Simulink model is buffering and unpacking these data for a continuous measurement.

*Table 2 IMU Packet Information*

| Measurement | Byte |
|---|---|
| Roll Angle | 2-5 |
| Pitch Angle | 6-9 |
| Yaw Angle | 10-13 |
| Angular Rate X | 14-17 |
| Angular Rate Y | 18-21 |
| Angular Rate Z | 22-25 |

Each of these measurements is unpacked and transformed into their values with using IEEE 754 conversion method. After unpacking the packet input according to the measurement information given in Table 1.

### 4.3 DC Motor and Motor Drive

As DC motor Maxon Amax Dc motor with 16 cpr quadrature encoder and a 19:1 planetary geartrain with ball bearing is used. This motor can be seen in Figure 27. The motor windings are 6V windings.

*Figure 27 Maxon Amax DC Motor.*

"VNH3SP30 Motor Driver Carrier MD01B" which is produced by Pololu Electronics and has a 9A continuous current limit is used as the motor driver. The used motor driver is shown in the figure 28.


*Figure 28 VNH3SP30 Motor Driver Carrier MD01B*

The maximum PWM (Pulse-width modulation) frequency of the motor driver is 10 kHz, which is not a perfect value, but the current limit is the critical point in the motor driver selection.

### 4.4. Brushless DC Motor and Motor Drive

Brushless motors are used in order to rotate the propellers. Art-Tech B2025-15L brushless motor which can be seen in Figure 29 is used as brushless motors. The motor has a 1.2 A idle and 15 A maximum current values. It has a mass of 60 grams and has an 8500 N thrust if the motor is used with an 11x4.7cm propeller. The brushless motor also has a 1/5 gear reduction.

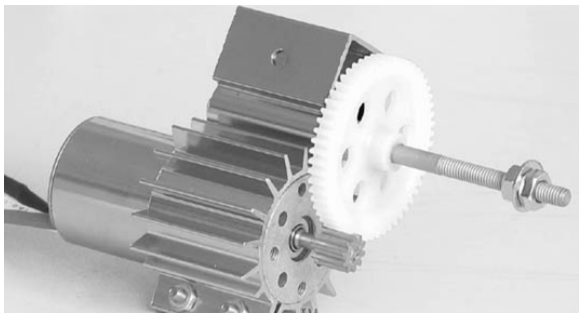

*Figure 29 Art-Tech B2025-15L Brushless Motor*

In order to drive the brushless motor, Electronic Speed Controller (ESC) is used. Art-Tech 18A Brushless ESC is used in order to drive the brushless motor. This ESC converts servo signal to single directional rotation. This means ESC drives the brushless motor with maximum speed when a pulse with 10% duty cycle and 20ms period is applied and the ESC drives the brushless motor with minimum speed when a pulse with 5% duty cycle and 20ms period is applied. The used ESC is shown in Figure 30.


*Figure 30 Art-Tech 18A Brushless ESC*

The brushless motor and ESC set is modeled as a DC motor in the mathematical modeling process. Pulse with 5% duty cycle and 20ms period is assumed as 0V and pulse with 10% duty cycle and 20ms period is assumed as 10V. A first order linear equation is fitted in order to convert these pulse and voltage values. Information about applied voltage and produced thrust for these voltages are given in Chapter 3.

### 4.5. Controller Software

The environment which the control actions will be carried is selected as Matlab Simulink, with using the Real Time Windows Target (RTWT) toolbox of Matlab, the control systems are implemented on the computer. The collected data from encoder and IMU sensor are processed and the control input u (voltage) is calculated and applied to the motor driver units as PWM signals. Different types of control systems like Error space approach, PID controller, LQR controller and bang bang controller are implemented by this controller software. The calibration of sensors and calculating the necessary PWM signals for the actuators are also processed with this software and finally the serial data package that IMU sends is indexed and seperate in this part also.

### 4.6. Controller Hardware

The control environment is selected as Matlab Simulink, so it is decided to use a DAQ card to get inputs from system and give outputs to the system. Humusoft MF624 DAQ Card is used for this reason. This card can be seen in Figure 31.

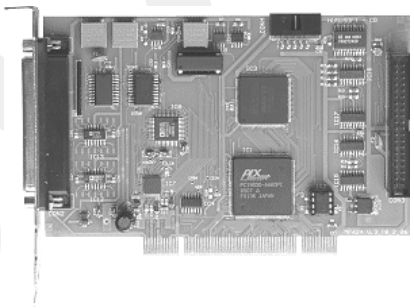

*Figure 31 MF624 DAQ Card*

The MF 624 contains 8 channel fast 14 bit A/D converter with simultaneous sample/hold circuit, 8 independent 14 bit D/A converters, 8 bit digital input port and 8 bit digital output port, 4 quadrature encoder inputs with single-ended or differential

interface and 5 timers/counters. The card is designed for standard data acquisition and control applications and optimized for use with Real Time Toolbox for Simulink. The DAQ card provides 50 Hz PWM signal for esc and brushless motors and 10 kHz PWM signal for DC motor driver and DC motor. DAQ card also collects the encoder and IMU data.

# CHAPTER 5

# DESIGN OF CONTROLLERS AND SIMULATIONS

Considering the ground motion of TWTR system, LQR and error space type controllers are designed and applied on the physical system. Similarly LQR is designed and tested on the system for attitude stabilization in flying mode. Latter is tested on TWTR attached to the special joint at its center of mass which only enables 3 rotations about that point. The implementation of these controllers on the system as it flies vertically and hovers while the system stabilizes itself on the ground is the future work of this thesis. Therefore it is out of the scope of the thesis. These controllers are designed utilizing the dynamic models derived for the TWTR system in Chapter 3.

## 5.1. Controller System Design for Ground Movements

The system is inherently unstable on the ground unless it is stabilised. The open loop response of the system is shown in Figure 32.

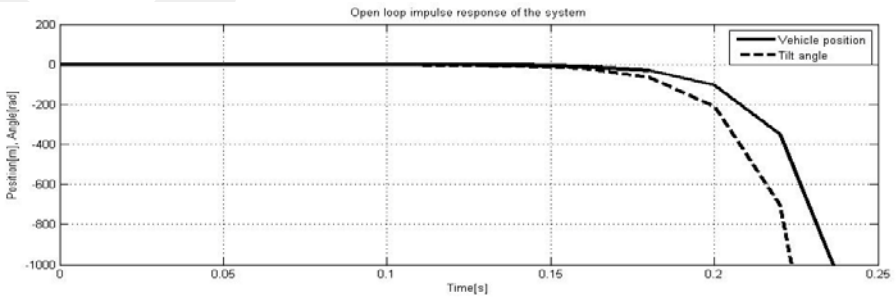


*Figure 32* Open Loop Response

In order to stabilise the system control action is needed. The open loop poles of the system are shown in Equation 5.1 and the pole zero map is shown in Figure 33;

$$P = [0 \quad 59.9883 \quad -3.0248 \quad 1.7804] \tag{5.1}$$

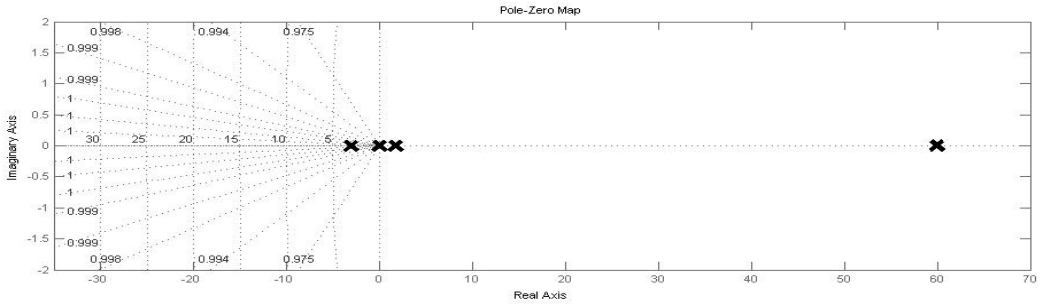


*Figure 33 Pole Zero Map*

There are poles on the right hand side of the pole zero map of the system and one of the poles is far at the right hand side; this means that the system will be unstable in a very short time period. This can also be seen in the open loop response given in Figure 32.

### 5.1.1. Linear Quadratic Regulator Design

The regulatory controllers control systems by using a mathematical algorithm that minimizes a cost function with weighting factors supplied by the user. The cost function is often defined as a sum of the deviations of key measurements from their desired values.

The LQR algorithm is an automated way of finding an appropriate state-feedback controller. For a continuous-time linear system described by;

$$\dot{x} = Ax + Bu \tag{5.2}$$

With a cost functional defined as;

$$J = \int_0^\infty (x^T Q x + u^T R u) dt \tag{5.3}$$

The feedback control law that minimizes the value of the cost is;

$$u = -Kx \tag{5.4}$$

Where *K* is given by;

$$K = R^{-1} B^T P \tag{5.5}$$

And *P* is found by solving the continuous time algebraic Riccati equation;

$$A^T P + PA - PBR^{-1} B^T P + Q = 0 \tag{5.6}$$

In equations 5.3, 5.6 and 5.7 used R and Q matrices can be described as the weighting matrices .

$$Q = \begin{bmatrix} W_x & 0 & 0 & 0 \\ 0 & W_{\dot{x}} & 0 & 0 \\ 0 & 0 & W_\phi & 0 \\ 0 & 0 & 0 & W_{\dot{\phi}} \end{bmatrix}, R = 1 \tag{5.7}$$

Every state has a weighting in Q matrix, in two wheeled balance robot system, phi is the critical state, so the weighting of the theta is selected as 500 and the weighting of the displacement is selected as 100. The weighting matrix R is a scalar value as there is only one control input to the system. The weightings of linear velocity and

rotational velocity are selected as 1. The calculation of the control matrix (K) has been carried out using Matlab software, the m-file succeeds this calculation is given in the Appendix A. The control matrix (K) is calculated in Matlab m-file as;

$$K = \begin{bmatrix} 3.1623 \\ -30.9939 \\ -35.6710 \\ -3.5923 \end{bmatrix} \tag{5.8}$$

The new poles of the system become;

$$P_{New} = \begin{bmatrix} -60.3120 \\ -0.3758 \\ -3.0537 + 1.4247i \\ -3.0537 - 1.4247i \end{bmatrix} \tag{5.9}$$

The poles of the closed loop system given in equation 5.9, means that the system has two real poles and one pair of complex conjugates, The model of the two wheeled balance robot is constructed in Matlab Simulink. This construction of the mathematical model is shown in the Figure 34. The stabilization of the states, output of the system and the control input of the system are shown in the Figure 35.

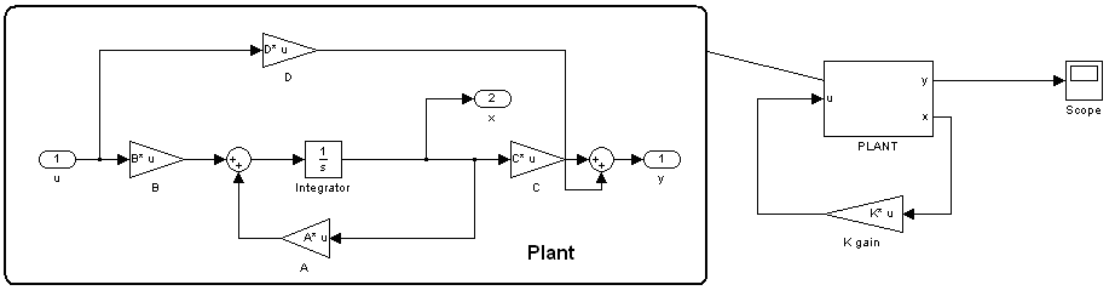


*Figure 34 Model of the System*

The control matrix K is applied to the state space model of the two wheeled balance robot system. A, B, C and D matrices are created in Matlab m-file which is given in the Appendix A.

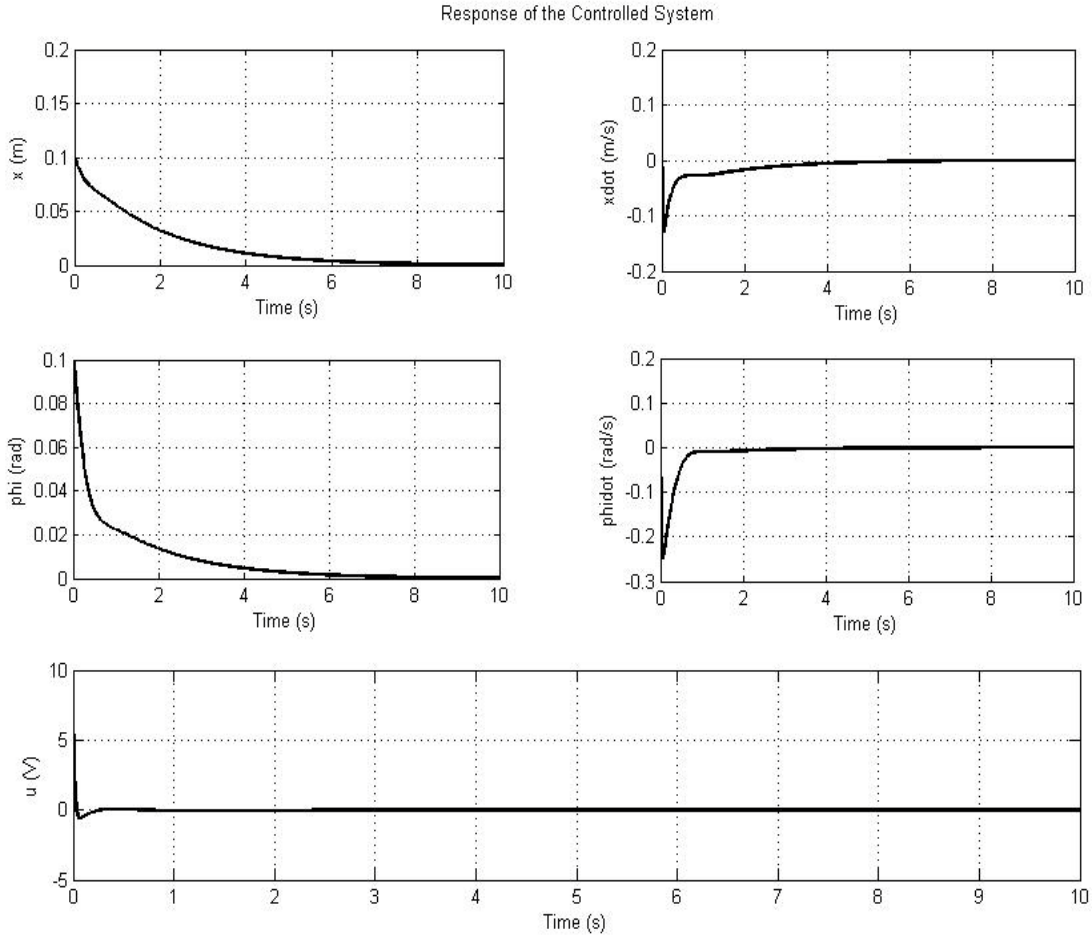


*Figure 35 Response of the Controlled System*

When the R weighting factor is increased to 100 in order to decrease the amount of control energy, the response of the system is shown in the Figure 36.

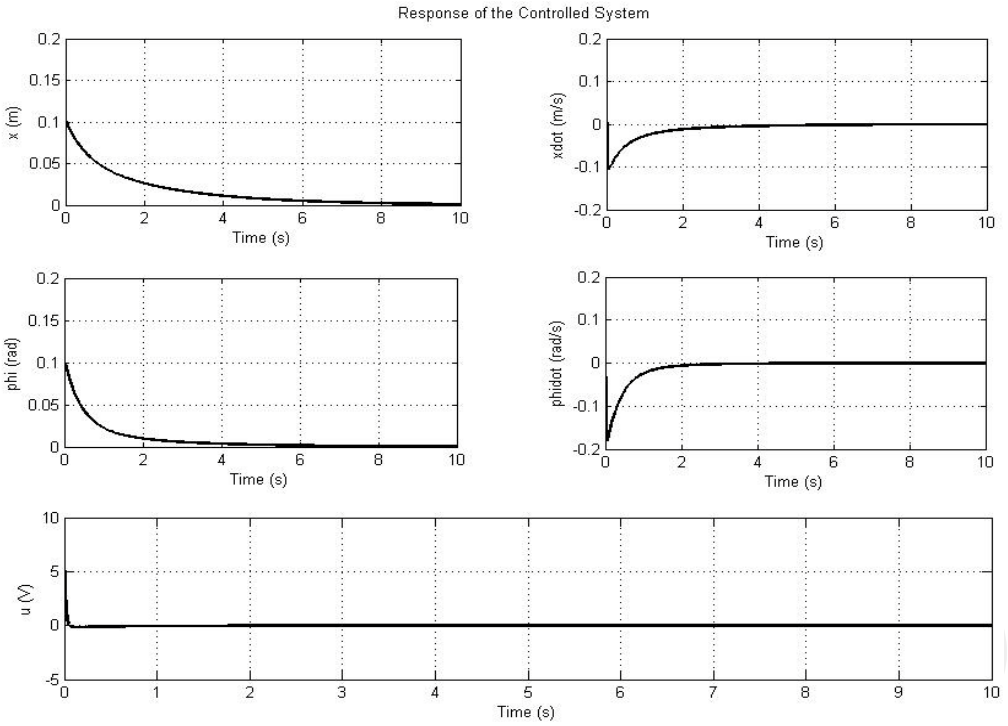


*Figure 36* Response of the Controlled System with High R (100) Weighting

It has been seen that the settling time of the system is decreased with a high R weighting. The settling time of the system is critical and should be set to a minimum value. This means this R weighting is more suitable.

### 5.1.2. Error Space Approach Design

The state space representation is;

$$\dot{x} = Ax + Bu + B_1 w \qquad (5.10)$$
$$y = Cx$$

The reference input satisfies the relation given in equation 5.11.

$$\ddot{r} + \alpha_1 \dot{r} + \sigma_2 r = 0 \qquad (5.11)$$

The disturbance also satisfies the same equation

$$\ddot{w} + \alpha_1 \dot{w} + \sigma_2 w = 0 \tag{5.12}$$

The tracking error is;

$$e = y - r \tag{5.13}$$

This formula can be written as;

$$\begin{aligned} \ddot{e} + \alpha_1 \dot{e} + \sigma_2 e &= \ddot{y} + \alpha_1 \dot{y} + \sigma_2 y \\ \ddot{e} + \alpha_1 \dot{e} + \sigma_2 e &= H\ddot{x} + \alpha_1 H\dot{x} + \sigma_2 Hx \end{aligned} \tag{5.14}$$

Replace the plant space vector with the error-space state

$$\xi = \ddot{x} + \sigma_1 \dot{x} + \sigma_2 x \tag{5.15}$$

Replace the control with the control space

$$\mu = \ddot{u} + \sigma_1 \dot{u} + \sigma_2 u \tag{5.16}$$

Replace eqn. 5.14 with;

$$\ddot{e} + \sigma_1 \dot{e} + \sigma_2 e = H\xi \tag{5.17}$$

State equation is given by;

$$\dot{\xi} = \dddot{x} + \sigma_1 \ddot{x} + \sigma_2 \dot{x} = F\xi + G\mu \tag{5.18}$$

The overal system in error space is;

$$
\begin{aligned}
&\dot{z} = Hz + Fu \\
&z = [e \quad \dot{e} \quad \xi^T]^T \\
&H = \begin{bmatrix} 0 & 1 & 0 \\ -\sigma_2 & -\sigma_1 & C \\ 0 & 0 & A \end{bmatrix} \\
&F = \begin{bmatrix} 0 \\ 0 \\ B \end{bmatrix}
\end{aligned}
\tag{5.19}
$$

After getting the overall system of error space, an LQR controller is designed for this new state space representation of the model. Using MATLAB, the algebraic Riccati equation is solved and the control gain K is evaluated for different values of Q and R weighting matrices. This m-file is given in the Appendix A, the Q matrix is assumed in the form of;

$$
Q = \begin{bmatrix} a & 0 & 0 & 0 & 0 & 0 \\ 0 & b & 0 & 0 & 0 & 0 \\ 0 & 0 & c & 0 & 0 & 0 \\ 0 & 0 & 0 & d & 0 & 0 \\ 0 & 0 & 0 & 0 & e & 0 \\ 0 & 0 & 0 & 0 & 0 & f \end{bmatrix}
\tag{5.20}
$$

Where the values of a, b, c, d are the weightings for the states while the weighting matrix R is a scalar value as there is only one control input to the system. The values in the Q matrix are adjusted according to the required response of the system; a higher value of the weightings indicates the importance of the states compared to others. The tuned Q and R values are shown in below;

- x is the weighting for the pendulum displacement
- y is the weighting for the pendulum angular position
- z is the weighting for the error terms

$$Q=\begin{bmatrix} x & 0 & 0 & 0 & 0 & 0 \\ 0 & 1 & 0 & 0 & 0 & 0 \\ 0 & 0 & y & 0 & 0 & 0 \\ 0 & 0 & 0 & 1 & 0 & 0 \\ 0 & 0 & 0 & 0 & z & 0 \\ 0 & 0 & 0 & 0 & 0 & z \end{bmatrix}, R=1 \tag{5.21}$$

#### 5.1.2.1. Error Space Approach for Sinusoidal Type Input

In order to design the error space approach for sinusoidal type of input, the reference input satisfies the differential equation is written as;

$$\ddot{r}=-w_0^2 r \tag{5.22}$$

This means;

$$\begin{aligned} \sigma_2 &= w_0^2 \\ \sigma_1 &= 0 \end{aligned} \tag{5.23}$$

Then the state matrices becomes;

$$A=\begin{bmatrix} 0 & 1 & 0 & 0 & 0 & 0 \\ -1 & 0 & 1 & 0 & 0 & 0 \\ 0 & 0 & 0 & 1 & 0 & 0 \\ 0 & 0 & 0 & 59.47 & 44.03 & -0.4795 \\ 0 & 0 & 0 & 0 & 0 & 1 \\ 0 & 0 & 0 & 119.6 & 93.94 & -0.73 \end{bmatrix}, B=\begin{bmatrix} 0 \\ 0 \\ 0 \\ -3.4190 \\ 0 \\ -5.4470 \end{bmatrix} \tag{5.24}$$

An LQR is designed with the weighting factors given in the form in equation 5.21, are given in equation 5.25 and calculated K gain of the controller is also given in equation 5.25;The simulation of this controller is constructed in Matlab Simulink and given in Figure 35.

$$K = \begin{bmatrix} -9.4405 \\ 70.0848 \\ 80.8548 \\ -23.8347 \\ -64.0588 \\ -9.0152 \end{bmatrix} \text{ for x=100, y=500 and z=5000} \quad (5.25)$$

As it can be seen in the Figure 37, a disturbance is applied to the system. The disturbance is applied to the system in order to see the performance of the system under the disturbance because real systems have some disturbances acting on the system. The weighting factors given in Equation 5.25 are in the form given in Equation 5.21. This means, the role of the tracking reference is important than the role of balancing operation in designed control system.

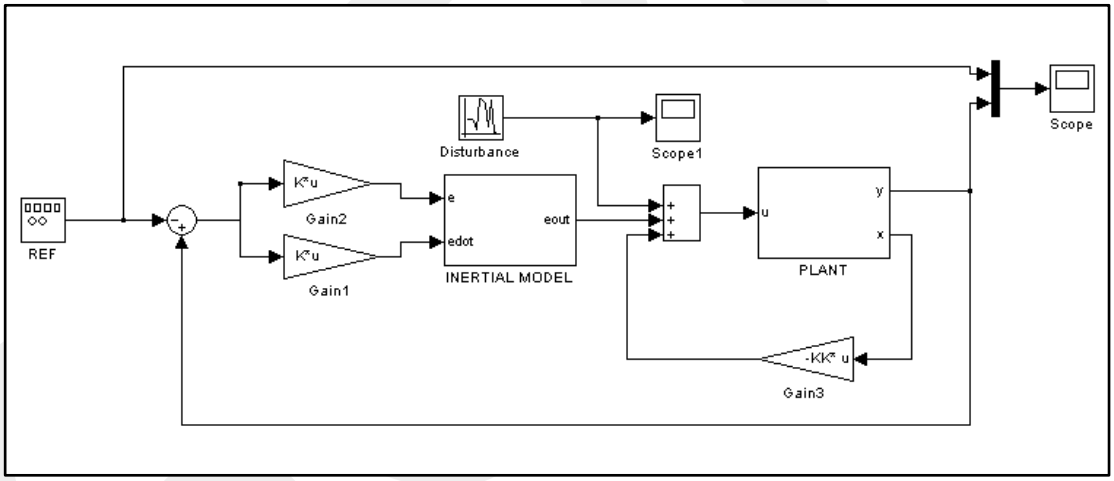


*Figure 37* Simulation of Error Space Controller

The disturbance added to the system, control input sent to the motors and the output of the plant and the reference signal is shown in Figure 36. This means, the effect of the disturbance on the control input and output of the system and the tracking performance of the system are shown in Figure 38.

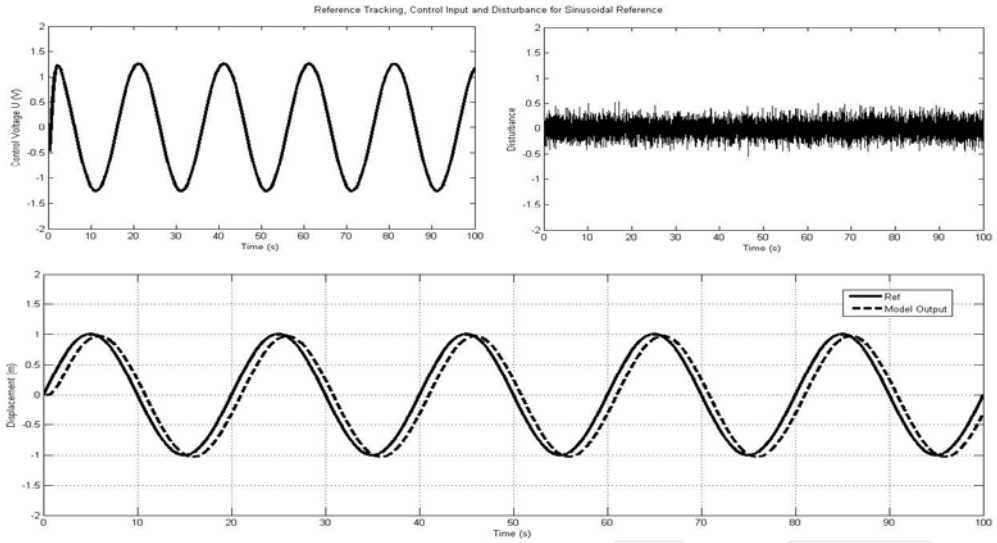


*Figure 38 Reference* Tracking, Control Input and Disturbance for Sinusoidal Reference

As it is shown in Figure 38 system tracks the reference under the effect of disturbance. The error space approach controller is simulated for 0.1Hz, 0.05Hz, 0.2Hz sinusoidal reference signals. The controller is simulated on a reference signal which is made with a summation of 0.1Hz and 1 Hz sinusoidal signal. These simulations are shown in Figure 39.

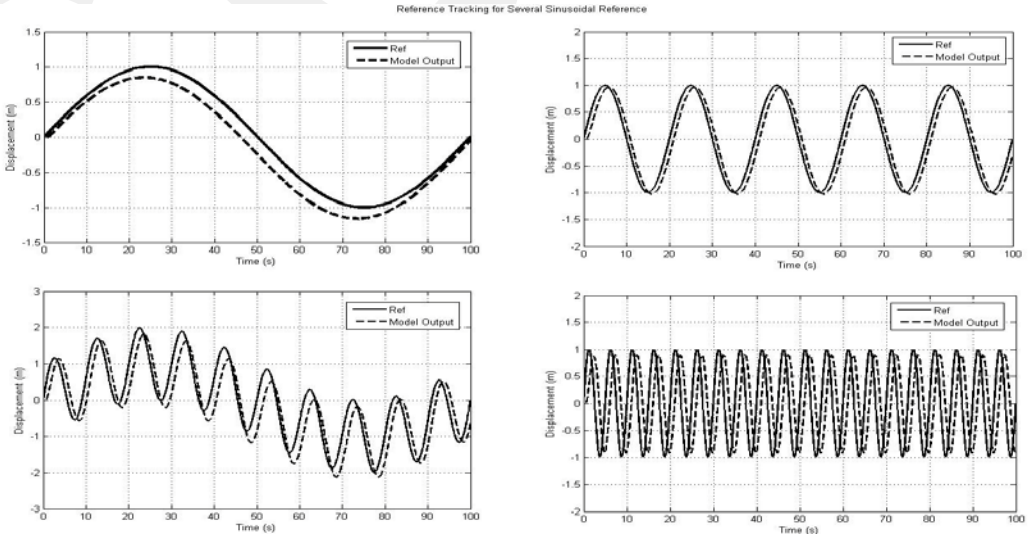


*Figure 39 Reference Tracking for Several Sinusoidal Reference*

As it can be seen in the Figure 39, the model tracks the reference between 0.05Hz and 1Hz and this is a sufficient range for the control system for tracking control in balancing system.

### 5.1.2.2. Error Space Approach for Step Type Input

In order to design the error space approach for step type of input, the reference input satisfies the differential equation is written as;

$$\ddot{r} = 0 \tag{5.26}$$

Then the state matrices becomes;

$$A = \begin{bmatrix} 0 & 1 & 0 & 0 & 0 \\ 0 & 0 & 1 & 0 & 0 \\ 0 & 0 & 59.47 & 44.03 & -0.4795 \\ 0 & 0 & 0 & 0 & 1 \\ 0 & 0 & 119.6 & 93.94 & -0.7302 \end{bmatrix}, B = \begin{bmatrix} 0 \\ 0 \\ -3.419 \\ 0 \\ -5.447 \end{bmatrix} \tag{5.27}$$

An LQR controller is designed with the weighting factors given in the form in Equation 5.21, are given in Equation 5.28 and calculated K gain of the controller is also given in Equation 5.28;

$$K = \begin{bmatrix} 70.7107 \\ 82.6380 \\ -23.6996 \\ -64.4633 \\ -9.1109 \end{bmatrix} \text{ for x=100, y=500 and z=5000} \tag{5.28}$$

As it can be seen in the equation 5.28, the role of the tracking reference is important than the role of balancing operation in designed control system. The simulation of this controller is constructed in Matlab Simulink software and shown in Figure 39. As it can be seen in Figure 40, a disturbance is added to the system also, the control system is expected to reject that disturbance.

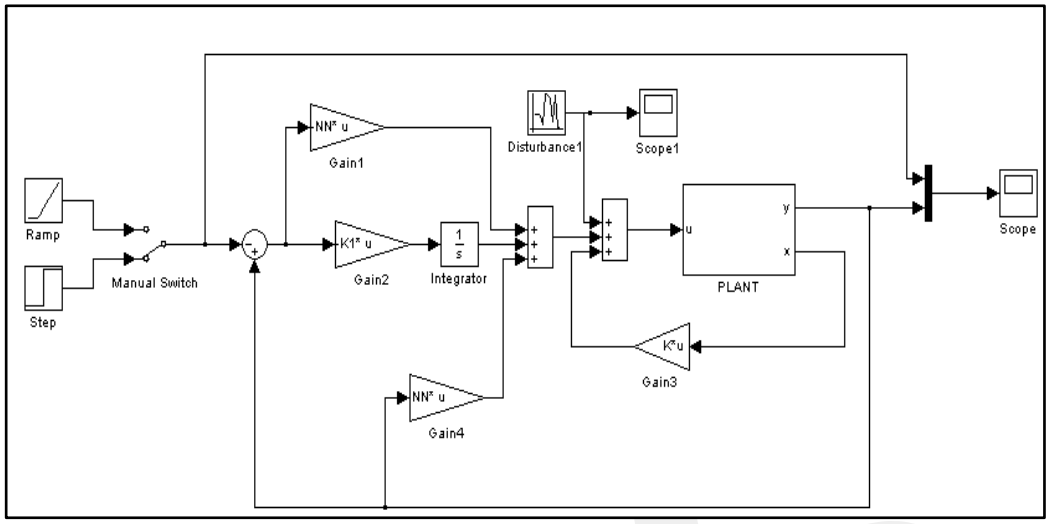


*Figure 40 Simulation* for Steps Type of Input

As it is shown in the Figure 40, a disturbance is added to the system. The disturbance added to the system, the control input u and the output of the plant and the reference signal is shown in Figure 41.

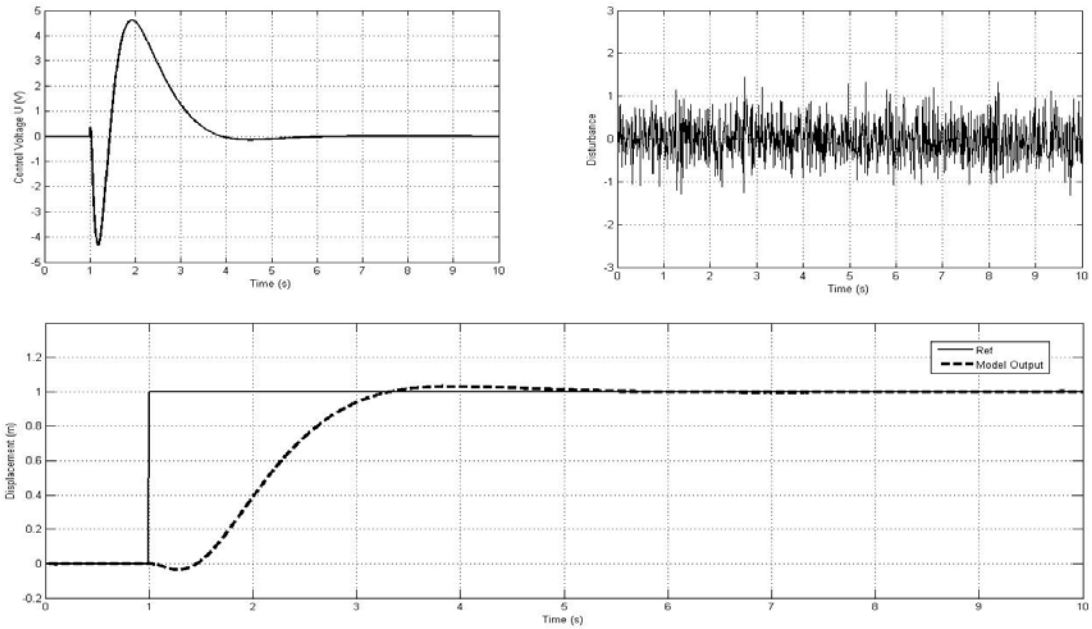


*Figure 41 Disturbance*, Control Input and Tracking of the system vs. Time Plots for Step Reference

As it is shown in Figure 41 system tracks the reference under the effect of disturbance. When a ramp input is applied to the system without any change in the control system, the control input and the output and the reference is shown in Figure 42.

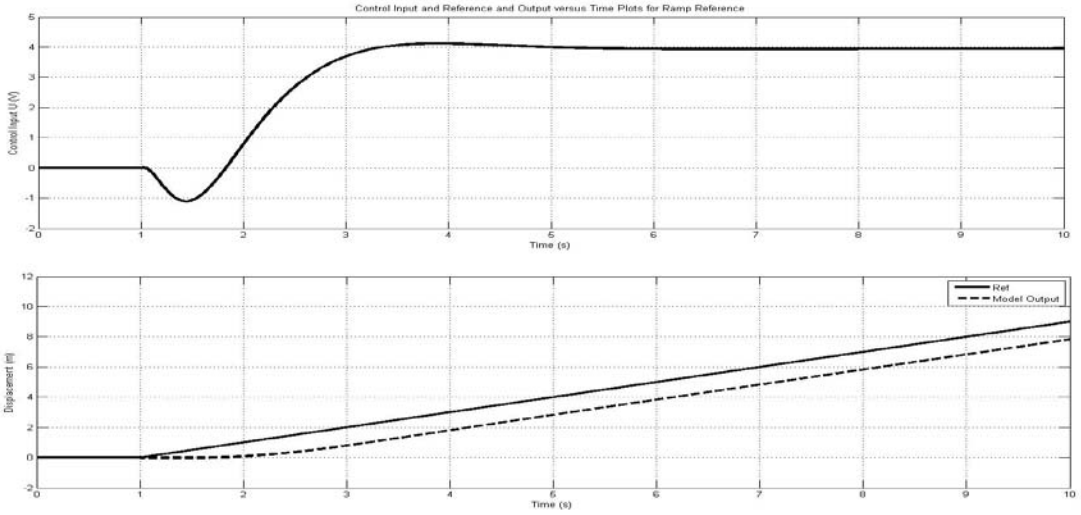


*Figure 42* Control Input and Reference and Output versus Time Plots for Ramp Reference

The same disturbance with the step type reference is applied to the system. It is obvious that there is a steady state error, this error is caused because of the input type, and this control system is designed for step type input and works well with the step type of input. The performance of the designed controller is simulated on the square wave references which have frequencies of 0.2, 0.1, 0.05 and 0.02Hz. These simulations are shown in Figure 43.

The square wave type of input has closer characteristics to the step type of input rather than the ramp type of input. Better results than the results given in Figure 42 because of the input type.

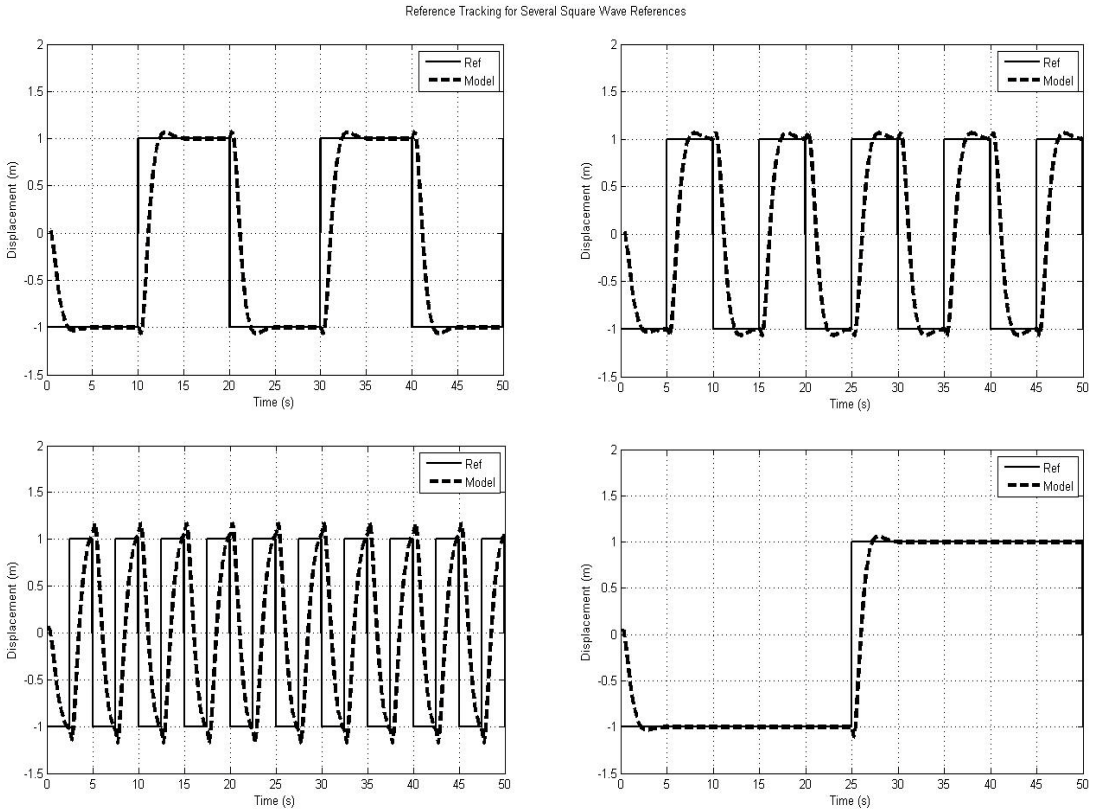


*Figure 43 Reference Tracking for Several Square Wave References*

It can be seen that, in Figure 43, the system cannot track a square wave reference which has a frequency of 0.2Hz, but the system can easily track a square wave reference which has a frequency of 0.1, 0.05, 0.02Hz. This result gives an idea about system dynamics and controller performance, when tracking a square wave type of reference; the frequency should be about 0.05Hz.

## 5.2. Controller System Design for Flying Movement

Similarly, the system is inherently unstable unless it is stabilized and controlled. Open loop response of the system is shown in the Figure 44.

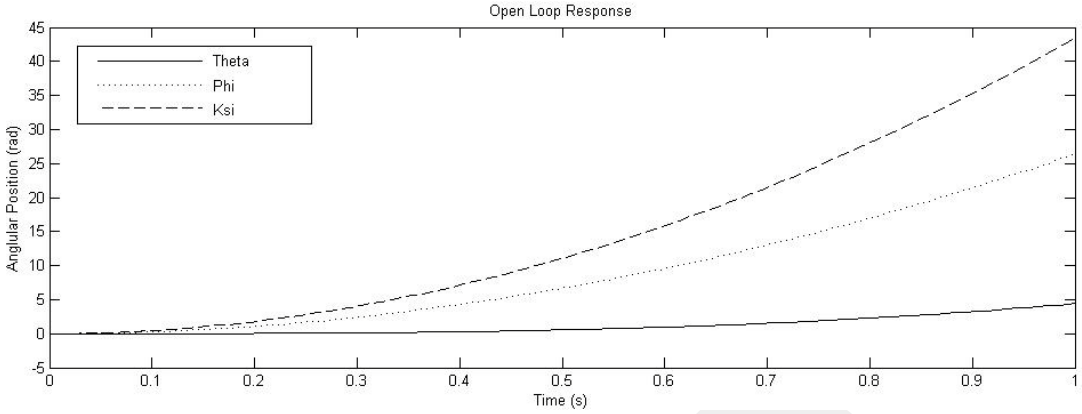


*Figure 44 Open Loop Response*

As it can be easily seen in the Figure 44, system is inherently unstable. In order to stabilize the system control action is needed. The open loop poles of the system are shown in equation 5.29.

$$P = [0 + 0.01i \quad 0 - 0.01i \quad 0 + 0.0076i \quad 0 - 0.0076i \quad 0 \quad 0] \qquad (5.29)$$

The pole zero map of the system is shown in figure 45;

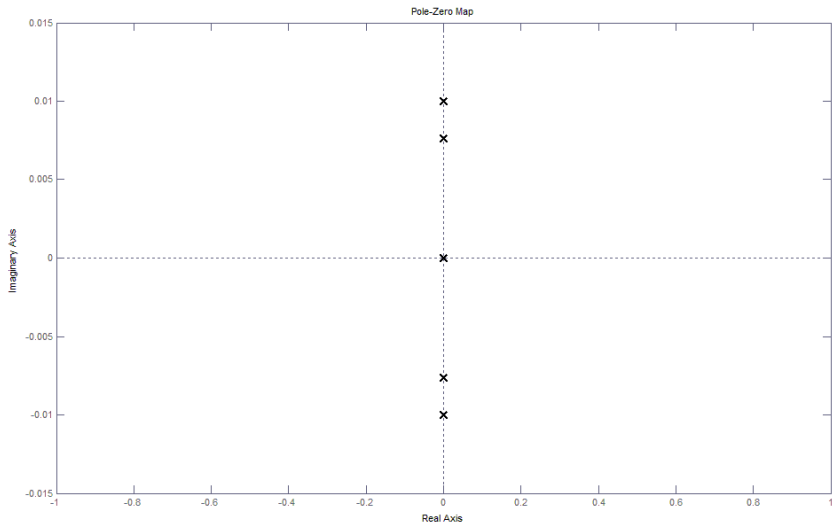


*Figure 45 Pole Zero Map*

### 5.2.2. Linear Quadratic Regulator Design

As control inputs, there are alternatives in flying mode. In addition to the inputs of propeller actuators, voltage to the ground wheel motors can be utilized with the pendulum angle or only voltage to the ground wheel motors can be used or only the pendulum angle can be used. When TWTR is attached to the special joint, voltage to the ground wheels is used in addition to $V_{1,2}$. Also, controllers are designed for the case when only the pendulum angle is used in addition to $V_{1,2}$. As it is mentioned before, regulatory controllers minimize a cost function which was shown in Equation 5.3, with weighting factors supplied by user. For a continuous-time linear system described by;

$$\begin{aligned} \dot{x} &= Ax + Bu \\ y &= Cx + Du \end{aligned} \tag{5.30}$$

Where *K* value which is the controller gain is calculated as in Equation 5.5 and the P is solved by using the continuous time algebraic Riccati equation given in Equation 5.6. R and Q matrices, in Equations 5.3, 5.6 and 5.7, can be described with the weighting coefficients.

$$Q = \begin{bmatrix} W_\phi & 0 & 0 & 0 & 0 & 0 \\ 0 & W_\theta & 0 & 0 & 0 & 0 \\ 0 & 0 & W_\psi & 0 & 0 & 0 \\ 0 & 0 & 0 & W_p & 0 & 0 \\ 0 & 0 & 0 & 0 & W_q & 0 \\ 0 & 0 & 0 & 0 & 0 & W_r \end{bmatrix}, R = \begin{bmatrix} 1 & 0 & 0 \\ 0 & 1 & 0 \\ 0 & 0 & 1 \end{bmatrix} \tag{5.31}$$

Then the control matrix (K) is calculated in Matlab m-file is given in equation 5.32 and the m-file calculates this control matrix (K) is given in Appendix A.

$$K = \begin{bmatrix} 0 & 0 & 0.0003 & 0.0002 & 0 & 0.0001 \\ -0.2861 & 0.0136 & -3.1620 & -1.5035 & -0.0001 & -0.9992 \\ 31.7788 & 0.1782 & -0.0286 & 334.3198 & 1.6581 & -0.3063 \end{bmatrix} \tag{5.32}$$

The new poles of the system become;

$$P_{New} = \begin{bmatrix} -5208.3 \\ -3.2 + 1.5i \\ -3.2 - 1.5i \\ -3.2 \\ -0.2 \\ -0.004 \end{bmatrix} \tag{5.9}$$

Every pole is on the left hand side, this means the system became stable. The simulation of the designed LQR control system is carried out with using Matlab/Simulink software and shown in Figure 46.

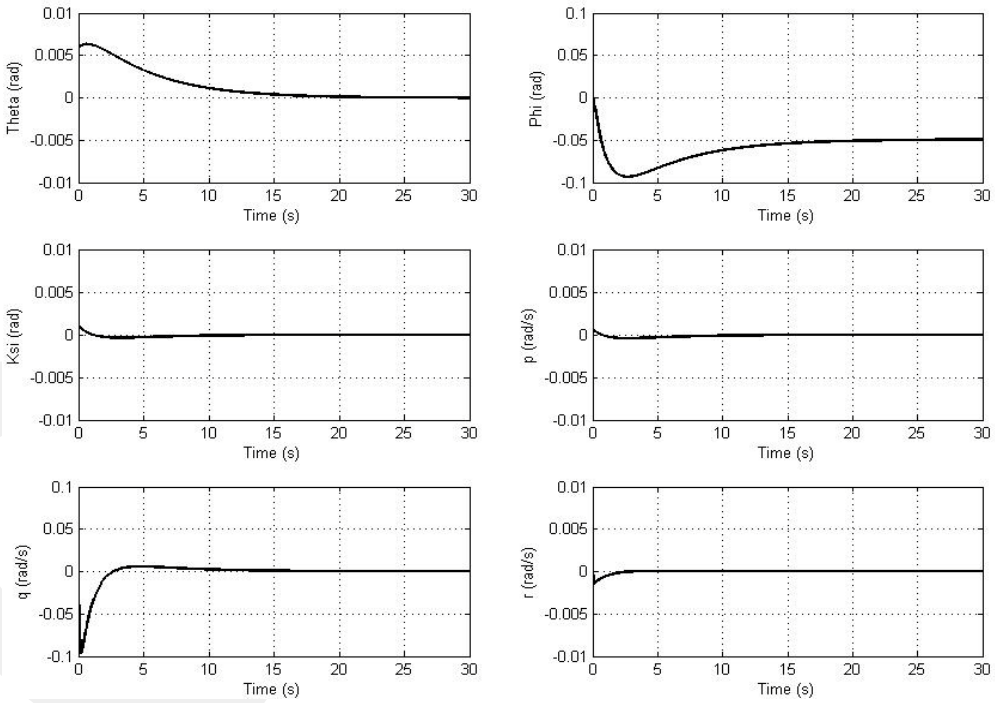


*Figure 46 LQR Control System Performance*

As it can be seen on Figure 46, the states of the model are stabilized with the designed LQR control system.

# CHAPTER 6

# EXPERIMENTS

As it is mentioned in Chapter 4, a physical prototype of the TWTR system is constructed with the control hardware. In this Chapter, the results of LQR and error space controllers for the ground movement and LQR and PID controller systems for attitude stabilization in flying motion are explained in detail and the comparison between physical system and the model is also given.

In order to perform the experiments on the physical system, two test stands are prepared. One test stand is prepared for testing the ground movements of the system and the other test stand is prepared for testing the flying movements of the TWTR system. The test stand for ground tests is shown in the Figure 47.

As it can be easily seen from Figure 47, the test stand contains TWTR structure (DC Motors, wheels, rods, etc…), IMU, encoder, DAQ card, motor driver, power supply, PC and control hardware and software. The measurements are taken from the encoders and IMU and collected with control hardware and processed and stored with the help of control software.

The data collection process is carried out with the help of the cables, the power delivered to the system and the motor signals (control input) are carried with cables. Noise shielded cables are used for data flow.

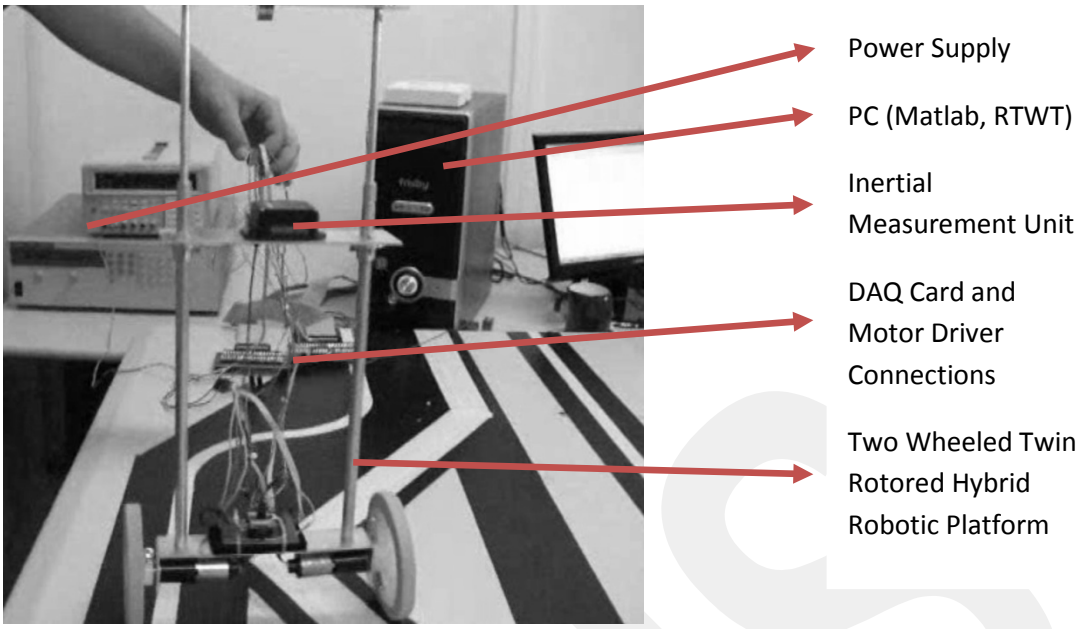


*Figure 47 Test Stand for Ground Movements*

The test stand for implementing control system designed for flying movements of TWTR system is shown in Figure 48.

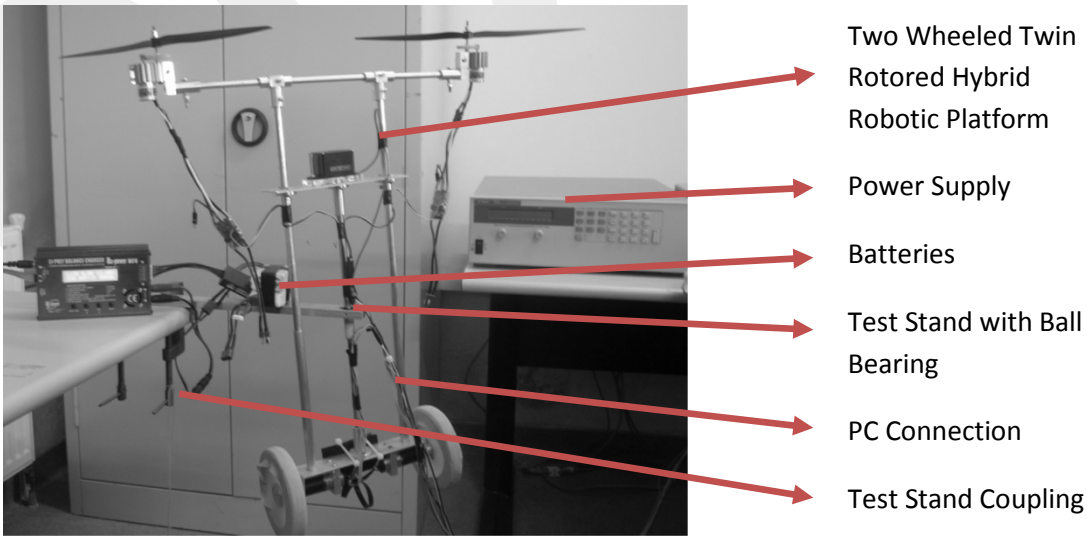


*Figure 48 Test Stand for Flying Movements*

The test stand, which is prepared for testing the flying movements of the twin rotor two wheeled hybrid robot is composed of a rod which assembles the stand to a fixed frame (table), a spherical joint mounted on the assembled rod which provides the ability of moving in roll, yaw and pitch axes, control software and hardware and power supply and batteries. The twin rotor two wheeled hybrid robot system is mounted to the spherical joint from its center of mass.

### 6.1. LQR Experiments for Ground Movement

In order to implement the designed linear quadratic regulator controller on the real system, a Matlab Simulink model using Real Time Windows Target is constructed. This model is shown in the Figure 49.

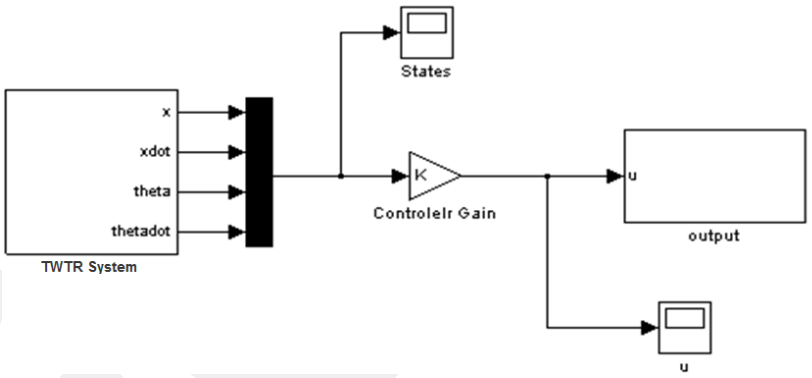


*Figure 49* Simulink Model for LQR Experiment

The model has package input block in order to get data from IMU, encoder input block in order to get encoder data, calibration blocks in order to have correct measurements from sensors, frequency output block in order to adjust the speed of the DC motors, digital output blocks for setting the direction of the DC motor turning and controller gain block in order to implement the LQR controller on the physical system. The controller gain K is calculated in Chapter 3 and it is adjusted during the

experiment to give the best results in LQR control. It is expected from the controller to damp all of the states to zero. The calculated controller gain from the mathematical model is given in below;

$$K = [3.1623 \quad 27.55 \quad -44.47 \quad -4.45] \tag{6.1}$$

The change in states of the system and the control input u, which makes the system states remain in zero is shown in Figure 50. From the change in states during the experiment which is shown in Figure 50, it can be seen that there is an oscillation in the system. The oscillation on the system can be seen in the linear and angular velocity states more, but in the linear and angular position states, the oscillation is not that much. There is an oscillation effect on the control input sent to the actuators; it is an expected result because there was an oscillation on the system. The critical point in the control input is not to exceed the actuators limit. In two wheeled balance robot experiment used actuators are DC Motors and have a maximum 10V voltage level. This means the actuator limit is not exceeded.

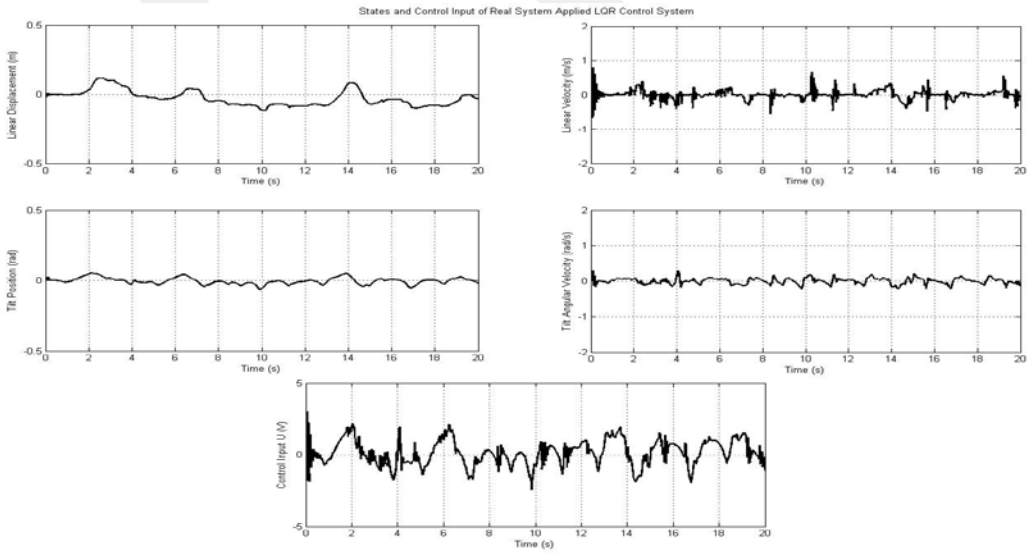


*Figure 50 Sta*tes and Control Input Graphs for Applied LQR Controller

The calculated LQR controller gain given in equation 6.1 is implemented on the mathematical model derived in Chapter 3. In order to make the model more realistic, a disturbance formed of Gaussian distributed random signal is added to the system. The linear position and tilt angular position of the real system and the model is shown in Figure 51.

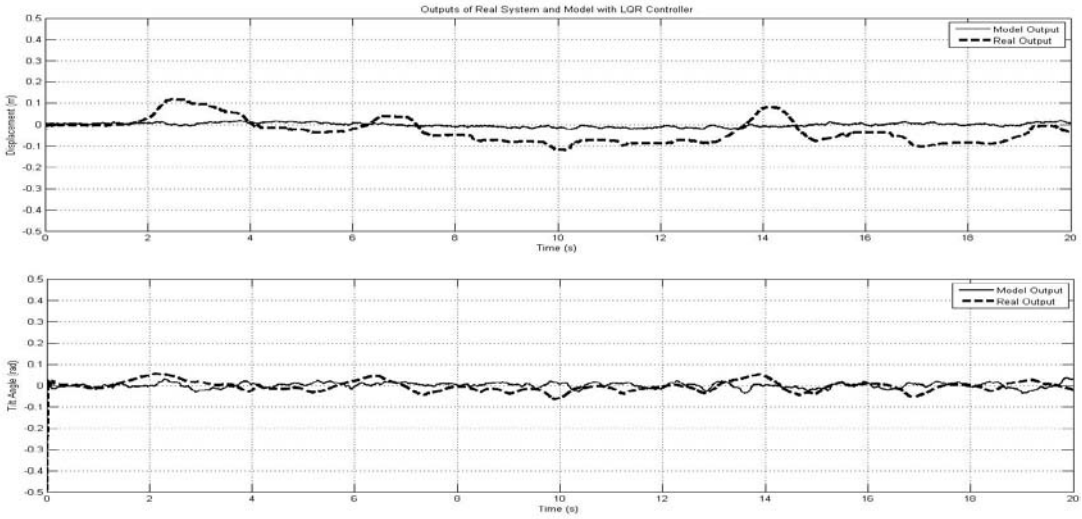


*Figure 51 Outputs of the Real System and Mathematical Model*

As it can be seen in Figure 51, the linear displacement of the real system nearly matches with the model and the tilt angular position of the real system exactly matches with the model. This means the derived mathematical model fits the real system well.

In Figure 51, the oscillation in linear displacement state is about limits of 0.1 meters and -0.1 meters, in order to damp this oscillation the weighting of linear displacement and linear velocity states in Q matrix is increased, the calculated controller gain is given in below;

$$K = [10 \quad 31.46 \quad -32.99 \quad -3.3643] \tag{6.2}$$

The change in states of the system and the control input u, for the calculated LQR controller gain given in Equation 6.2 is shown in Figure 52.

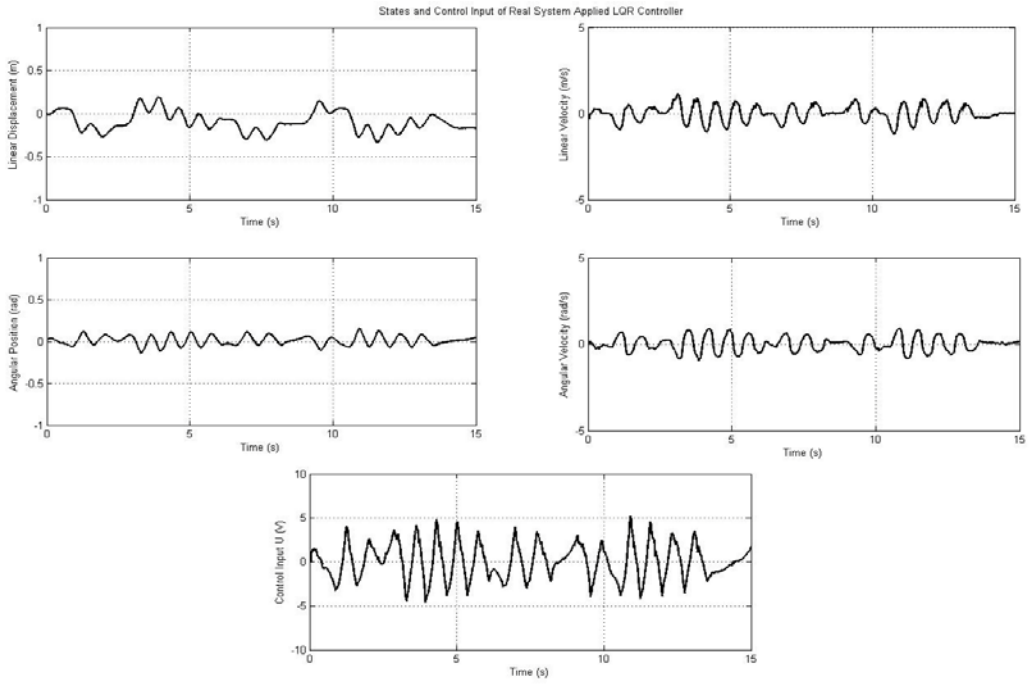


*Figure 52 States and Control Input Graphs for Applied LQR Controller Gain Calculated with High Linear Velocity and Linear Position Weightings*

As it can be seen Figure 51, that the oscillation in tilt angular position and tilt angular velocity states are increased, and this oscillation in tilt angle effects the linear displacement and linear velocity states of the system. As it is mentioned before in Chapter 3, the critical states in two wheeled balance system are tilt angular position and tilt angular velocity. The weightings of these states in Q matrix should be higher than the weightings of other states.

In order to damp the oscillations shown in Figure 51, the weightings of the tilt angular position and tilt angular velocity in Q matrix are increased. The weightings of the linear displacement and linear velocity states were increased before; this means the weightings of all of the states are increased when the Q matrix is

compared with the matrix used in experiment shown in Figure 50. The calculated LQR gain matrix K is shown in below;

$$K = [18 \;\; 35.73 \;\; -62.68 \;\; -5.26] \tag{6.3}$$

The calculated LQR controller gain given in equation 6.2 is implemented on the mathematical model also. The linear position and tilt angular position of the real system and the model is shown in the figure 53.

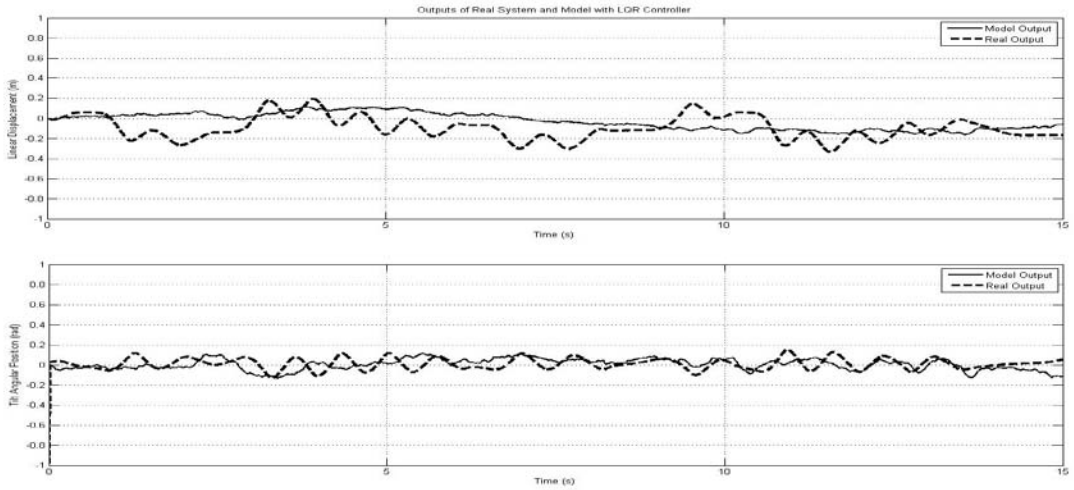


*Figure 53 Outputs of the Real System and Mathematical Model for LQR Gain Given in Eqn. 6.2*

As it can be seen in Figure 53, the linear displacement and the tilt angular position of the real system exactly matches with the model with using the LQR controller gain given in Equation 6.2. The linear displacement state has a oscillation but the angular position state fits very well with the results of the simulations.

The change in states of the system and the control input u, for the calculated LQR controller gain given in Equation 6.3 is shown in Figure 5.

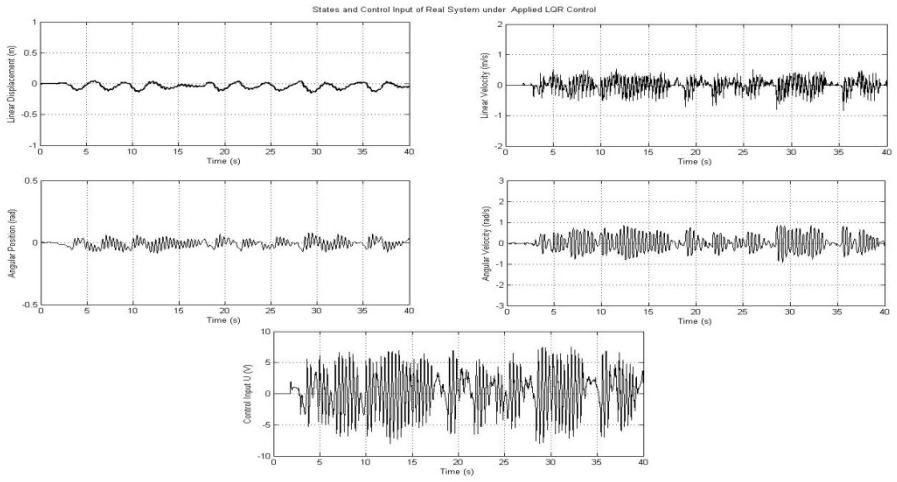


*Figure 54 States and Control Input Graphs for Applied LQR Controller Gain Calculated with High Weightings*

As it can be seen in Figure 54, the oscillation in linear displacement state is damped; the system oscillates between 0.05m and -0.05m, but the oscillation in other states is increased. This increased oscillation affects the calculated control input u also.

### 6.2. Error Space Approach Experiments for Ground Movement

In order to implement the designed error space controller on the real system, a Matlab Simulink model using Real Time Windows Target is constructed. This model is shown in the Figure 55.

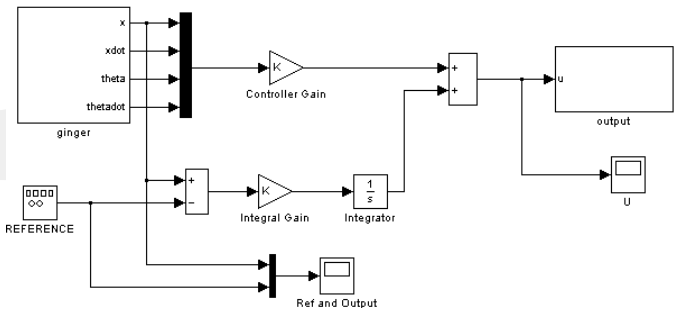


*Figure 55 Error Space Controller Implementation Model*

As it is mentioned in Chapter 4 before, in designing the error space approach controllers, the characteristics for the reference which will be tracked should be known. The error space controller is designed and implemented for sinusoidal and step type references.

### 6.2.1. Error Space Approach for Step Type Reference

The controller gain K and integral action gain for the step type of reference are calculated from the mathematical model. This mathematical model is given in Chapter 3 and the calculation of the controller gains are shown in Chapter 4. These calculated controller gains are adjusted during the experiment to give the best results in error space control. It is expected to track the reference given to the system. The system is designed to track reference in displacement state. The change in states while tracking the reference, the reference tracked and corresponding control input u is shown in Figure 56. The controller is designed for step type of reference but a square wave type of reference is given for the system to track.

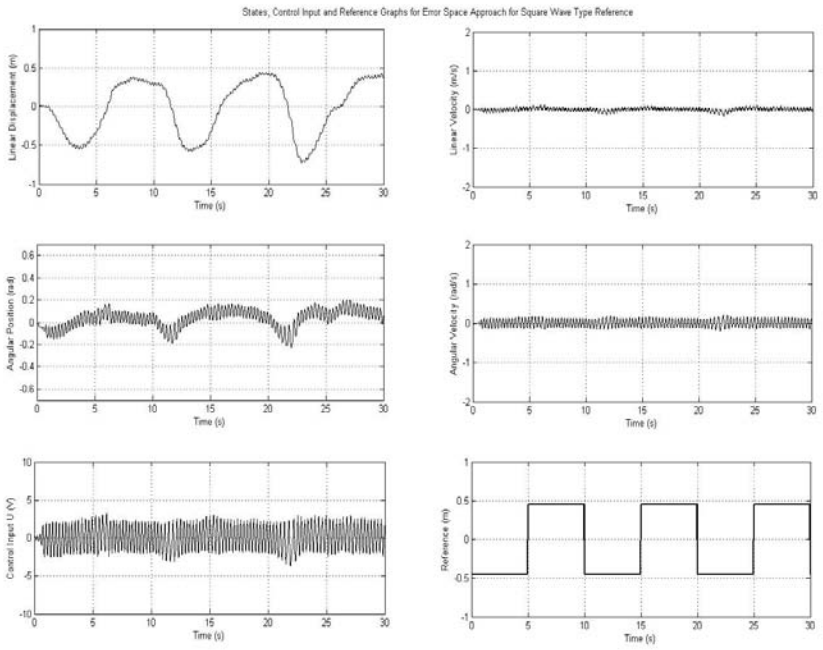


*Figure 56 Change in States, Control Input U and the Reference Tracked for Step Type Reference*

From the change in states shown in Figure 56, it can be seen that the linear displacement state tracks a reference and angular position, angular velocity and the linear velocity states have an oscillation because of the tracking operation. The linear displacement state also has oscillations but the main tendency is to track the reference. The tilt angular position state has a little oscillation and it is about zero level. This means the system is in balance.

There is an oscillation on the control input sent to the actuators which can be also seen in Figure 56; it is expected because this oscillation is caused from balancing control action applied from the tilt angular position and velocity. Another point is not to exceeding the actuators limit, it is seen that the control input does not exceed the actuator limit. The linear displacement of the system and the reference tracked is shown on the same plot in Figure 57.

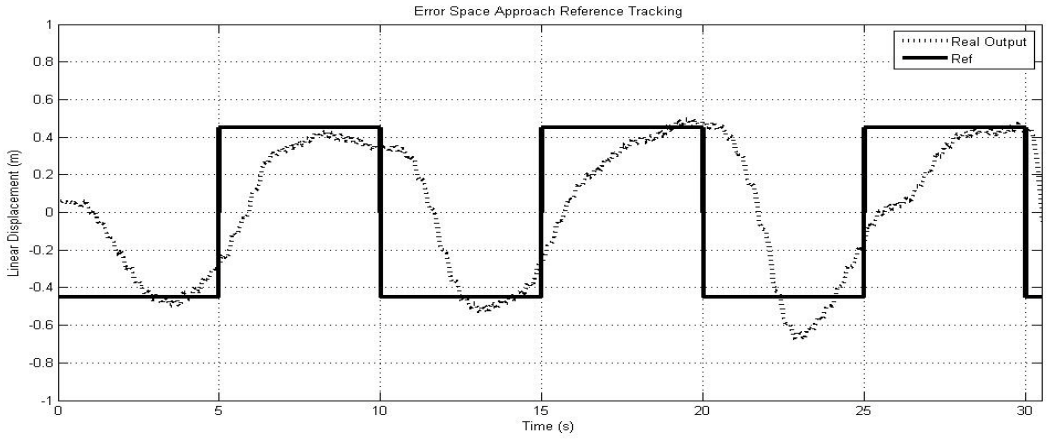


*Figure 57 Reference Tracking of the System for Step Type Reference*

In Figure 57, it can be seen that the system tracks the reference but there is a delay occurred in tracking the reference.

The adjusted controller gain and integral action gain is applied to the twin rotor two wheeled hybrid robot mathematical model for ground movements which is derived in Chapter 3 in Matlab Simulink. The reference tracking of the model and the real

system is shown on the same plot given in Figure 57. The tracked reference is also shown in the figure 57.

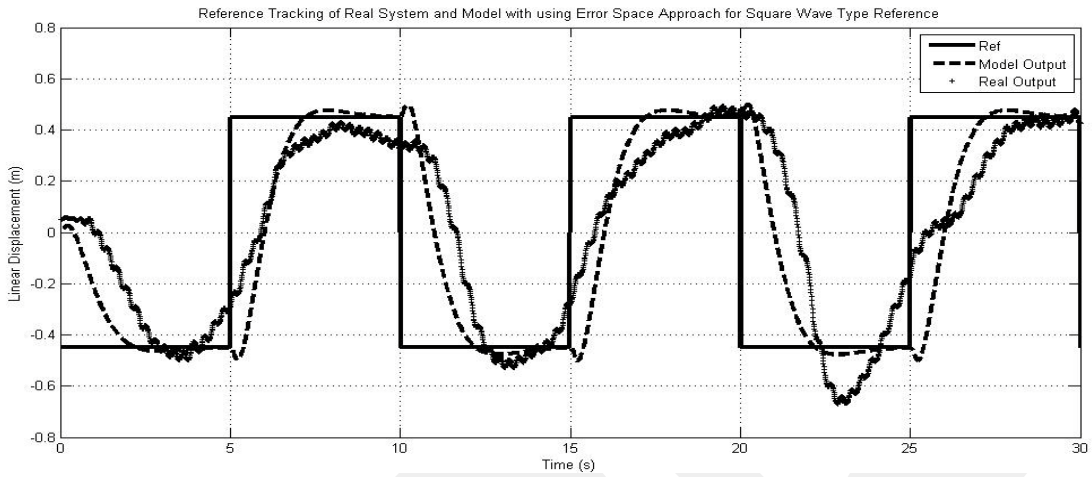


*Figure 58 Reference Tracking of Model and Real System for Step Type Reference*

From the comparison between model and the real system, it has been seen that the output of the mathematical model fits with the output of the real system very well. The occurred delay in reference tracking is also occurred in mathematical model. To sum up, it can be stated that the error space controller designed for step type of references tracks the reference very well.

### 6.2.2 Error Space Approach for Sinusoidal Type Reference

The controller gain K and integral action gain for the sinusoidal type of reference are calculated from the mathematical model. These calculated controller gains are again adjusted as implementing the error space controller for step type of reference, during the experiment to give the best results. The system is designed to track reference in displacement state. The change in states while tracking the reference, the reference tracked and corresponding control input u is shown in Figure 59.

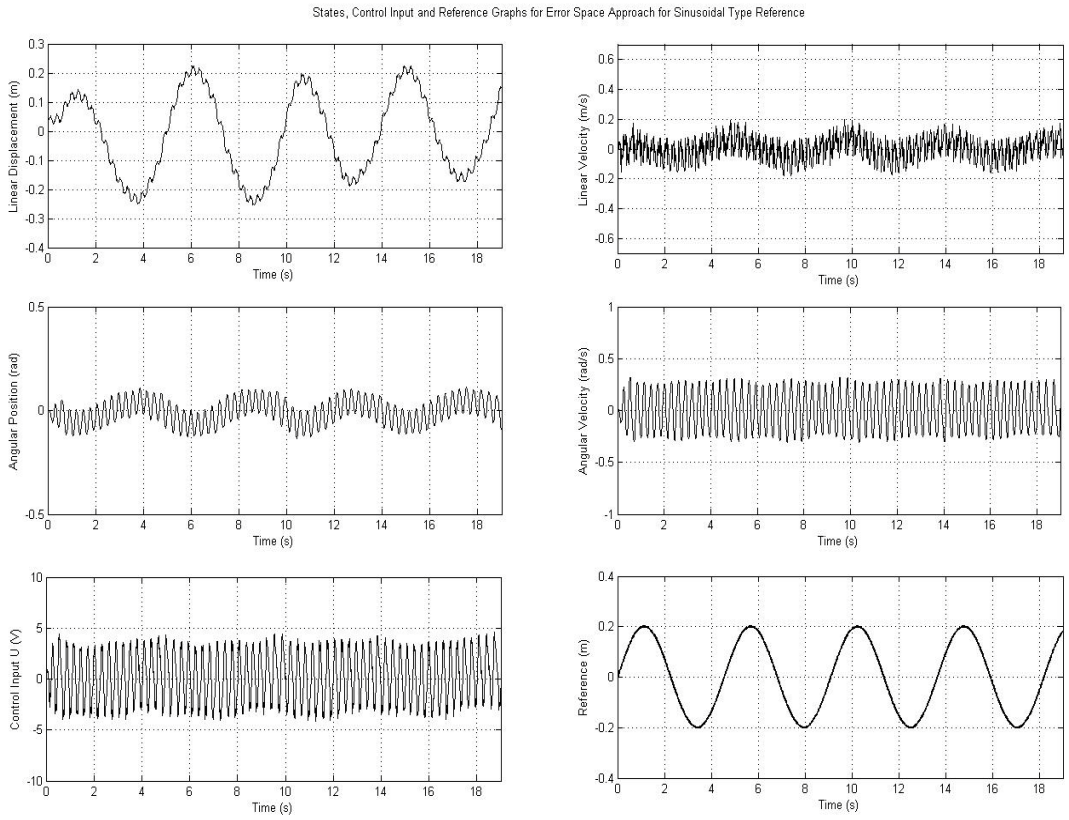


*Figure 59 Change in States, Control Input and the Reference Tracked for Sinusoidal Type Reference*

From the change in states shown in Figure 59, it can be seen that the linear displacement state tracks a reference but it has small oscillations during this tracking operation. These small oscillations can be seen well on angular position, angular velocity and the linear velocity states. The linear displacement state has also oscillations but the main tendency is to track the reference. There is an oscillation on the control input sent to the actuators which can be also seen in Figure 59.

The linear displacement of the system and the reference tracked is shown on the same plot in Figure 60.

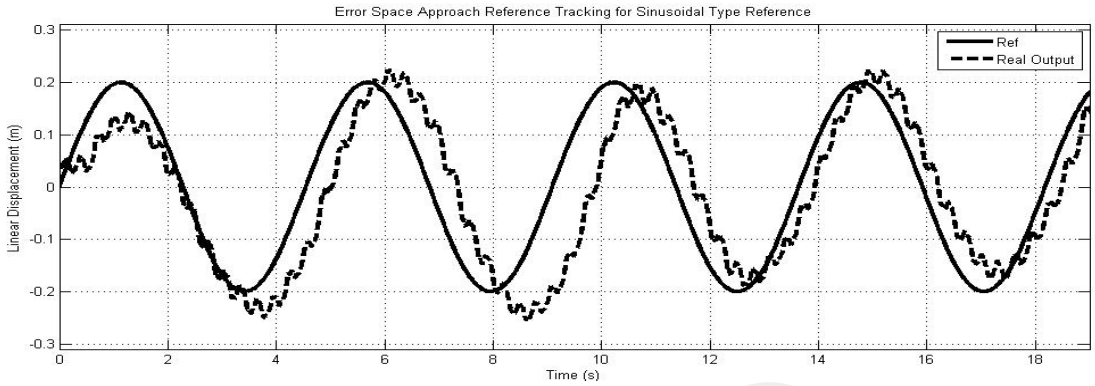


*Figure 60 Reference Tracking of the System for Sinusoidal Type Reference*

In Figure 60, it can be seen that the system tracks the reference well, but there is a delay occurred in tracking the reference. The adjusted controller gain and integral action gain is applied to the twin rotor two wheeled hybrid robot mathematical model for ground movements which is derived in Chapter 3 in Matlab Simulink. The reference tracking of the model and the real system is shown on the same plot given in Figure 61. The tracked reference is also shown in Figure 61.

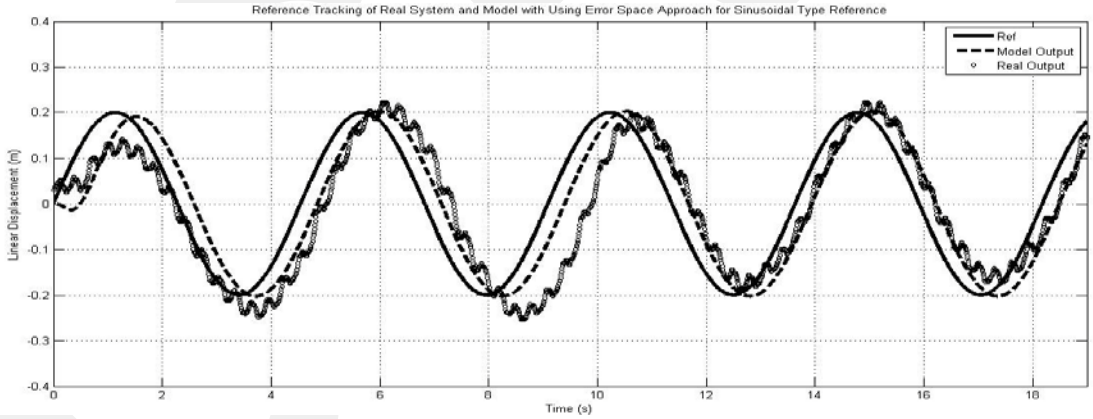


*Figure 61 Reference Tracking of Model and Real System for Step Type Reference*

As it can be seen in Figure 62, the same delay which the physical system has, also be seen in the reference tracking of the model. Actually, the real system fits very well with the reference tracking of the model, but there is small oscillations in the real system, this means there are small disturbances acting on the system which are not concluded in mathematical model.

### 6.3. PID Control Experiments for Stabilization in Flying Movement

In order to stabilize the TWTR system which means holding roll, yaw and pitch angles at zero position in flying movements, three PID controllers are tuned for each axis. This PID controller schematic is shown in the Figure 62.

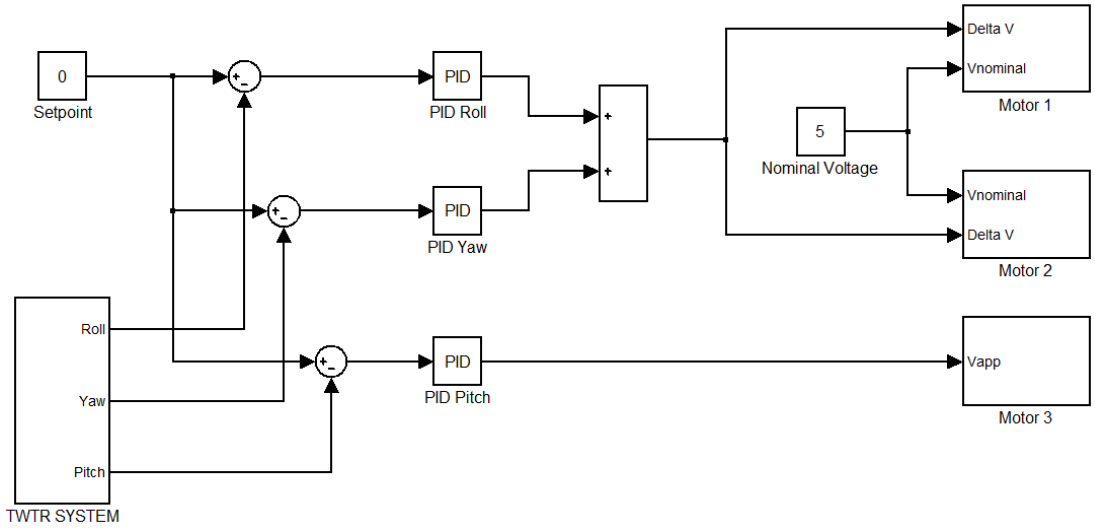


*Figure 62 PID Controller Schematic for TWTR System*

As it can be seen from Figure 62, the roll and yaw dynamics of the system are coupled and controlled by the motor 1 and motor 2 which has the propellers and the pitch dynamic of the system is controlled by the motor 3 which has the wheel. The roll, yaw and the pitch angles are measured with the IMU sensor as radians and the input of the control system are the voltages applied to the actuators. The PID parameters are tuned experimentally and shown in the Table 3.

*Table 3 Tuned PID Controller Parameters for Stabilization*

| | Roll Axis | Yaw Axis | Pitch Axis |
|---|---|---|---|
| P | 2.9 | 2.2 | 7.15 |
| I | 2.1 | 1.3 | 1.3 |
| D | 0.9 | 0.8 | 2.05 |

The performances of the tuned PID controllers are shown in the Figure 63. It can be seen from the Figure 63 that, the roll and yaw dynamics are stabilized, but the pitch dynamic cannot be stabilized. The main effect in the pitch dynamic of the system is the acceleration of the wheel rotation. If the system cannot stabilize itself on a disturbance or initial condition in a short time period, the wheel which controls the pitch dynamic reaches its maximum acceleration and cannot stabilize itself again.

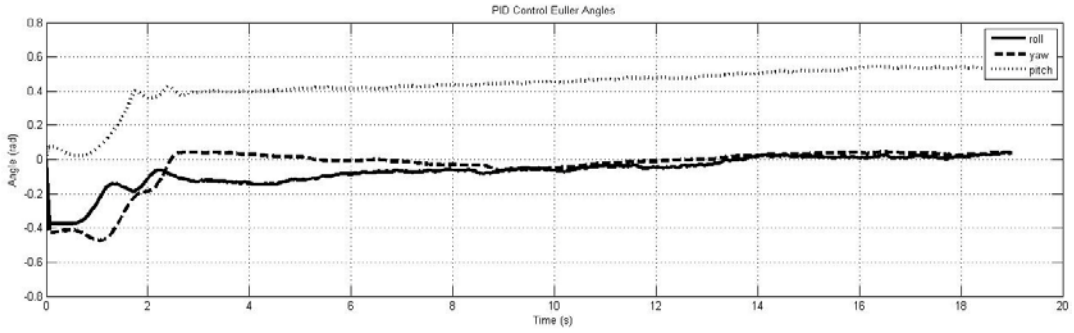


*Figure 63 Performance of Tuned PID Controllers on Each Axis*

Because of these reasons a bang bang (Three position controller) controller is implemented on pitch axis and PID controllers are implemented for roll and yaw axes. The implemented bang bang controller is shown as a graph in the Figure 64.

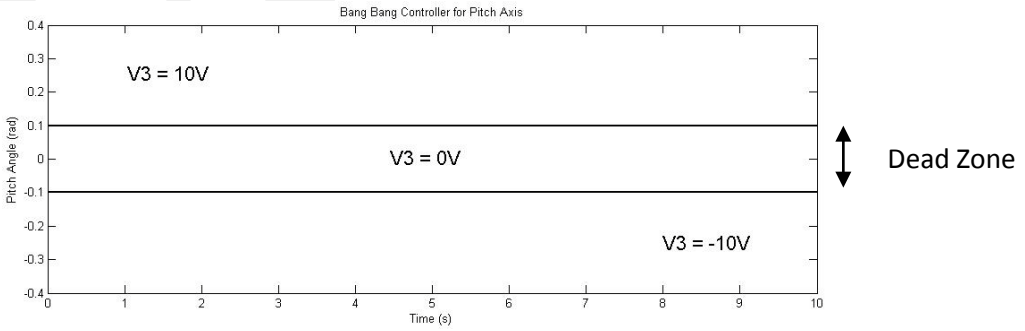


*Figure 64 Bang Bang (Three position controller) Controller Designed for Pitch Axis*

The Pitch angle values 0.1 radian and -0.1 radian are the dead zone limits for the bang bang controller. When the bang bang controller shown in Figure 64 is applied to the system the schematic of the control system becomes as in Figure 65. The tuned PID values for yaw and roll axes given in Table 3 are used in order to stabilize these axes and the bang bang controller is used in order to stabilize the pitch axis.

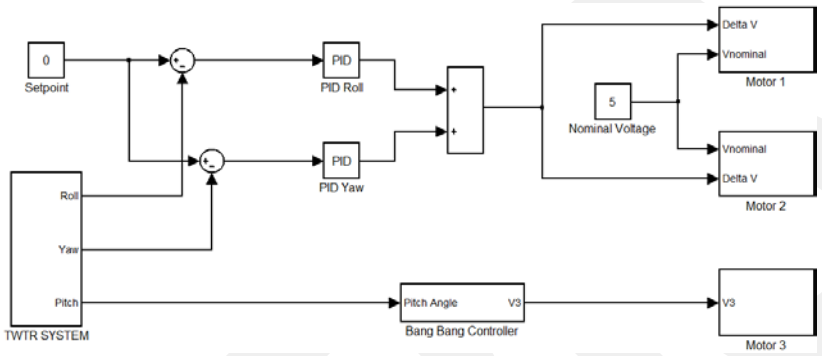


*Figure 65 Implementation of Bang Bang Controller for Pitch Axis*

The performance of the control system shown in Figure 65 is shown in the Figure 66 as two experiments with different initial conditions for each axis are ;

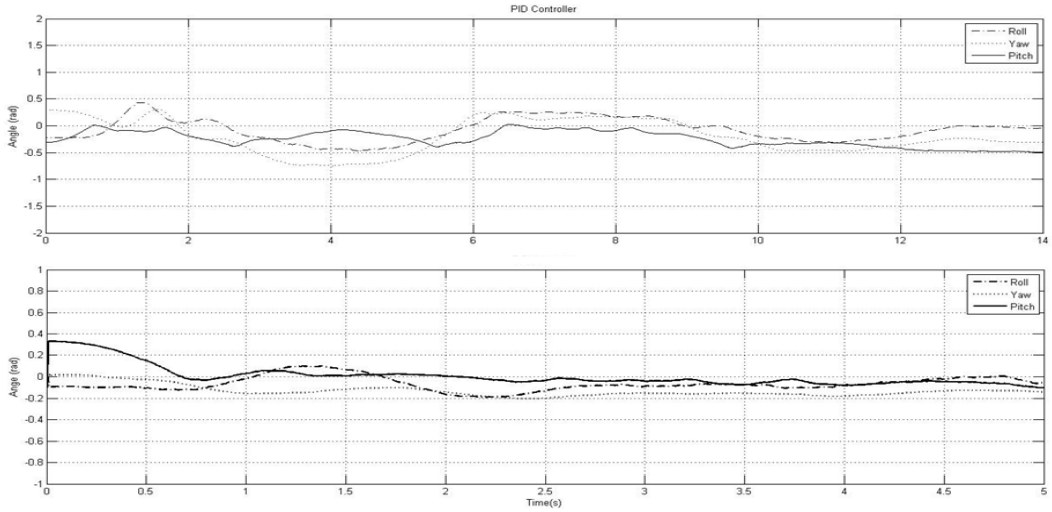


*Figure 66 Performance of the PID and Bang Bang Controllers*

From Figure 65, it can be seen that the pitch dynamic is stabilized with the use of bang bang controller, it can be seen that the system is able to stabilize itself from a initial condition about 0.4 rad in pitch axis, the roll and yaw axes are stabilized with the tuned PID controller parameters also.

### 6.4. Vertical Take-off Preparation Experiment

TWTR system has ability of two wheeled balance and vertical take-off. As it is mentioned before, the switching between the control systems are succeeded with the proximity sensor or switches. In Figure 67, the performance of the TWTR system on two wheeled ground motion with effect of the propeller motion.

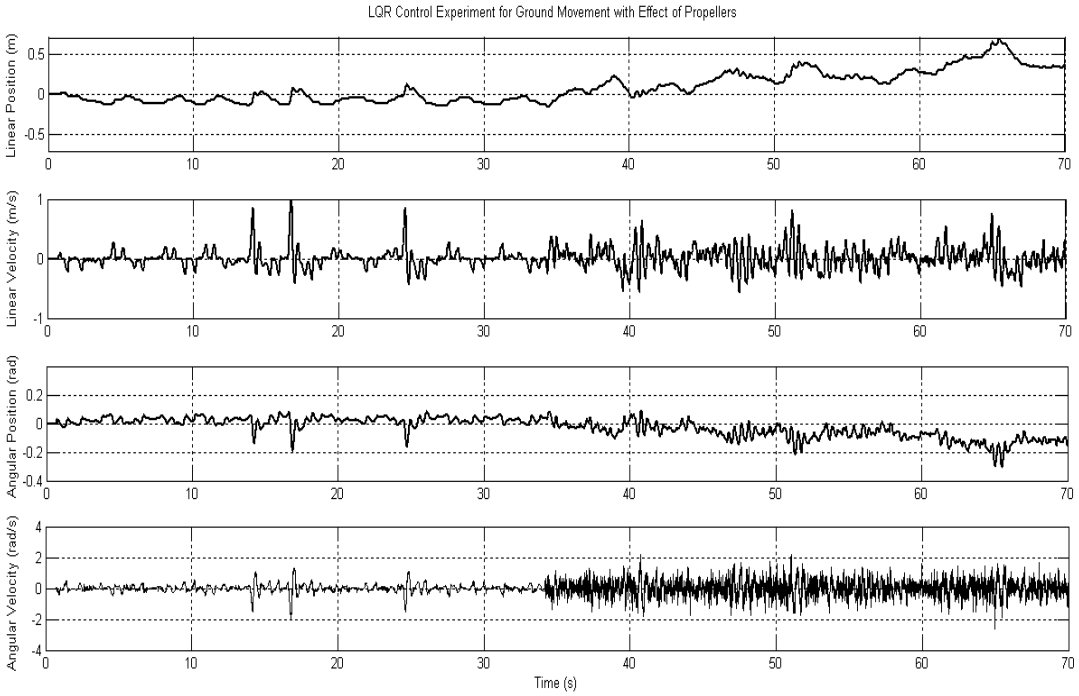


*Figure 67 Performance of the Ground Motion under Propeller Motion Disturbance*

In Figure 67, at time 35 s, the propellers stars motion and the effect of these propeller motion are clearly seen, but the system is still stabilized under this disturbance.

# CHAPTER 7

# RESULTS AND CONCLUSION

This thesis is the starting point of a study that aims to design and build up a hybrid robot navigating on ground while stabilizing itself on 2 wheels. It is also desired to hover and navigate in air by using the propellers, ground wheels, and the pendulum. The scope of the thesis covers to design a prototype based on mechatronics design principles including the actuators, drivers, sensor set, microcontroller to drive the digital servo, control hardware and algorithm.

The sensor set is composed of an IMU, encoder, and the proximity sensor. All data are acquired and processed in real time. Necessary algorithm is derived in Matlab, Simulink and Real Time Windows Target blockset. Blocks are constructed to read out the sensor measurements and to send the control inputs to the actuators.

Prototype is modified throughout the study to analyze the dynamics on ground and in air. One of the major goals of this thesis is to physically observe the dynamics of the hybrid system. It is important to see that control algorithms are different for each mode. This means that, the controllers should be switched from one mode to the other. This is a really critical task. Behavior should be switched. Proximity sensor is placed to aid the switching operation. However, additional sensors, such as force sensors, should be placed to achieve a proper switching between the control modes.

It is seen that TWTR can stabilize itself on ground and can track the reference position inputs. System can reject disturbances that can be seen in recorded data and videos. While stabilizing on the ground, propellers are ignited and accelerated by increasing the nominal voltage applied to the propellers. As it is increased, the thrust generated by the propellers also increase. This results the decrease in the weight of

the structure on ground. Consequently the traction between the wheels and ground is also reduced. Stabilizing on the ground becomes more difficult. However, the controller can cope with these effects up to a certain level. Since the switching procedure is not completely studied, platform starts to float on ground and may become unstable before taking off vertically. Managing the taking off vertically while the platform stabilizes itself on ground is one the future aims of this study.

Attitude stabilization is also studied in the thesis. Alternatives exist in selecting the control inputs. Use of ground wheels together with propeller inputs is the major aim. However, it is seen that inertia of the wheel may not be sufficient to generate the enough torque to stabilize the pitch dynamics. Therefore, an active pendulum is also utilized in the system. Battery packs of the brushless DC motors are placed at the tip of the pendulum. Location of the packs is changed by the servo motor that rotates the pendulum. Use of such additional subsystem may be advantageous during the critical take off period. On ground stabilization actions and take off stabilization actions may be decoupled by using the pendulum. Wheels are employed to stabilize the system on ground. Pendulum may assist the system during this period.

A combination of ground wheels and pendulum in the attitude stabilization and take-off period should be studied. Due to the weight reduction in the take-off phase and switching phases adaptive and/or robust control algorithms should be employed. In addition to the attitude and heading stabilization, altitude control will be studied by using the data from proximity sensor.

Use of embedded control hardware is planned as a future work in the project. Cables may cause some undesired disturbances. In addition, structural modifications are also necessary due to the vibration problem seen with the operation of the propellers. This problem also causes the saturation of the inertial sensors. This vibration and saturation degrades the performance of the IMU and accuracy of the Euler angles is decreased enormously. Therefore, structural design should be revised.

The thesis proposed a novel hybrid robotic platform. Basic mathematical models are constructed and basic controllers are designed. It is seen that the prototype can be modified and used in certain indoor and outdoor applications. The hovering ability of

the TWTR hybrid platform may be used for various tasks. Taking over the obstacles by flying over them is one of the major skills of the designed robot. It will gain this kind of skills in the future phases of the project.

# REFERENCES


1. J. A. Smith, I. Sharf and M. Trentini, 2006, "PAW, A Hybrid Wheeled-Leg Robot", *Proceedings of the 2006 IEEE International Conference on Robotics and Automation*, pp.4043-4048, Orlando, U.S.A.
2. G. Besseron, Ch. Grand, F. B. Amar and Ph. Bidaud, 2008, "Decoupled Control ofthe High Mobility Robot Hylos based on a Dynamic Stability Margin", *IEEE/RSJ International Conference on Intelligent Robots and Systems*, pp.2435-2440, Acropolis Convention Center, U.S.A.
3. M. Kumagai and K. Tamada, 2008, "Wheel Locomotion of a Biped Robot Using Passive Rollers", *Journal of Robotics and Mechatronics*, Vol.20, No.2, pp. 206-212
4. B. Yamauchi and P. Rudakevych, 2004, "Griffon: A Man-Portable Hybrid UGV/UAV", *Industrial Robot*, vol. 31, no. 5, pp. 443-450.
5. R. J. Bachmann, F. J. Boria, P. G. Ifju, R. D. Quinn, J. E. Kline, and R. Vaidyanathan, 2005, "Utility of a sensor platform capable of aerial and terrestrial locomotion", *International Conference on Advanced Intelligent Mechatronics*, pp.1581–1586.
6. P. Deegan, B. J. Thibodeau and R. Grupen, 2006, "Designing a Self Stabilizing Robot For Dynamic Mobile Manipulation", University of Massachusetts Amherst, Amherst
7. Y. Takahashi, T. Takagaki, J. Kishi, and Y. Ishii, 2001, "Back and Forward Moving Scheme of Front Wheel Raising for Inverse Pendulum Control Wheel Chair Robot", *Proceedings of the 2001 IEEE International Conference on Robotics & Automation*, pp. 3189-3194.
8. Wei-chen Lee, Hung-yan Gu, Kuo-Liang Chung, C.Y. Lin, Chin-Shyurng Fahn, Yah–Syun Lai, Chih–Cheng Chang, Chia–Lun Tsai, 2007, "The Realization of a

Music Reading and Singing Two-Wheeled Robot", *Advanced Robotics and Its Social Impacts, ARSO 2007*, pp. 1-6.

9. S. W. Nawawi, M. N. Ahmad and J. H. S. Osman, 2006, "Variable Structure Control of Two-Wheels Inverted Pendulum Mobile Robot", *Regional Postgraduate Conference on Engineering and Science*, pp. 197-201, Johore
10. E. Minnaert, B. Hemmelman and D. Dolan, 2008, "Inverted Pendulum Design With Hardware Fuzzy Logic Controller", *Journal of Systemics, Cybernetics and Informatics*, Vol. 6, No. 3, pp. 34-39.
11. K. Pathak, J. Franch and S. K. Agrawal, 2005, "Velocity and Position Control of a Wheeled Inverted Pendulum by Partial Feedback Linearization", *IEEE Transactions on Robotics*, Vol.21, No.3, pp. 505-513.
12. S. Kalra, D. Patel and K. Stol, 2007, "Design and Hybrid Control of a Two Wheeled Robotic Platform", *In Proceedings 2007 Australasian Conference on Robotics and Automation*.
13. R. C. Ooi, 2003 ,"*Balancing a Two-Wheeled Autonomous Robot*", University of Western Australia
14. W. Zhou, 2008 ,"Platform for ergonomic steering methods investigation of "Segway-style" balancing scooters", University of Waikato.
15. Y. Kim, S. H. Kim, and Y. K. Kwak, 2005, "Improving Driving Ability for a Two-Wheeled Inverted-Pendulum-Type Autonomous Vehicle", *Proceedings of the Institution of Mechanical Engineers. Part D, Journal of Automobile Engineering*, Vol. 220, n 2, pp. 165-175
16. S. W. Nawawi, M. N. Ahmad and J. H. S. Osman, 2006, "Control of Two-wheels Inverted Pendulum Mobile Robot Using Full Order Sliding Mode Control", *Proceedings of International Conference on Man-Machine Systems*, Langkawi, Malaysia
17. S. W. Nawawi, M. N. Ahmad and J. H. S. Osman, 2008, "Real-Time Control of a Two-Wheeled Inverted Pendulum Mobile Robot", *International Journal of Computer, Information and Systems Science, and Engineering*, Winter 2008, pp. 70-76.

18. F. Grasser, A. D'Arrigo, S. Colombi and A. Rufer, 2002, "JOE: A Mobile, Inverted Pendulum", *IEEE Transactions on Industrial Electronics*, Vol 49, pp. 107-114.
19. V. Coelho, S. Liew, 2008, "Hardware Integration of a Mobile Two-Wheel Balancing Platform for Autonomous Applications", *The UoA Undergraduate Mechatronics Research Journal*, Vol. 1, pp. 21-26.
20. M. Baloh and M. Parent, 2003, "Modeling and Model Verification of an Intelligent Self-Balancing Two-Wheeled Vehicle for an Autonomous Urban Transportation System", *The Conference on Computational Intelligence, Robotics, and Autonomous Systems*, Dec. 15 2003, Singapore.
21. H. Ozaki, T. Ohgushi, T. Shimogawa and C. Lin, , 2001 "Position and Orientation Control of a Wheeled Inverted Pendulum", *JSME Int Journal. Ser C. Mech Systems, Mach Elem Manuf,* Vol.44, No.1, Pg.188-195.
22. Tayebi and S. McGilvray, 2006, "Attitude Stabilization of a VTOL Quadrotor Aircraft", *IEEE Transactions on Control Systems Technolohy*, Vol. 14, No. 3, pp. 562 -571.
23. S. Bouabdallah, P. Murrieri and R. Siegwart, 2004, "Design and control of an indoor micro quadrotor", *IEEE International Conference on Robotics and Automation*, No. 21, pp. 4393-4398, New Orleans, U.S.A.
24. S. Bouabdallah, A. Nothand and R. Siegwart, 2004, "PID vs LQ Control Techniques Applied to an Indoor Micro Quadrotor" *Intelligent Robots and Systems Proceedings 2004 IEEE/RSJ International Conference*, Volume: 3, pp. 2451- 2456 .
25. S. Bouabdallah and R. Siegwart, 2005, "Backstepping and Sliding-mode Techniques Applied to an Indoor Micro Quadrotor", *Proceedings of the 2005 IEEE International Conference on Robotics and Automation*, pp. 2259-2264, Barcelona, Spain.
26. Ö. Kıvrak, 2006, "Design of Control Systems for a Quadrotor Flight Vehicle Equipped with Inertial Sensors" Msc. Thesis, Mechatronics Eng. Dept., Atılım University, ANKARA

27. T. T. Nwe, T. Htike, K. M. Mon, Z. M. Naing and Y. M. Myint, 2008, "Application of an Inertial Navigation System to the Quad-rotor UAV using MEMS Sensors", *World Academy of Science, Engineering and Technology*, Vol. 42, pp. 578-582
28. S. D. Hanford, L. N. Long, and J. F. Horn, 2005, "A Small Semi-Autonomous Rotary-Wing Unmanned Air Vehicle (UAV)", *American Institute of Aeronautics and Astronautics, Infotech, Aerospace Conference*, Paper No. 2005-7077
29. G. Angeletti, J.R. Pereira Valente, L. Iocchi, D. Nardi, 2008, "Autonomous Indoor Hovering with a Quadrotor", *Intl. Conf. On Simulation, Modeling and Programing for Automous Robots*, pp. 472-481, Venice, Italy.
30. G. V. Raffo, M. G. Ortegaand, F. R. Rubio, 2008, "Backstepping/Nonlinear $H_\infty$ Control for Path Trackingof a QuadRotor Unmanned Aerial Vehicle", *American Control Conference*, pp. 3356-3361, Westin Seattle Hotel, Seattle, Washington, U.S.A.
31. J. Escareno, A. Sanchez, O. Garcia, R. Lozano, 2008, "Triple Tilting Rotor mini-UAV: Modeling and Embedded Control of the Attitude", *American Control Conference*, pp. 3476-3481 Westin Seattle Hotel, Seattle, Washington, U.S.A.
32. S. Salazar-Cruz, F. Kendoul, R. Lozano and I. Fantoni, 2008, "Real-Time Control of a Small-Scale Helicopter Having Three Rotors", *IEEE Transactions on Aerospace and Electronics Systems*, Vol. 44, No. 2, pp. 783-794.
33. P. Rongier, E. Lavarec and F. Pierrot, 2005, "Kinematic and Dynamic Modeling and Control of a 3-Rotor Aircraft", *Robotics and Automation (ICRA)*, pp. **2**606-2611.
34. Budiyono, S. S. Wibowo, 2007, "Optimal Tracking Controller Design for a Small Scale Helicopter", *Journal of Bionic Engineering* 4, pp. 271−280.
35. S. M. Ahmad, A. J. Chipperfield and M. O. Tokhi, 2003, "Dynamic Modelling and Linear Quadratic Gaussian Control of a Twin-rotor Multi-input Multi-output System", *Proc. Instn Mechanical Engineers*, Vol. 217, Part I, pp. 203-227.
36. J. Verhaevert and J. Beyens, 2007, "Study and Realisation of Controlling a Twin Rotor", *Vehicular Technology Conference IEEE 65th***,** pp. 2535-2539, Dublin, Irland.

37. F. Kendoul, I. Fantoni, R. Lozano, 2005, “Modeling and control of a small autonomous aircraft having two tilting rotors”, *Proceedings of the 44th IEEE Conference on Decision and Control, and the European Control Conference*, pp.8144-8149, Seville, Spain.
38. Tayebi and S. McGilvray, 2006, “Attitude Stabilization of a VTOL Quadrotor Aircraft”, IEEE Transactions on Control Systems, Vol. 14, No. 3, pp. 562 -571.
39. P. Bauer, G. Ritzinger, A. Soumelidis and J. Bokor, 2008, “LQ Servo control design with Kalman filter for a quadrotor UAV”, *Periodica Polytechnica Transportation Engineering*, Vol. 33 1-2, pp. 9-14.
40. Uy-Loi Ly, 1997, “Stability and Control of Flight Vehicle”, Department of Aeronautics and Astronautics, University of Washington.

# APPENDIX

## APPENDIX A MATLAB CODES

```
% ------------------------------------------------------------------
%            Mathematical Model of the TWTR System on Ground
%                     Prepated by Doğanç KÜÇÜK
% Msc Thesis Atılım University Mechatronics Engineering Department
% ------------------------------------------------------------------

clear all; clc

% Setting the symbolic values.
syms Mb Mw r Iw n Kt Ke b R L Ib g x dx ddx th dth ddth Va f1 f2 f3
f4

% Equations from free body diagram and implementation of Newton's
2nd law
% EOM 1.
E1=(-0.5*Mb*r-
Mw*r)*ddx+((Iw+n*n*Kt*Ke+b*R)/r)*dx+(0.5*Mb*r*L*cos(th))*ddth-
(0.5+Mb+r+L+sin(th))*dth*dth-((n*Kt*Ke+b*R)/R)*dth-((n*Kt)/R)*Va;

% EOM 2.
E2=(Ib+2*Mb*((L*cos(th))^2+(L*sin(th))^2))*ddth+((2*n*Kt*Ke-
2*b*r)/r)*dth+(-2*Mb*L*cos(th))*ddx+((2*n*n*Kt*Ke-
2*n*r)/(R*r))*dx+((2*n*Kt)/R)*Va-2*Mb*g*L*R*sin(th);

% Solving the equations.
S=solve(E1,E2,ddth,ddx)

% Collecting the equations.
(collect(S.ddx,[x,dx,th,dth,Va]))
(collect(S.ddth,[x,dx,th,dth,Va]))
f1=dx;
f2=S.ddx;
f3=dth;
f4=S.ddth;

% Declaring the states and control input.
x = [x dx th dth];
u=[Va];

% Linearization.
As=jacobian([f1;f2;f3;f4],x)
Bs=jacobian([f1;f2;f3;f4],u)


%The Numerical Values
Ke=0.0059;                      %Back EMF constant (Vs/rad)
```

```
Kt=0.0059;                          %Motor torque constant (Nm/A)
R=1.71;                             %Nominal Terminal Resistance (Ohm)
Ib=0.0044;                          %Inertia of the body(kg*m^2)
Iw=0.000237;                        %Inertia of the wheel(kg*m^2)
g=9.81;                             %Gravity(m/s^2)
L=0.6;                              %Length of body (m)
n=19;                               %Gear Ratio
r=0.115;                            %Radius of wheel(m)
Mw=0.144;                           %Mass of wheel(kg)
Mb=1.323;                           %Mass of body(kg)
th=0;                               %initial conditions
dth=0;                              %initial conditions
dx=0;                               %initial conditions
Va=0;                               %Sampling Time
Ts=0.01;
b=0.001;

As=subs(As);
A=double(As);

Bs=subs(Bs);
B=double(Bs);

C=[1 0 0 0;0 0 1 0];
D=[0;0];
SYS=ss(A,B,C,D)

Co=ctrb(SYS);
Ob=obsv(SYS);

disp('Controllability and Observability Matrix RANKS')
Controllability=RANK(Co)
Observability=RANK(Ob)


%x is the weighting for the TWTR System Linear Position
%y is the weighting for the TWTR System Angular Position

x = 100; y =400;

Q = [x 0 0 0;
     0 1 0 0;
     0 0 y 0;
     0 0 0 1];

R =5;

%Finding the LQR Gain for the SS System
[K,S,E] = LQR(A,B,Q,R)
```

```
% ------------------------------------------------------------------
%       Mathematical Model of the TWTR System for Flying Motion
%                      Prepated by Doğanç KÜÇÜK
% Msc Thesis Atılım University Mechatronics Engineering Department
% ------------------------------------------------------------------

clear all; clc;
syms p q r theta phi ksi L Lp F1 F2 Tw mp g bw Kt Ke R J n Md1 Md2
dtw Tw dMd1 dMd2 b Omega0 Ke Km R V1 V2 V3 d n dphi dtheta dksi dp
dq dr J beta h Ix Iy Iz Mx My Mz beta M1 M2 d b k1 k2

I=[Ix 0 0;0 Iy 0;0 0 Iz];

w=[p;q;r];

F1=b*(k1*V1+k2)^2;
F2=b*(k1*V2+k2)^2;
M1=(d/b)*F1;
M2=(d/b)*F2;
Tw=0;

Mx=(F1-F2)*L/2;
My=Tw+mp*g*Lp*cos(theta)*sin(beta);
Mz=M1-M2;
M=[Mx;My;Mz];

ddtw=(n*Kt/(J*R))*V3-((n*Kt*Ke+R*bw)/(J*R))*dtw;
dphi=(p+q*tan(theta)*sin(phi)+r*tan(theta)*cos(phi));
dtheta=(q*cos(phi)-r*sin(phi));
dksi=(q*sec(theta)*sin(phi)+r*sec(theta)*cos(phi));

dw=inv(I)*(-(cross(w,I*w))+M);

dp=dw(1);
dq=dw(2);
dr=dw(3);


x=[phi;theta;ksi;p;q;r];
u=[V1;V2;beta];
dxnn=[dphi;dtheta;dksi;dp;dq;dr];
dxnn=subs(dxnn);

As=jacobian(dxnn,x);
Bs=jacobian(dxnn,u);

% Parameters and operating point;

V1=7;
V2=7;
V3=0;
b=9.81*0.0023/1000;
d=58*b;
phi=0;
```

```
theta=0;
ksi=10*pi/180;
p=0;
q=0;
r=0.01;
beta=0;

Ix = 66480231.70e-9;
Lxy = 7903.96e-9;
Lxz = -253.96e-9;
Lyx = 7903.96e-9;
Iy = 83273387.20e-9;
Lyz = -47689.61e-9;
Lzx = -253.96e-9;
Lzy = -47689.61e-9;
Iz = 17663034.71e-9;

Ke=0.0059;
Kt=0.0059;
R=1.71;
bw=0.0023;
n=19;
J=0.000237;
mp=0.270;
Lp=0.125;
k1=64.51;
k2=93.26;
g=9.81;
L=0.4;

As=subs(As);
A=double(As);

Bs=subs(Bs);
B=double(Bs);


C=eye(6);
D=[zeros(6,3)];

SYS=ss(A,B,C,D)
P=pole(SYS)
pzmap(SYS)

Co=ctrb(SYS);
Ob=obsv(SYS);

disp('Controllability and Observability Matrix RANKS')
Controllability=RANK(Co)
Observability=RANK(Ob)
```

```
%%%%%%%%%%%%%%%%%
%LQR control design
%%%%%%%%%%%%%%%%%

Q = [100 0 0 0 0 0;
     0 100 0 0 0 0;
     0 0 100 0 0 0;
     0 0 0 10 0 0;
     0 0 0 0 10 0;
     0 0 0 0 0 10];

R =[10 0 0; 0 10 0; 0 0 10];

%Calculation of LQR Gain
[K,S,E] = LQR(A,B,Q,R)
```

## APPENDIX B TECHNICAL DRAWINGS

| PART NO. | PART NAME | QTY. |
|---|---|---|
| 1 | Link 1 | 2 |
| 2 | Link 2 | 2 |
| 3 | T Connector | 2 |
| 4 | Link 3 | 1 |
| 5 | U Connector | 1 |
| 6 | Maxon Motor | 2 |
| 7 | Wheel Connector | 2 |
| 8 | Wheel | 2 |
| 9 | Link Holder | 2 |
| 10 | Middle Link | 1 |
| 11 | Sensor Holder | 1 |
| 12 | Sensor Connector | 2 |
| 13 | Microstrain Gx2 IMU | 1 |
| 14 | Brushless Motor Holder | 2 |
| 15 | Brushless Motor Set | 2 |
| 16 | Propeller | 2 |
| 17 | Motor Holder | 2 |

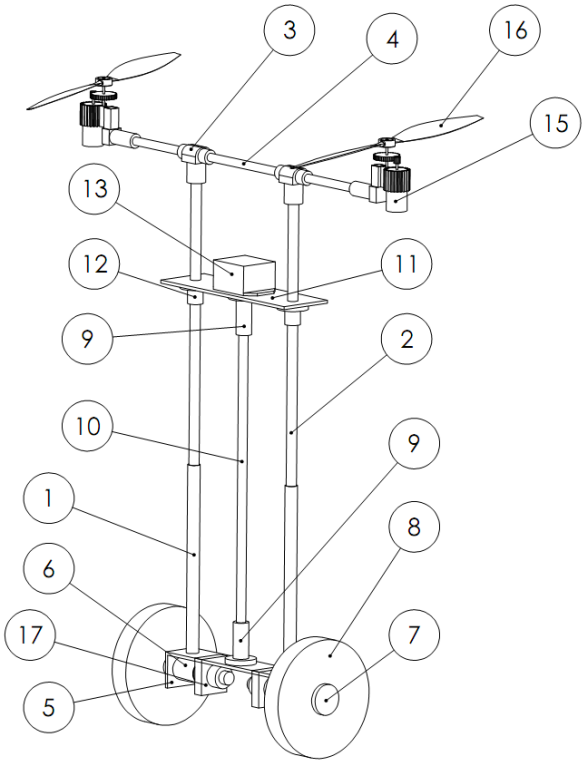


Atılım University
Mechatronics Engineering Department

DO NOT SCALE THE DRAWINGS | REVISION

Doğanç KÜÇÜK MSc. Thesis

| | NAME | SIGNATURE | DATE |
|---|---|---|---|
| DRWN | D. KÜÇÜK | | |
| CHK | | | |
| APP | | | |
| MNF | | | |
| QUA | | | |

TITTLE:

Full Assembly

MATERIALS:

DRAWING NO:

A4

WEIGHT: 1.236 Kg

SCALE: 1:5

PAGE 1 / 1

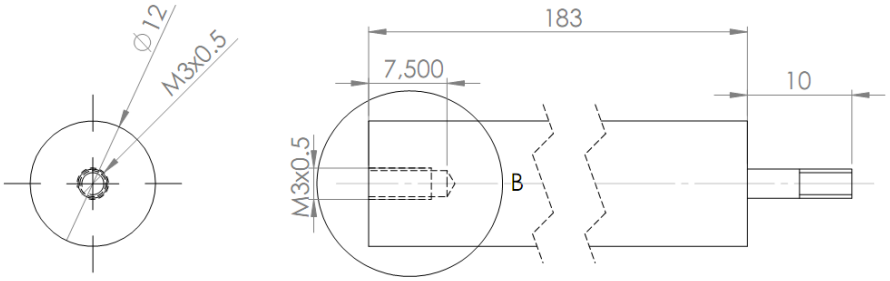


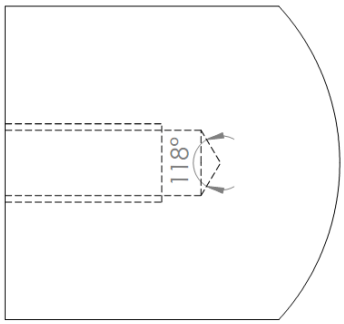


DETAIL B
SCALE 5 : 1

| | | | | | | |
|---|---|---|---|---|---|---|
| Atılım University<br>Mechatronics Engineering Department | | | | DO NOT SCALE THE DRAWINGS | | REVISION |
| | | | | Doğanç KÜÇÜK MSc. Thesis | | |
| | NAME | SIGNATURE | DATE | TITLE: | | |
| DRWN | D. KÜÇÜK | | | Link 1 | | |
| CHK | | | | | | |
| APP | | | | | | |
| MNF | | | | | | |
| QUA | | | | MATERIALS: | DRAWING NO: 1 | A4 |
| | | | | | | |
| | | | | | | |
| | | | | | SCALE: 2:1 | PAGE 1 / 1 |

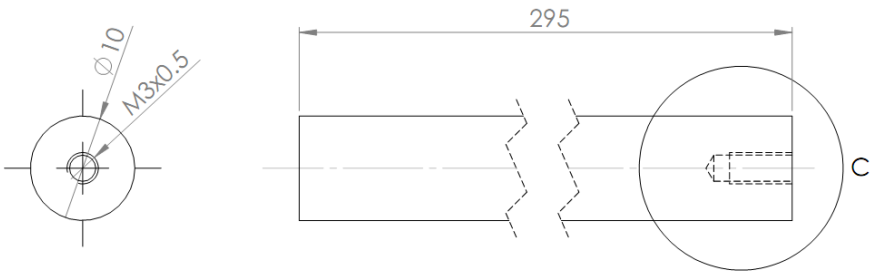


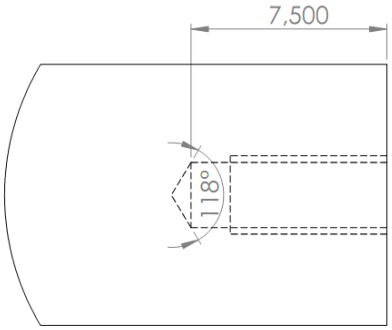


DETAIL C
SCALE 5 : 1

| | | | | | | |
|---|---|---|---|---|---|---|
| Atılım University<br>Mechatronics Engineering Department | | | | DO NOT SCALE THE DRAWINGS | | REVISION |
| | | | | Doğanç KÜÇÜK MSc. Thesis | | |
| | NAME | SIGNATURE | DATE | TITLE: | | |
| DRWN | D. KÜÇÜK | | | Link 2 | | |
| CHK | | | | | | |
| APP | | | | | | |
| MNF | | | | | | |
| QUA | | | | MATERIALS: | DRAWING NO: 2 | A4 |
| | | | | | | |
| | | | | | | |
| | | | | | SCALE: 2:1 | PAGE 1 / 1 |

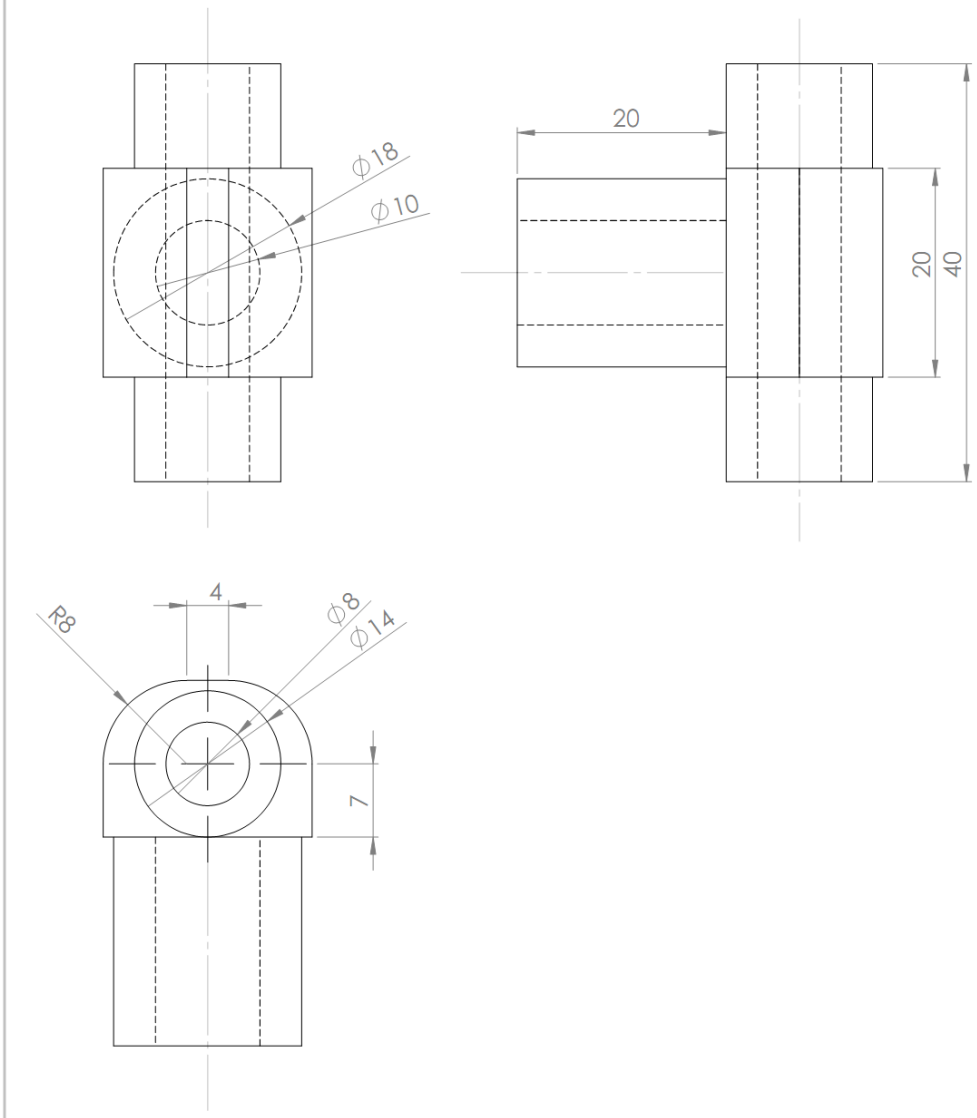


| | | | | | | |
|---|---|---|---|---|---|---|
| Atılım University<br>Mechatronics Engineering Department | | | | | DO NOT SCALE THE DRAWINGS | REVISION |
| | | | | | Doğanç KÜÇÜK MSc. Thesis | |
| | NAME | SIGNATURE | DATE | | TITLE: | |
| DRWN | D. KÜÇÜK | | | | T Connector | |
| CHK | | | | | | |
| APP | | | | | | |
| MNF | | | | | | |
| QUA | | | | MATERIALS: | DRAWING NO: 3 | A4 |
| | | | | | SCALE: 2:1 | PAGE 1 / 1 |

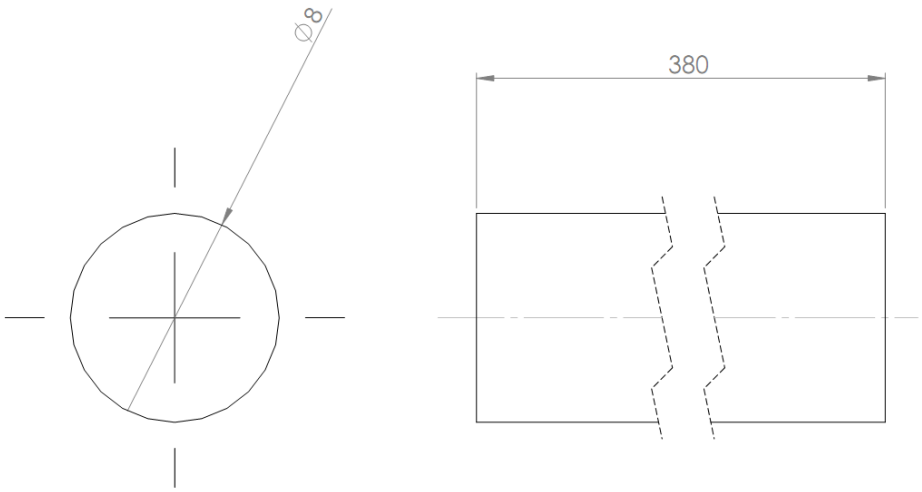


| | | | | | | |
|---|---|---|---|---|---|---|
| Atılım University<br>Mechatronics Engineering Department | | | | DO NOT SCALE THE DRAWINGS | | REVISION |
| | | | | Doğanç KÜÇÜK MSc. Thesis | | |
| | NAME | SIGNATURE | DATE | TITLE: | | |
| DRWN | D. KÜÇÜK | | | Link 3 | | |
| CHK | | | | | | |
| APP | | | | | | |
| MNF | | | | | | |
| QUA | | | | MATERIALS: | DRAWING NO: 4 | A4 |
| | | | | | | |
| | | | | | | |
| | | | | | SCALE: 2:1 | PAGE 1 / 1 |

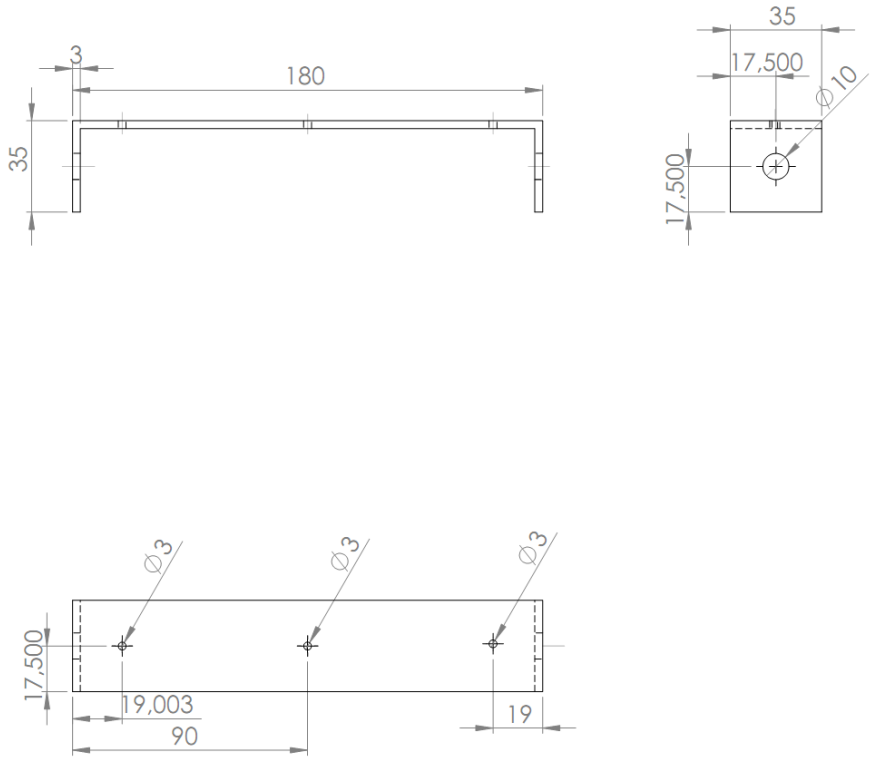


| | | | | | | |
|---|---|---|---|---|---|---|
| Atılım University<br>Mechatronics Engineering Department | | | | DO NOT SCALE THE DRAWINGS | REVISION | |
| | | | | Doğanç KÜÇÜK MSc. Thesis | | |
| | NAME | SIGNATURE | DATE | TITLE: | | |
| DRWN | D. KÜÇÜK | | | U Connector | | |
| CHK | | | | | | |
| APP | | | | | | |
| MNF | | | | | | |
| QUA | | | | MATERIALS: | DRAWING NO: 5 | A4 |
| | | | | | | |
| | | | | | | |
| | | | | | SCALE: 1:2 | PAGE 1 / 1 |

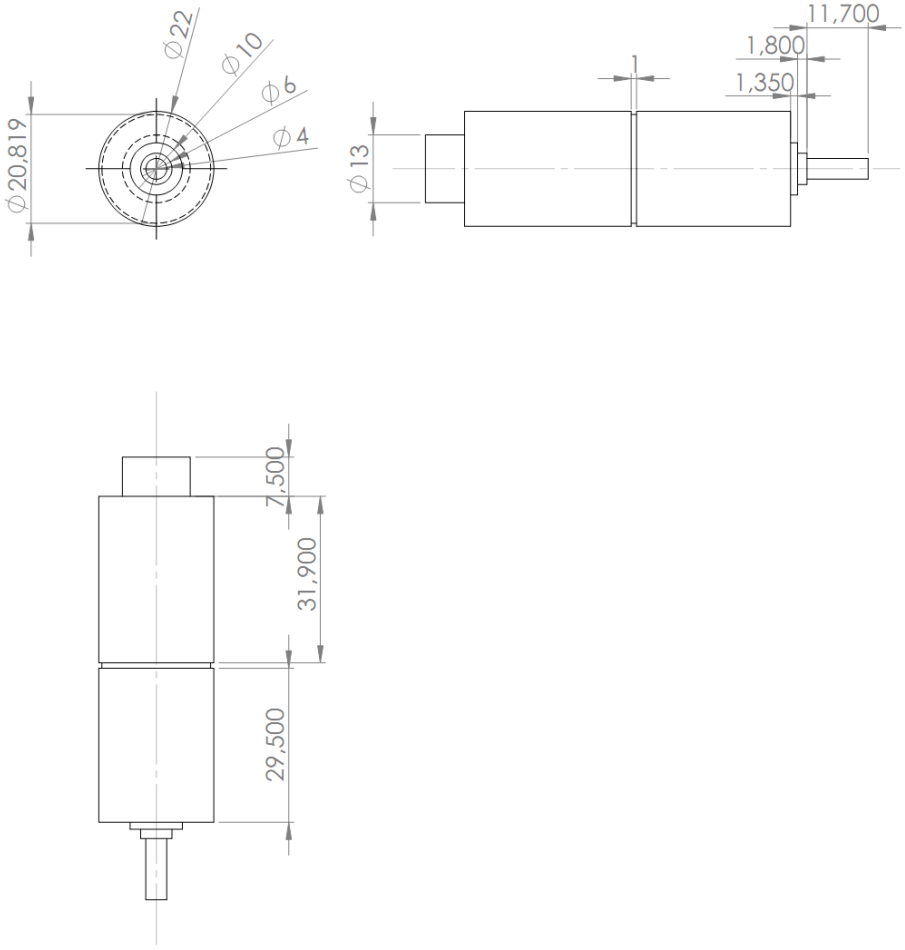


| | | | | | | |
|---|---|---|---|---|---|---|
| Atılım University<br>Mechatronics Engineering Department | | | | | DO NOT SCALE THE DRAWINGS | REVISION |
| | | | | | Doğanç KÜÇÜK MSc. Thesis | |
| | NAME | SIGNATURE | DATE | | TITLE: | |
| DRWN | D. KÜÇÜK | | | | Maxon Motor | |
| CHK | | | | | | |
| APP | | | | | | |
| MNF | | | | | | |
| QUA | | | | MATERIALS: | DRAWING NO: 6 | A4 |
| | | | | | SCALE: 1:1 | PAGE 1 / 1 |

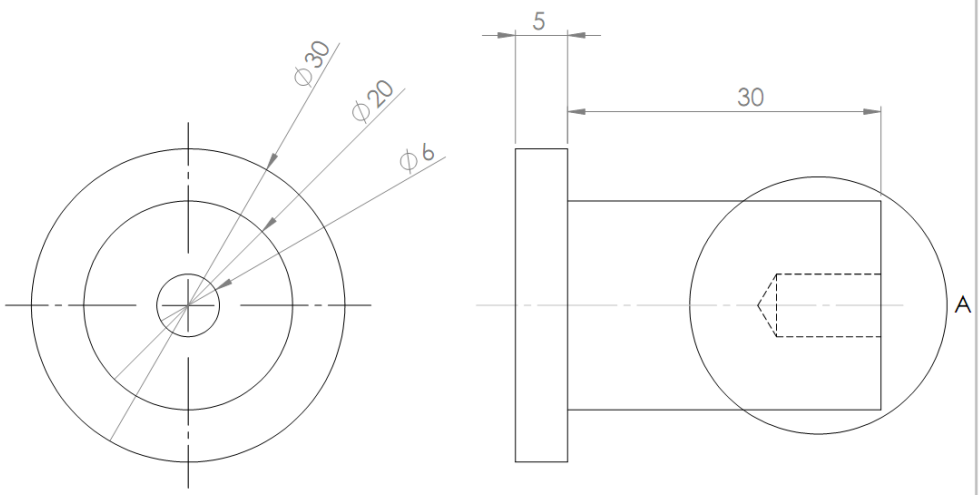


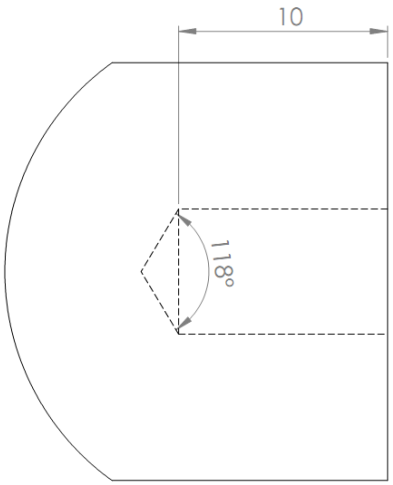


DETAIL A
SCALE 4 : 1

| | | | | | | |
|---|---|---|---|---|---|---|
| Atılım University<br>Mechatronics Engineering Department | | | | DO NOT SCALE THE DRAWINGS | REVISION | |
| | | | | Doğanç KÜÇÜK MSc. Thesis | | |
| | NAME | SIGNATURE | DATE | TITLE: | | |
| DRWN | D. KÜÇÜK | | | Wheel Inner | | |
| CHK | | | | | | |
| APP | | | | | | |
| MNF | | | | | | |
| QUA | | | | MATERIALS: | DRAWING NO: 7 | A4 |
| | | | | | SCALE: 2:1 | PAGE 1 / 1 |

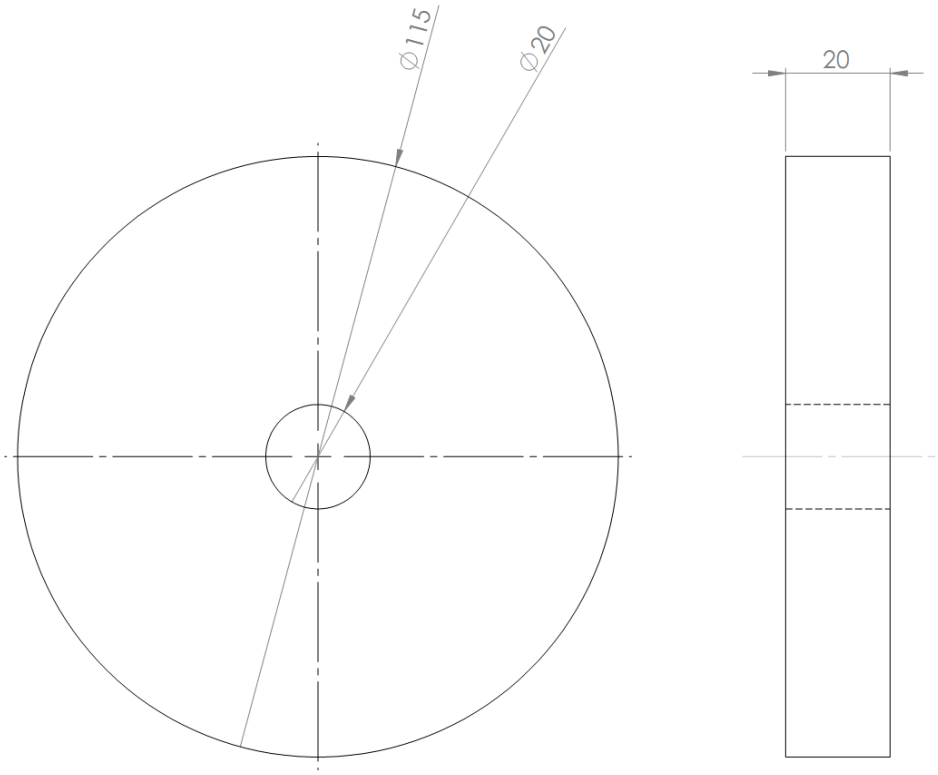


| | | | | | | |
|---|---|---|---|---|---|---|
| Atılım University<br>Mechatronics Engineering Department | | | | | DO NOT SCALE THE DRAWINGS | REVISION |
| | | | | | Doğanç KÜÇÜK MSc. Thesis | |
| | NAME | SIGNATURE | DATE | | TITLE: | |
| DRWN | D. KÜÇÜK | | | | Wheel | |
| CHK | | | | | | |
| APP | | | | | | |
| MNF | | | | | | |
| QUA | | | | MATERIALS: | DRAWING NO: 8 | A4 |
| | | | | | SCALE: 2:1 | PAGE 1 / 1 |

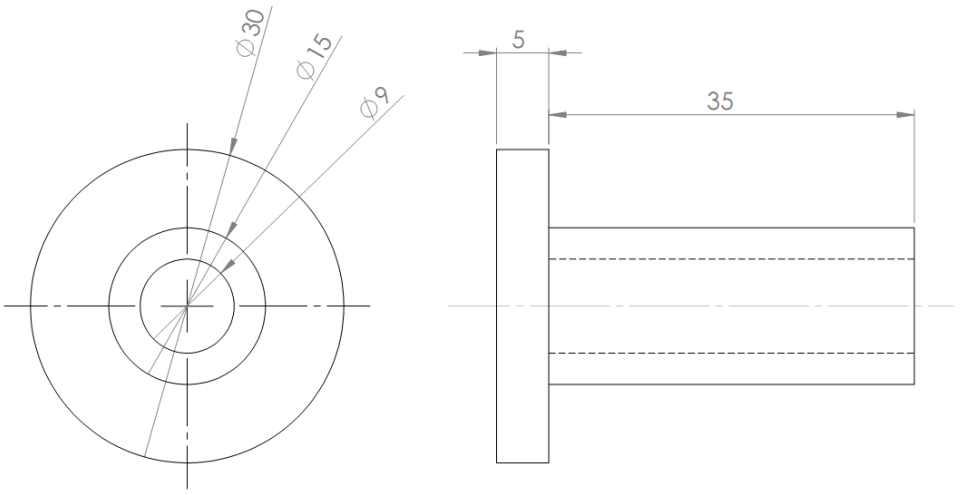


| | | | | | | |
|---|---|---|---|---|---|---|
| Atılım University<br>Mechatronics Engineering Department | | | | DO NOT SCALE THE DRAWINGS | | REVISION |
| | | | | Doğanç KÜÇÜK MSc. Thesis | | |
| | NAME | SIGNATURE | DATE | TITLE: | | |
| DRWN | D. KÜÇÜK | | | Link Holder | | |
| CHK | | | | | | |
| APP | | | | | | |
| MNF | | | | | | |
| QUA | | | | MATERIALS: | DRAWING NO: 9 | A4 |
| | | | | | | |
| | | | | | | |
| | | | | | SCALE: 2:1 | PAGE 1 / 1 |

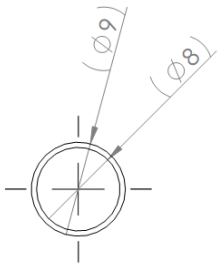


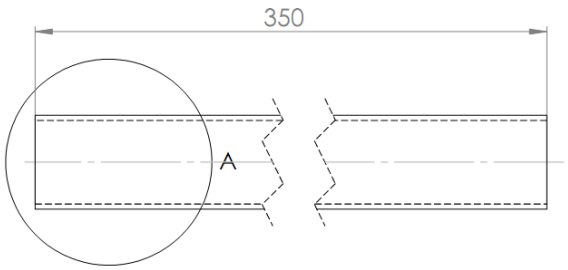


DETAIL A
SCALE 5 : 1

| | | | | | | |
|---|---|---|---|---|---|---|
| Atılım University<br>Mechatronics Engineering Department | | | | DO NOT SCALE THE DRAWINGS | | REVISION |
| | | | | Doğanç KÜÇÜK MSc. Thesis | | |
| | NAME | SIGNATURE | DATE | TITLE: | | |
| DRWN | D. KÜÇÜK | | | Middle Link Standard 3 View | | |
| CHK | | | | | | |
| APP | | | | | | |
| MNF | | | | | | |
| QUA | | | | MATERIALS: | DRAWING NO: 10 | A4 |
| | | | | | | |
| | | | | | | |
| | | | | | SCALE: 2:1 | PAGE 1 / 1 |

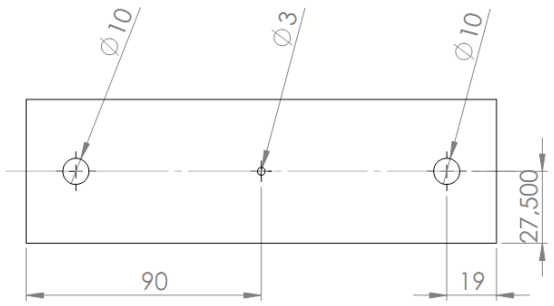


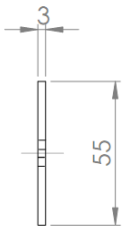


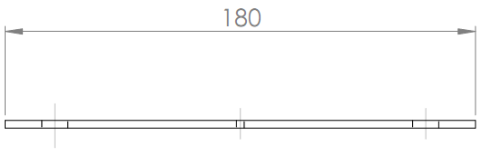


| | | | | | | |
|---|---|---|---|---|---|---|
| Atılım University<br>Mechatronics Engineering Department | | | | DO NOT SCALE THE DRAWINGS | | REVISION |
| | | | | Doğanç KÜÇÜK MSc. Thesis | | |
| | NAME | SIGNATURE | DATE | TITLE: | | |
| DRWN | D. KÜÇÜK | | | Sensor Holder | | |
| CHK | | | | | | |
| APP | | | | | | |
| MNF | | | | | | |
| QUA | | | | MATERIALS: | DRAWING NO: 11 | A4 |
| | | | | | | |
| | | | | | | |
| | | | | | SCALE: 1:2 | PAGE 1 / 1 |

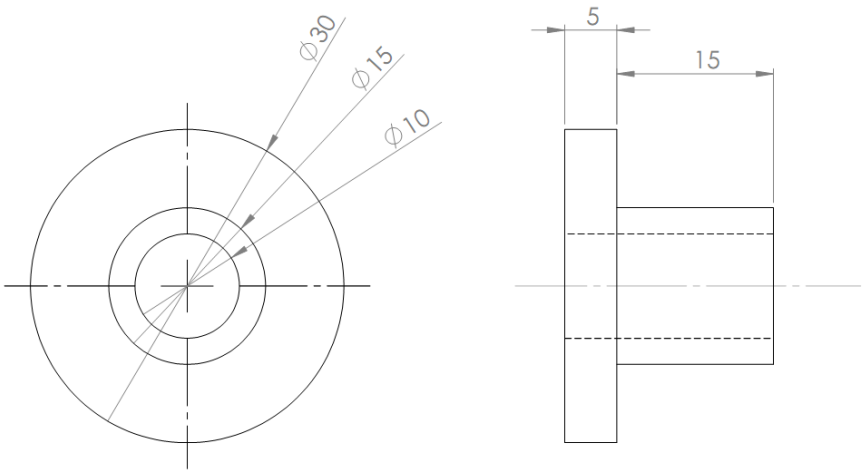


| | | | | | | |
|---|---|---|---|---|---|---|
| Atılım University<br>Mechatronics Engineering Department | | | | DO NOT SCALE THE DRAWINGS | | REVISION |
| | | | | Doğanç KÜÇÜK MSc. Thesis | | |
| | NAME | SIGNATURE | DATE | TITLE: | | |
| DRWN | D. KÜÇÜK | | | Sensor Connector | | |
| CHK | | | | | | |
| APP | | | | | | |
| MNF | | | | | | |
| QUA | | | | MATERIALS: | DRAWING NO: 12 | A4 |
| | | | | | | |
| | | | | | | |
| | | | | | SCALE: 2:1 | PAGE 1 / 1 |

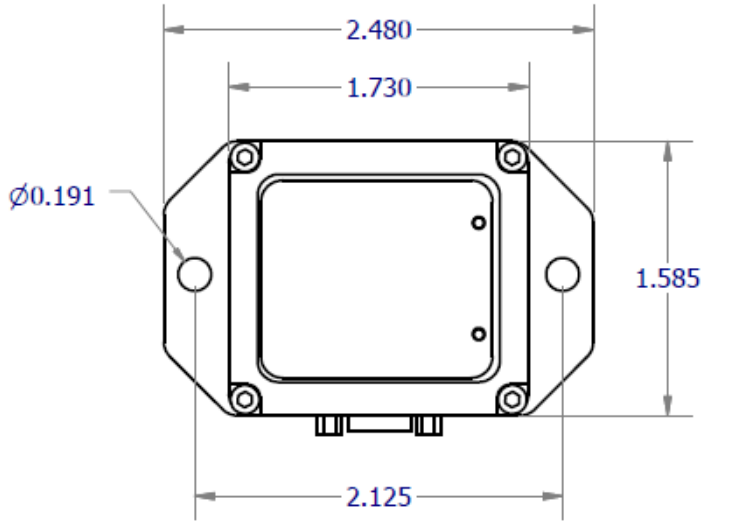


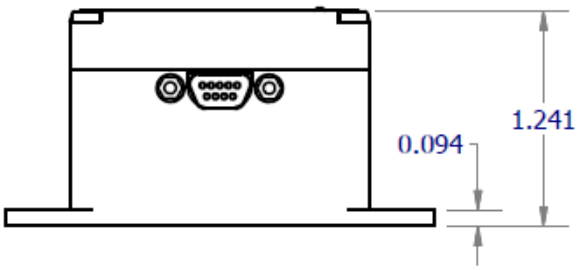


| | | | | | | |
|---|---|---|---|---|---|---|
| Atılım University<br>Mechatronics Engineering Department | | | | DO NOT SCALE THE DRAWINGS | | REVISION |
| | | | | Doğanç KÜÇÜK MSc. Thesis | | |
| | NAME | SIGNATURE | DATE | | | |
| DRWN | D. KÜÇÜK | | | TITLE: | | |
| CHK | | | | Microstrain GX2 | | |
| APP | | | | | | |
| MNF | | | | | | |
| QUA | | | | MATERIALS: | DRAWING NO: | A4 |
| | | | | | 13 | |
| | | | | | SCALE 1:1 | PAGE 1 / 1 |

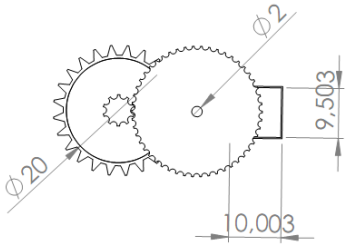


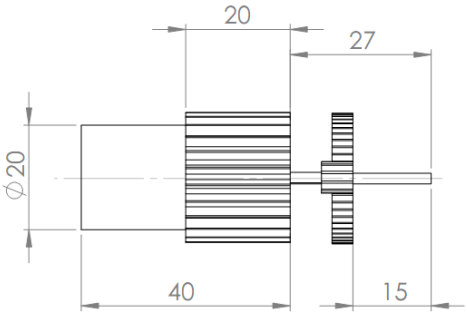


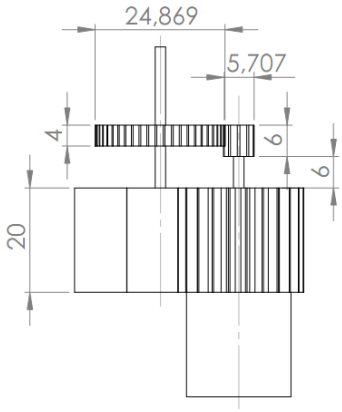


| | | | | | | |
|---|---|---|---|---|---|---|
| Atılım University<br>Mechatronics Engineering Department | | | | | DO NOT SCALE THE DRAWINGS | REVISION |
| | | | | | Doğanç KÜÇÜK MSc. Thesis | |
| | NAME | SIGNATURE | DATE | | TITLE: | |
| DRWN | D. KÜÇÜK | | | | Art Tech Brushless Motor | |
| CHK | | | | | | |
| APP | | | | | | |
| MNF | | | | | | |
| QUA | | | | MATERIALS: | DRAWING NO: 15 | A4 |
| | | | | | SCALE: 1:1 | PAGE 1 / 1 |

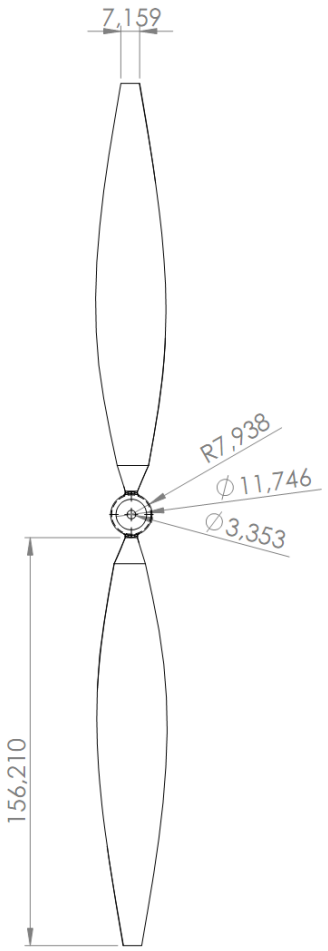


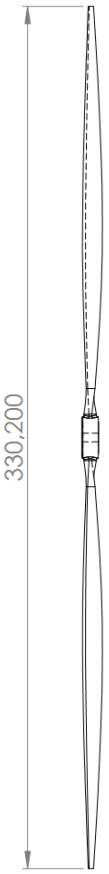


| | | | | | | |
|---|---|---|---|---|---|---|
| Atılım University<br>Mechatronics Engineering Department | | | | DO NOT SCALE THE DRAWINGS | | REVISION |
| | | | | Doğanç KÜÇÜK MSc. Thesis | | |
| | NAME | SIGNATURE | DATE | TITLE: | | |
| DRWN | D. KÜÇÜK | | | Propeller | | |
| CHK | | | | | | |
| APP | | | | | | |
| MNF | | | | | | |
| QUA | | | | MATERIALS: | DRAWING NO: 16 | A4 |
| | | | | | | |
| | | | | | | |
| | | | | | SCALE: 1:2 | PAGE 1 / 1 |

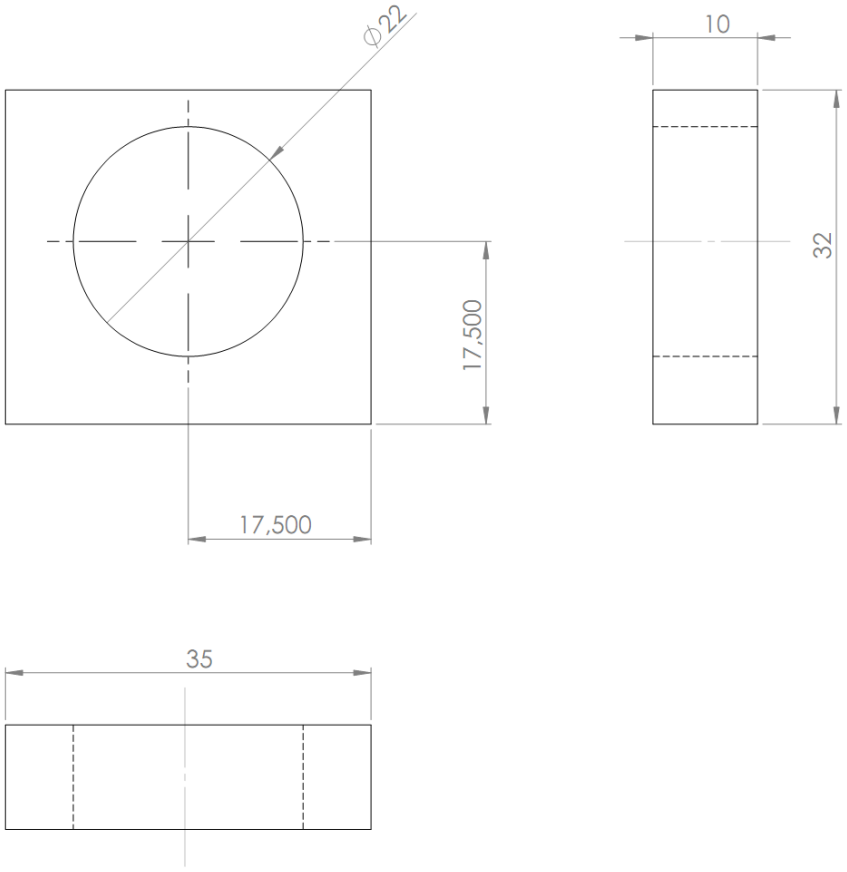


| | | | | | | |
|---|---|---|---|---|---|---|
| Atılım University<br>Mechatronics Engineering Department | | | | | DO NOT SCALE THE DRAWINGS | REVISION |
| | | | | | Doğanç KÜÇÜK MSc. Thesis | |
| | NAME | SIGNATURE | DATE | | TITLE: | |
| DRWN | D. KÜÇÜK | | | | Motor Holder | |
| CHK | | | | | | |
| APP | | | | | | |
| MNF | | | | | | |
| QUA | | | | MATERIALS: | DRAWING NO: 17 | A4 |
| | | | | | SCALE: 2:1 | PAGE 1 / 1 |